Herbicide detection: A review of enzyme- and cell-based biosensors

Guillaume Octobre, Nicolas Delprat, Bastien Doumèche, Béatrice Leca-Bouvier

Journal Pre-proof

Herbicide detection: A review of enzyme- and cell-based biosensors

Guillaume Octobre, Nicolas Delprat, Bastien Doumèche, Béatrice Leca-Bouvier

PII: S0013-9351(24)00234-2

DOI: https://doi.org/10.1016/j.envres.2024.118330

Reference: YENRS 118330

To appear in: *Environmental Research*

Received Date: 23 October 2023

Revised Date: 18 January 2024

Accepted Date: 27 January 2024

Please cite this article as: Octobre, G., Delprat, N., Doumèche, B., Leca-Bouvier, Bé., Herbicide detection: A review of enzyme- and cell-based biosensors, *Environmental Research* (2024), doi: https://doi.org/10.1016/j.envres.2024.118330.

Herbicide detection: a review of enzyme- and cell- based biosensors

Guillaume Octobre[1*], Nicolas Delprat[1], Bastien Doumèche[1], Béatrice Leca-Bouvier[1*]

[1] Univ Lyon, Université Claude Bernard Lyon 1, CNRS, ICBMS UMR5246, 69622 Villeurbanne, France

* corresponding authors

Graphical abstract

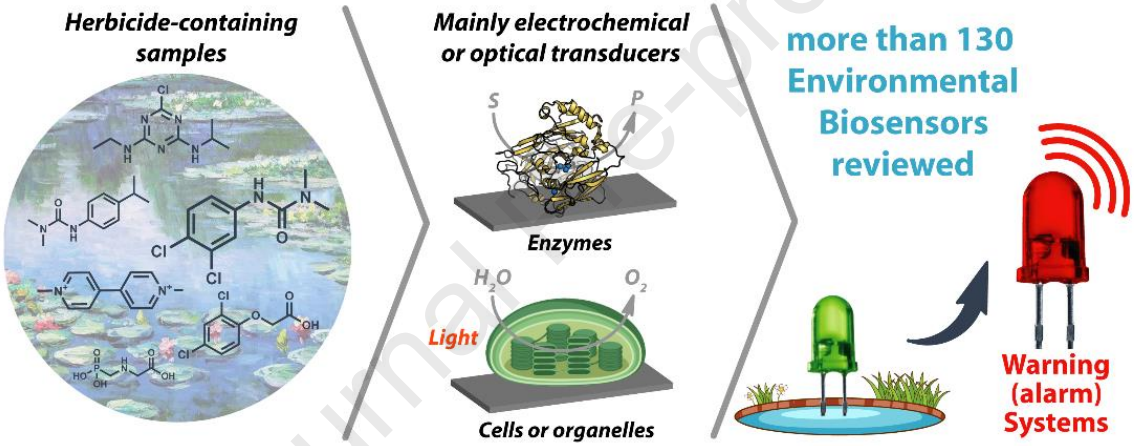

Abstract

Herbicides are the most widely used class of pesticides in the world. Their intensive use raises the question of their harmfulness to the environment and human health. These pollutants need to be detected at low concentrations, especially in water samples. Commonly accepted analytical techniques (HPLC-MS, GC-MS, ELISA tests) are available, but these highly sensitive and time-consuming techniques suffer from high cost and from the need for bulky equipment, user training and sample pre-treatment. Biosensors can be used as complementary early-warning systems that are less sensitive and less selective. On the other hand, they are rapid, inexpensive, easy-to-handle and allow direct detection of the sample, onsite, without any further step other than dilution. This review focuses on enzyme- and cell- (or subcellular elements) based biosensors. Different enzymes (such as tyrosinase or peroxidase) whose activity is inhibited by herbicides are presented. Photosynthetic cells such as algae or cyanobacteria are also reported, as well as subcellular elements (thylakoids, chloroplasts). Atrazine, diuron, 2,4-D and glyphosate appear as the most frequently detected herbicides, using amperometry or optical transduction (mainly based on chlorophyll fluorescence). The recent new WSSA/HRAC classification of herbicides is also included in the review.

Keywords: review, biosensors, herbicides, enzymes, cells, inhibition.

Abbreviations

ACP: acid phosphatase
AChE: acetylcholinesterase
A2P: ascorbic acid-2-phosphate
AFM: atomic force microscopy
AFS: atomic force spectroscopy
ALP: alkaline phosphatase
ALS: acetolactate synthase
AMPA: aminomethylphosphonic acid
ANN: artificial neural network
AuNPs: gold nanoparticles
BQ: benzoquinone
BSA: bovine serum albumin
CB: carbon black
CDs: carbon dots
CNTs: carbon nanotubes
CPEs: carbon paste electrodes
ChOx: choline oxidase
CV: cyclic voltammetry
DAD: diaminodurene
DAP: 2,3-diaminophenazine
DCMU: N′-(3,4-dichlorophenyl)-N,N-dimethylurea
DEA: desethylatrazine
DIA: desisopropylatrazine
2,4-D: 2,4-dichlorophenoxyacetic acid
DNOC: dinitro-o-cresol
DPV: differential pulse voltammetry
L-DOPA: 3,4-dihydroxy-L-phenylalanine
DXP: deoxy-D-xylulose phosphate
EDC: N-(3-dimethylaminopropyl)-N′-ethylcarbodiimide
ECL: electrochemiluminescence
EGDGE: ethylene glycol diglycidyl ether
ELISA: enzyme-linked immunosorbent assay
EPSPS: 5-enolpyruvylshikimate-3-phosphate synthase
ERGO: electrochemically reduced graphene oxide
ENFEC: enzyme field effect capacitive
ENFET: enzyme-field-effect transistor
FAD: flavin adenine dinucleotide
FET: field effect transistor
GC: gas chromatography
GCE: glassy carbon electrode
G6P: glucose-6-phosphate
GFET: gated field effect transistor
GST: glutathione-S-transferase
GlyOx: glycine oxidase
GOx: glucose oxidase

HGOFET: hydrogel-gated organic field-effect transistor
hPG: porous gold electrode
HPLC: high-pressure liquid chromatography
HQ: hydroquinone
HRAC: herbicide resistance action committee
HRP: horseradish peroxidase
ITO: indium tin oxide
LIFT: laser-induced forward transfer
LIG: laser-induced graphene
LOD: limit of detection
LSV: linear sweep voltammetry
µPADs: microfluidic paper-based analytical devices
MCPA: 2-methyl-4-chlorophenoxyacetic acid
MFC: microbial fuel cell
MIPs: molecular imprinted polymers
MPA: 3-mercaptopropionic acid
MS: mass spectrometry
MWCNTs: multiwalled carbon nanotubes
NHS: N-hydroxysuccinimide
NPs: nanoparticles
NQ: 1,2-naphtoquinone
OEC: oxygen-evolving complex
OPD: *o*-phenylenediamine
OPEEs: organic phase enzyme electrodes
PAM: pulse amplitude modulated
PEDT: polyethylenedioxythiophene
PET: photosynthetic electron transport
PGE: pencil graphite electrode
polySBQ: poly-mercapto-*p*-benzoquinone
PPO: polyphenol oxidase
PS: photosystem
PVA-SbQ: polyvinyl alcohol-styrylpyridinium
PAP: polyazetidine prepolymer
PSS: poly(4-styrenesulfonic acid)
PSF: polysulfone
SAM: self-assembled monolayer
SCE: saturated calomel electrode
SPEs: screen-printed electrodes
SPCEs: screen-printed carbon electrodes
SWCNTs: single-walled carbon nanotubes
SWV: square wave voltammetry
TMB: 3,3’5,5’-tetramethylbenzidine
UHPLC: ultra high performance liquid chromatography
WSSA: weed science society of America

1. Introduction

Worldwide pesticide usage was recently reported (Sharma *et al.*, 2019). As many as 2 million tonnes of pesticides are used annually all over the world, with *ca*. 50 % herbicides, 30 % insecticides and 20 % fungicides, thus pointing out the intensive use of herbicides. Considering the number of publications dealing with the development of systems for pesticide and for herbicide detection since the 1990's (Figure 1), a noticeable increase appears over time for pesticide detection, even more pronounced since COVID disturbance. Such a drastic increase cannot be observed for herbicide detection, with *ca*. 120 articles published per year. For pesticides, it is well-known that organophosphorous and carbamate insecticides inhibiting acetylcholinesterase are among the most reported and studied pesticides in the literature. On the other hand, and even if herbicide detection gives rise to a lower number of publications, their intensive use is harmful for the environment, as well as for human health, and should motivate research.

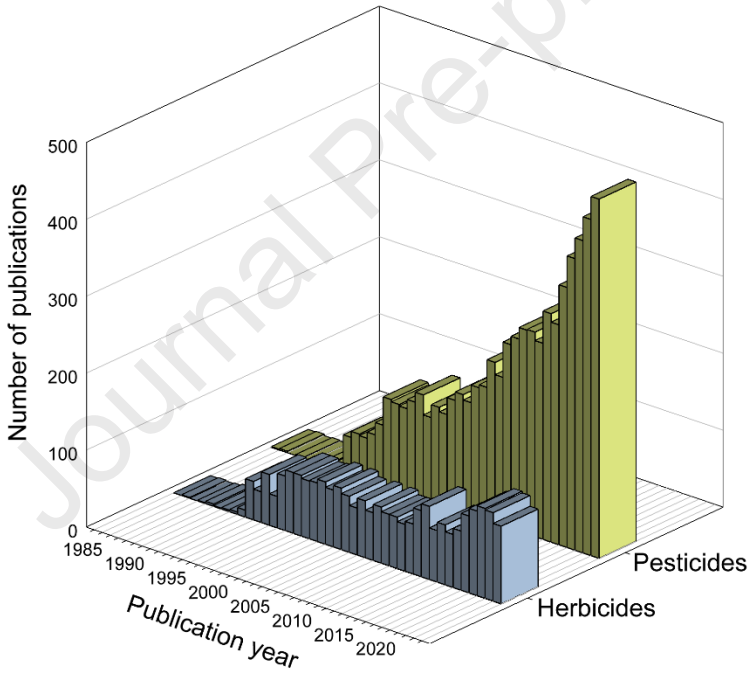

Figure 1. Time trend in the number of published articles in the field of bioassays and biosensors for the detection of pesticides or herbicides. Data were obtained from Web of Science (2023, july, 28th) using the two following requests (specific terms for pesticides and for herbicides are in italic). Herbicides: "*herbicide or atrazine or simazine or prometryne or terbutryne or terbuthylazine or sulcotrione or diuron or linuron or chlorotoluron or isoproturon or 2,4-D or MCPA or dicamba or bromacil or glyphosate or glufosinate or alachlor or paraquat*" or Pesticides: "*pesticide or insecticide or fungicide or organophosphorus or carbamate or organophosphorous",* each one being coupled with AND "enzyme or oxidase or peroxidase or tyrosinase or urease or phosphatase or whole cell or algae or bacteria or thylakoids or PSII or photosystem" AND "biosensor or assay".

From a regulatory point of view, maximum admissible pesticide concentrations in drinking water vary between countries. The European Union sets a maximum level of 0.1 ppb (0.1 µg.L^{-}

[1]) per pesticide, whereas this limit grows to 700 ppb in the USA or 280 ppb in Canada. Common specific and very sensitive chromatographic detection techniques such as GC-MS and HPLC-MS, or ELISA (Enzyme-Linked Immunosorbent Assay) immunoassays can be used, with a limit of detection (LOD) as low as 1 to 10 ppt for individual pesticides. However, sample preparation is very often required for preconcentration before analysis, by solid phase extraction for instance. Unlike these time-consuming and expensive procedures requiring skilled users, biosensors represent simple and low-cost alternatives, which are also usable onsite. A biosensor is defined as the intimate association of a specific biological recognition element (enzyme, antibody, tissue, organelle or whole cell, for instance) immobilized on a transducer which transforms an electrical, thermal or optical signal into a numerical signal. Enzyme- and photosynthesis (cells and subcellular elements)-based biosensors for herbicide detection will be considered in this review.

1.1. Herbicides

The Global Herbicide Resistance Action Committee (HRAC) updated the mode of action classification system for herbicides on March 1, 2020. A single numerical code is now shared by WSSA (Weed Science Society of America) and Global HRAC. Table 1 presents the classification of herbicides based on their cellular mode of action, including inhibitors of lipid or amino acid synthesis, photosynthesis, cell wall synthesis, microtubule assembly, and auxin mimics.

Table 1. Legacy HRAC and new WSSA / HRAC (2020) herbicide classifications.

Classification group		Mode and site of action	Chemical family	Main examples
New WSSA / HRAC (2020)	Legacy HRAC			
1	A	Lipid synthesis inhibition →acetyl-CoA carboxylase inhibitors	Cyclohexanediones	alloxydim, cycloxydim, sethoxydim
			Aryloxyphenoxy-propionates	diclofop-methyl, fenoxaprop-ethyl
			Phenylpyrazoline	pinoxaden
2	B	Branched-chain amino acid synthesis inhibition →acetolactate synthase (ALS) inhibitors	Pyrimidinyl benzoates	pyriftalid, pyriminobac-methyl
			Sulfonanilides	pyrimisulfan, triafamone
			Triazolopyrimidine - Type 1	cloransulam-methyl, diclosulam
			Triazolopyrimidine - Type 2	penoxsulam, pyroxsulam
			Sulfonylureas	chlorsulfuron,sulfometuron-methyl

			Imidazolinones	imazamethabenz-methyl, imazethapyr
			Triazolinones	propoxycarbazone-Na, thiencarbazone-methyl
3	K1	Root growth inhibition →microtubules assembly inhibitors	Dinitroanilines	benefin (=benfluralin), butralin, nitralin
			Pyridines	dithiopyr, thiazopyr
			Phosphoroamidates	butamifos, DMPA
			Benzoic acid	chlorthal-dimethyl
			Benzamides	pronamide
4	O	Plant growth inhibition →agonist action on auxin hormone receptor: transport inhibitor response protein 1	Pyridine-carboxylates	picloram, clopyralid, halauxifen
			Pyridyloxy-carboxylates	triclopyr, fluroxypyr
			Phenoxy-carboxylates	2,4,5-T, 2,4-D, 2,4-DB, dichlorprop, MCPA
			Benzoates	dicamba, chloramben
			Quinoline-carboxylates	quinclorac, quinmerac
			Pyrimidine-carboxylates	aminocyclopyrachlor
			Phenyl carboxylates	chlorfenac, chlorfenprop
			Other	benazolin-ethyl
5	C1, C2	Photosynthesis inhibition →photosystem II inhibitors (D1 protein Serine 264 binding)	Triazines	atrazine, cyanazine, simazine, terbutryne
			Triazolinone	amicarbazone
			Triazinones	ethiozin, hexazinone
			Uracils	bromacil, lenacil, terbacil
			Phenylcarbamates	chlorprocarb, desmedipham
			Pyridazinone	brompyrazon, chloridazon(=pyrazon)
			Ureas	diuron, benzthiazuron, bromuron, isoproturon

			Amides	chloranocryl (=dicryl), pentanochlor, propanil
6	C3	Photosynthesis inhibition →photosystem II inhibitors (D1 protein Histidine 215 binding)	Nitriles (also uncouplers "M")	bromofenoxim, bromoxynil, ioxynil
			Phenyl-pyridazines	pyridate
			Benzothiadiazinone	bentazon
9	G	Aromatic amino acid synthesis inhibition → EPSPS inhibitors	Glycines	glyphosate
10	H	Inhibition of Glutamine Synthetase	Phosphinic acids	glufosinate ammonium, bialaphos
12	F1	Inhibition of Phytoene Desaturase	Phenyl-ethers	picolinafen, diflufenican
			N-Phenyl heterocycles	flurochloridone, norflurazon
			Diphenyl heterocycles	fluridone, flurtamone
13	F4	Inhibition of DXP synthase	Isoxazolidinone	clomazone, bixlozone
14	E	Inhibition of Protoporphyrinogen Oxidase	Diphenyl ethers	acifluorfen, bifenox, fluoronitrofen
			Phenylpyrazoles	pyraflufen-ethyl
			N-Phenyl-oxadiazolones	oxadiargyl, oxadiazon
			N-Phenyl-triazolinones	azafenidin, carfentrazone-ethyl
			N-Phenyl-imides	fluthiacet-methyl
			N-Phenyl-imides	butafenacil, saflufenacil
			Other	pyraclonil
15	K3	Inhibition of Very Long Chain Fatty Acid Synthesis	Azolyl-carboxamides	cafenstrole, fentrazamide
			α-Thioacetamides	anilofos, piperophos
			Isoxazolines	pyroxasulfone, fenoxasulfone
			Oxiranes	indanofan, tridiphane
			α-Chloroacetamides	acetochlor, alachlor, allidochlor
			α-Oxyacetamides	mefenacet, flufenacet

			Thiocarbamates	butylate, cycloate, dimepiperate
			Benzofurans	benfuresate, ethofumesate
18	I	Inhibition of Dihydropteroate Synthase	Carbamate	asulam
19	P	Auxin transport inhibition	Aryl-carboxylates	naptalam
22	D	PS-I electron diversion	Pyridiniums	paraquat, cyperquat, diquat
23	K2	Inhibition of Microtubule Organization	Carbamates	barban, carbetamide, chlorbufam
24	M	Uncouplers	Dinitrophenols	dinosam, dinoseb, DNOC, dinoterb
27	F2	Inhibition of Hydroxyphenyl Pyruvate Dioxygenase	Triketones	mesotrione, sulcotrione
			Triketone	benzobicyclon
			Pyrazoles	benzofenap, pyrasulfotole
			Isoxazoles	isoxaflutole
29	L	Inhibition of Cellulose Synthesis	Triazolecarboxamide	flupoxam
			Benzamide	Isoxaben
			Alkylazines	triaziflam, indaziflam
			Nitriles	dichlobenil, chlorthiamid
30	Q	Inhibition of Fatty Acid Thioesterase	Benzyl ether	cinmethylin, methiozolin
31	R	Inhibition of serine-threonine protein phosphatase	Other	endothall
32	S	Inhibition of Solanesyl Diphosphate Synthase	Diphenylether	aclonifen
33	T	Inhibition of homogentisate solanesyltransferase	Phenoxypyridazine	cyclopyrimorate
34	F3	Inhibition of Lycopene Cyclase	Triazole	amitrole
0	Z	Unknown mode of action		cumyluron, difenzoquat

(DXP: deoxy-D-xylulose phosphate; EPSPS: 5-enolpyruvylshikimate-3-phosphate synthase)

In the literature, biosensors for herbicide detection have been developed, particularly through immobilization of enzymes, whole cells or subcellular components. As reported later in this review, the main herbicides that are detected are atrazine, diuron, 2,4-D and glyphosate

(structures in Figure 2), acting on hormone-based regulation, photosynthesis and aromatic amino acid synthesis, respectively (Figure 3).

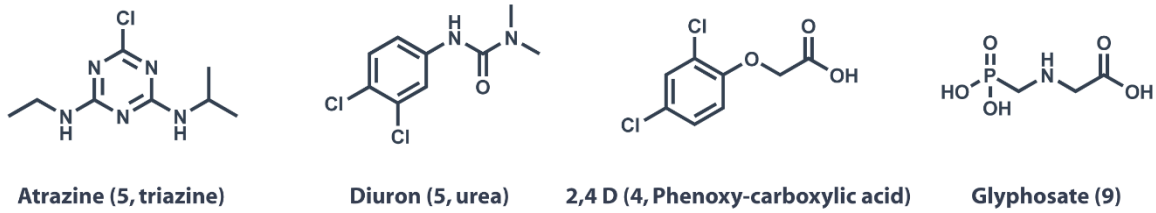

Figure 2. Structures of the main herbicides detected by enzyme- or cell-based biosensors (HRAC group numbers and chemical families are indicated in parentheses).

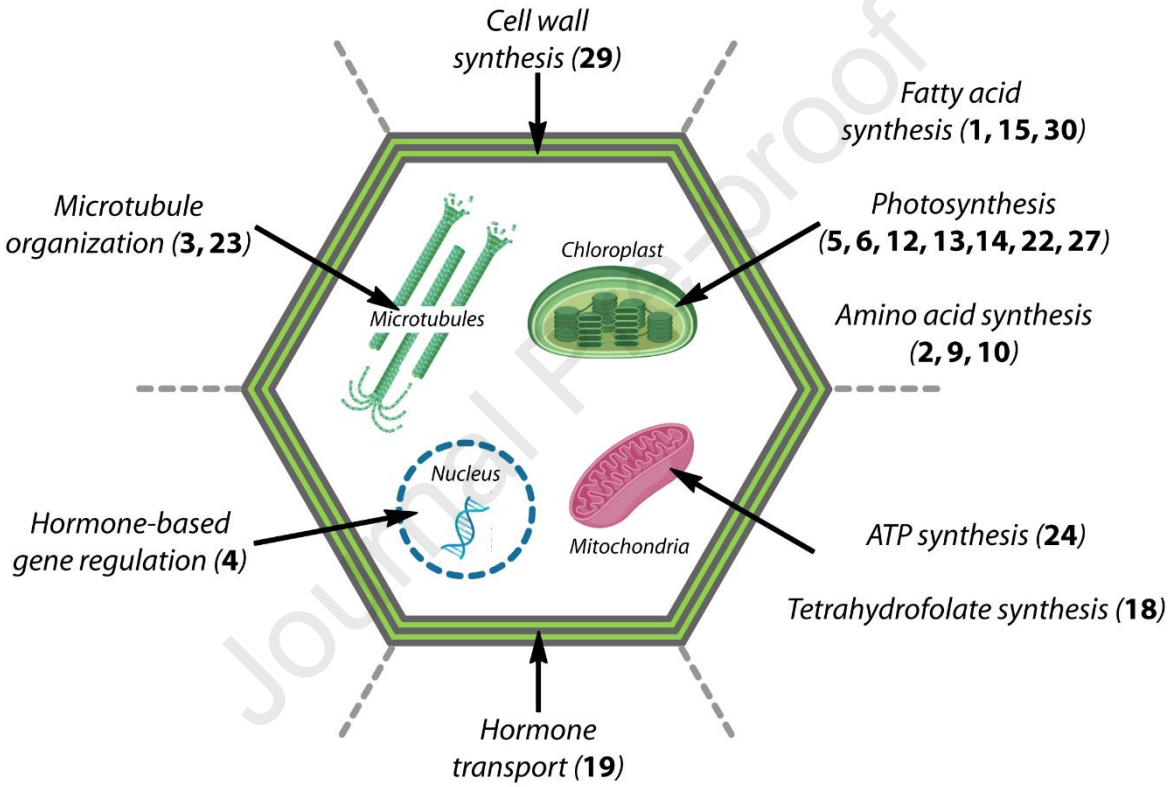

Figure 3. Modes of action of herbicides on a plant cell according to the HRAC classification (group number in bold case, *Figure adapted from* (Délye *et al.*, 2013).

1.2. Herbicide detection

Several detection formats can be distinguished, as previously reported in the literature (Sassolas *et al.*, 2011). Soluble bioelements can be employed for homogeneous assays using a single liquid phase. On the other hand, heterogeneous assays rely on immobilization of the bioelement on a surface that is not a transducer, and unbound binding partners can be removed by washing or by magnetic separation. In a biosensor, contrary to heterogeneous enzyme-based assays, immobilization is achieved directly onto a transducer surface.

In this study, only biosensors meeting the above definition will be considered. Heterogeneous assays have also been reported in the literature, either enzyme-based (using acetolactate synthase (ALS) (Marty *et al.*, 1993), 5-enolpyruvylshikimate-3-phosphate synthase (EPSPS) (Döring *et al.*, 2019), alkaline phosphatase (ALP) (Tong *et al.*, 2023), glyphosate oxidase (Delprat *et al.*, 2023) or whole cell-based (using algae (Prudkin-Silva *et al.*, 2021), bacteria (Rocaboy-Faquet *et al.*, 2014) or thylakoids (Euzet *et al.*, 2005), but they will not be considered in this review. Biochip systems have also been proposed, such as the one described by Podola and Melkonian (2005) (Podola and Melkonian, 2005) using multiple microalgal strains. Optical detection was achieved by measuring variations in chlorophyll fluorescence after treatment with herbicide. However, this type of biochip system is considered as an heterogeneous assay and is not developed in this review.

Among the biosensors developed for herbicide detection, different biological elements have been immobilized on an appropriate transducer surface, not only enzymes and cells/organelles that are considered in this review, but also aptamers, antibodies or molecular imprinted polymers (MIPs). As shown in Figure 4, enzymes and cells/organelles obviously represent the main biological elements (*ca*. 60 %, comprising 35 % enzymes) used in biosensors for herbicide detection. Immunosensors are also widely cited among biosensors for herbicide detection (35 %). Other less developed biosensors are aptasensors or MIP-based biosensors.

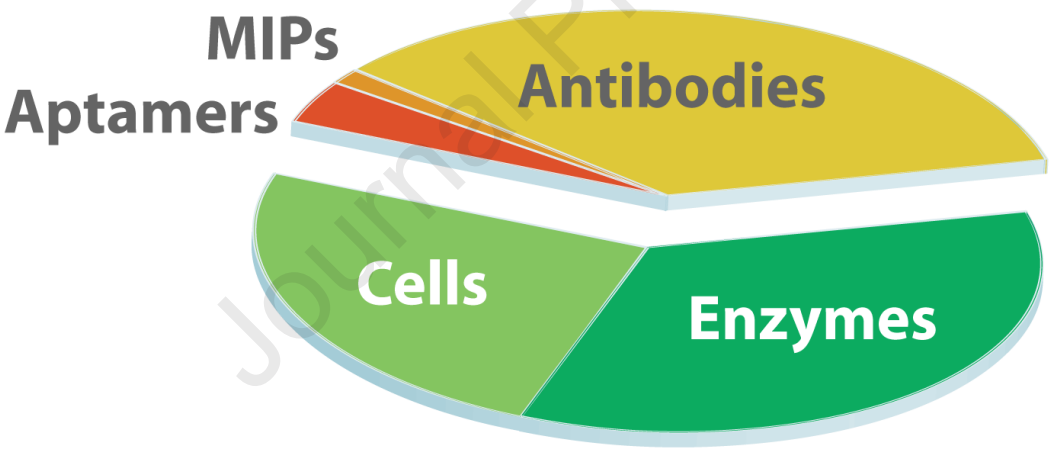

Figure 4. Repartition of biosensors for herbicide detection with respect to the recognition element. Data were obtained from Web of Science (2023, july 28th) using the following request: **"**herbicide or atrazine or simazine or prometryne or terbutryne or terbuthylazine or sulcotrione or diuron or DCMU or linuron or chlorotoluron or chlortoluron or isoproturon or 2,4-D or MCPA or dicamba or bromacil or glyphosate or glufosinate or alachlor or paraquat or bromoxynil or mesotrione" AND "biosensor" AND "aptamer or aptasensor or MIP or immuno or antibody or immunosensor or enzyme or oxidase or peroxidase or tyrosinase or urease or phosphatase or whole cell or algae or bacteria or thylakoids or PSII or photosystem". For simplicity, the term "cells" is used in the figure to refer to cells/organelles.

Immunosensors for pesticide detection have been reviewed several times in the literature (Jiang *et al.*, 2008)(Raman Suri *et al.*, 2009)(Fang *et al.*, 2020). Nucleic acid-based and aptasensors have also been reported. For example, an electrochemical DNA biosensor was recently described (Congur, 2021) for 2,4-D detection using a single-use pencil graphite

electrode (PGE). The guanine oxidation signal measured at 1 V *vs*. Ag|AgCl by differential pulse voltammetry (DPV) decreased after surface-confined interaction of 2,4-D and DNA at the electrode surface. Aptasensors for pesticide (Phopin and Tantimongcolwat, 2020) or for atrazine (Sun *et al.*, 2019) detection have also been proposed. In the signal-on aptasensor format (Sun *et al.*, 2019), when atrazine is present, graphene combined with aptamer is released and a photocurrent is recovered. MIPs have also been described for pesticide detection (Nageib *et al.*, 2023). Readers are also referred to a review on biosensors based on antibodies, aptamers and MIPs (Majdinasab *et al.*, 2021).

As described hereafter in this review, the development of biosensors based on enzyme, cell or subcellular element immobilization relies on two main transduction modes: electrochemical (amperometry) and optical (fluorescence). Amperometry can be used for any biological element, while fluorescence measurements are only suitable for photosynthesis-based biosensors. Main advantages and disadvantages of these two detection modes are recapitulated in Table 2. As an example, comparison in terms of LOD is supported by the values obtained for atrazine detection and based on algae PSII inhibition described by Antonacci *et al.* (2021).

Table 2. Advantages and drawbacks of optical (fluorescence) and electrochemical (amperometry) detection used in biosensors for herbicide detection.

	Optical (fluorescence)	Electrochemical (amperometry)
low LOD (Antonacci *et al.*, 2021)	++ (1 ppt atrazine)	+ (0.4 ppb atrazine ; O_2 sensing)
easily miniaturized	+	++
low cost	+	++
user-friendly instrumentation, simple set-up	+	++
usable in complex and turbid matrices	-	+

2 Enzymatic biosensors

Herbicides are known for causing metabolic perturbation in plants by inhibiting specific enzymes. Based on this feature, enzymes can be used as biological recognition elements in biosensors, keeping in mind that an enzyme can be inhibited by several herbicides as well as other compounds, leading to specificity issues. Herbicides can also be directly used as substrates for enzymatic reactions, thus overcoming specificity limitation. However, very few biosensors based on such direct detection have been described.

Table 3. Enzymatic biosensors for herbicide detection.

Herbicide	Enzyme	Immobilization method	Detection method	LOD (ppm or ppb)	Linear range (ppm or ppb)	Reference
Biosensors based on inhibition of enzyme activity (signal-off systems)						
glyphosate	AChE	entrapment in chitosan	FET	6.4 x 10^{-8} ppb	1.7 x 10^{-7}- 1.7 x 10^{-3} ppb (semi-log)	(Yu *et al.*, 2021)
glyphosate	ACP	glutaraldehyde cross-linking	amperometry	15 ppb	50 - 500 ppb	(Butmee *et al.*, 2021)
2,4-D	ALP	covalent coupling *via* polyazetidine	amperometry	0.5 ppb	1.5 - 60 ppb	(Mazzei *et al.*, 2004)
2,4-D; 2,4,5-T	ALP	entrapment in silica sol-gel / chitosan	amperometry	0.5 ppb 2,4-D, 0.8 ppb 2,4,5-T	1 - 60 ppb 2,4-D or 2,4,5-T	(Shyuan *et al.*, 2008)
2,4-D	ALP	entrapment in a sol-gel silica / chitosan matrix	amperometry	0.3 ppb	0.5 - 30 ppb	(Loh *et al.*, 2008)
2,4-D	ALP	entrapment in PVA-SbQ under UV illumination	amperometry	1 ppb	2.1 - 110 ppb	(Bollella *et al.*, 2016)
2,4-D	ALP	glutaraldehyde cross-linking	CV	3.5 x 10^{-3} ppb	9 x 10^{-3} - 5 ppb (semi-log)	(Gianvittorio *et al.*, 2023)
2,4-D	catalase	entrapment in hierarchical porous calcium phosphate microspheres	amperometry (flow injection system)	3.3 ppb	6.6 - 660 ppb	(Liu *et al.*, 2016)
atrazine	GOx	adsorption on aligned CNTs	SWV	8.4 ppb	0.1 - 9 ppm	(Yang *et al.*, 2010)
glyphosate	HRP	electrostatic adsorption	CV	(incorrect value)	0.25 - 14 ppb	(Songa *et al.*, 2009a)
glyphosate	Atemoya peroxidase	entrapment	SWV	30 ppb	0.1 - 4.55 ppm	(Oliveira *et al.*, 2012)
glyphosate	HRP	adsorption	CV	(incorrect value)	1.7 x 10^{-2} ppb - 1.9 ppm (semi-log)	(Cahuantzi-Muñoz *et al.*, 2019)

glyphosate	HRP	adsorption (electrodeposition)	electrochemical	5.44 ppb	16.9 ppb – 16.9 ppm (semi-log)	(Roman *et al.*, 2020)
glyphosate	HRP	interaction biotinylated HRP with streptavidin	SWV	$4{,}5 \times 10^{-2}$ ppb	8×10^{-2} - 11 ppb	(Kergaravat *et al.*, 2021)
2,4-D and 2,4,5-T	HRP	covalent immobilization then cross-linking	amperometry	2.6 ppb 2,4,5-T, 5 ppb 2,4-D	33 - 220 ppb	(Sok and Fragoso, 2021)
atrazine	HRP	glutaraldehyde cross-linking	amperometry	0.35 ppm	nd	(Kucherenko *et al.*, 2021)
glyphosate	HRP	entrapment in MWCNT-doped PSF membrane	amperometry	25 ppb	0.1 - 10 ppm	(Zambrano-Intriago *et al.*, 2023)
atrazine and diuron	tyrosinase	entrapment in a polythiophene film	amperometry	1 ppm atrazine, 0.5 ppm diuron	5 - 40 ppm atrazine	(Védrine *et al.*, 2003)
atrazine	tyrosinase	entrapment in polypyrrole	electrochemical (LSV)	(incorrect value)	0.05 - 0.5 ppm	(El Kaoutit *et al.*, 2004)
atrazine and diuron	tyrosinase	cross-linking with BSA and glutaraldehyde vapour	conductometry	1 ppb	2.3 ppb - 2.33 ppm diuron, 2.15 ppb - 2.15 ppm atrazine	(Anh *et al.*, 2004)
atrazine	tyrosinase	adsorption on κ-carrageenan	amperometry (oxygen consumption)	0.1 ppm	4.3×10^{-1} - 43 ppm	(Campanella *et al.*, 2005)
alachlor	tyrosinase	cross-linking with BSA and glutaraldehyde	conductance	41 ppb	nd	(Wang *et al.*, 2006)
2,4-D, atrazine	mushroom tyrosinase	covalent immobilization	amperometry	0.35×10^{-3} ppb atrazine, 0.55×10^{-3} ppb 2,4-D	0.1×10^{-2} - 0.5 ppb 2,4-D or atrazine	(Kim *et al.*, 2008)
atrazine	tyrosinase	glutaraldehyde cross-linking then entrapment	amperometry	32 ppb	0.17 - 2.2 ppm	(Vidal *et al.*, 2008)

atrazine	tyrosinase	adsorption before glutaraldehyde cross-linking	amperometry	0.1 x 10^{-3} ppb	0.2 x 10^{-3} - 2 ppb	(Yu *et al.*, 2010)
chlortoluron	tyrosinase	glutaraldehyde cross-linking	electrochemical (*o*-quinone reduction)	0.1 ppb	0.2 - 21 ppb	(Haddaoui and Raouafi, 2015)
atrazine	tyrosinase	entrapment in poly(L-DOPA) and Nafion	amperometry	10 ppb	50 ppb - 30 ppm	(Guan *et al.*, 2016)
atrazine	tyrosinase	entrapment in PVA-SbQ	amperometry	0.3 ppm	0.5 - 20 ppm	(Tortolini *et al.*, 2016)
glyphosate	tyrosinase	covalent immobilization	amperometry	1.1 ppb	2.5 - 1.7 x 10^{3} ppb	(Sok and Fragoso, 2019)
atrazine	tyrosinase	adsorption before Nafion coating	ECL	8 x 10^{-5} ppb	1 x 10^{-4} - 1 x 10^{-2} ppb	(Wu *et al.*, 2019)
atrazine	urease	glutaraldehyde cross-linking	ENFEC	28 ppb	28 - 2.8 x 10^{6} ppb	(Braham *et al.*, 2013)
atrazine	urease	glutaraldehyde cross-linking	graphene-based FET	5 x 10^{-5} ppb	2 x 10^{-4} - 20 ppb	(Cao *et al.*, 2016)
glyphosate	urease	entrapment in agarose-guar gum matrix	potentiometry	0.5 ppm	0.5 - 50 ppm	(Vaghela *et al.*, 2018)
2,4-D	ALP GOx	polyazetidine prepolymer (PAP)	amperometry	10 ppb	15 - 4.2 x 10^{3} ppb	(Botrè *et al.*, 2000)
glyphosate	AChE ChOx	adsorption on graphene oxide NPs	ECL	8.5 x 10^{-2} ppb	0.17 - 169 ppb	(Liu *et al.*, 2020)
2,4-D, atrazine	ALP tyrosinase	adsorption on carbon paper working electrode	amperometry	50 ppb 2,4-D, 2 ppb atrazine	100 - 600 ppb 2,4-D, 10 - 100 ppb atrazine	(Arduini *et al.*, 2019)
2,4-D, glyphosate	ALP HRP	adsorption on carbon paper working electrode	amperometry	50 ppb 2,4-D, 10 ppb glyphosate	100 - 600 ppb 2,4-D, 50 - 150 ppb glyphosate	(Caratelli *et al.*, 2022)

glyphosate	HRP	adsorption on carbon paper working electrode	amperometry	75 ppb	100 - 700 ppb	(Moro *et al.*, 2023)
Biosensors based on specific interactions						
atrazine	tyrosinase (banana extract)	covalent immobilization on cantilever tip	AFS	7.75 ppb	nd	(Martinazzo *et al.*, 2018)
glyphosate	peroxidase (zucchini extract)	covalent immobilization on cantilever tip	AFS	28 ppb	nd	(Muenchen *et al.*, 2018)
Biosensors based on signal-on systems (herbicide used as an enzymatic substrate						
glyphosate	GlyOx	glutaraldehyde cross-linking	amperometry	0.5 ppm	1.7 - 44 ppm	(Johnson *et al.*, 2022)
atrazine	GST	glutaraldehyde cross-linking	colorimetry	0.18 ppm	0.4 - 21 ppm	(Andreou and Clonis, 2002)
2,4-D	laccase from *Trametes versicolor*	entrapment in gelatin then glutaraldehyde cross-linking	amperometry	nd	1.1 - 4.4 ppb	(Sezgintrk *et al.*, 2010)

(AChE: acetylcholinesterase ; ACP: acid phosphatase ; AFS: atomic force spectroscopy ; ALP: alkaline phosphatase ; BSA: bovine serum albumin ; ChOx: choline oxidase ; CV: cyclic voltammetry ; ECL: electrochemiluminescence ; ENFEC: Enzyme Field Effect Capacitive ; FET: field effect transistor ; GlyOx: glycine oxidase ; GOx: glucose oxidase ; GST: glutathione-S-transferase ; L-DOPA: 3,4-dihydroxy-L-phenylalanine ; LSV: linear sweep voltammetry ; PVA-SbQ: polyvinyl alcohol-styrylpyridinium ; SWV: square wave voltammetry ; nd: not determined*)*

Table 3 and Figure 5 summarize enzymatic biosensors developed for herbicide detection. It can be observed that atrazine detection is mainly achieved using tyrosinase inhibition, whereas glyphosate and 2,4-D detection rely on peroxidase and alkaline phosphatase (ALP) inhibition, respectively. Only a few studies describe the detection of other herbicides, such as alachlor, diuron or chlortoluron. Electrochemical detection is obviously noticeably favored. Given the abundance of literature on inhibition-based biosensors, three primary enzymes are used to detect three key herbicides (representing more than 60 % of the detected herbicides) (Figure 2). The three target herbicides are among the most frequently detected, except for diuron (Figure 5) known as a photosynthetic herbicide, thus mainly detected using photosynthetic cells (cf. § 3.) or subcellular elements (cf. § 4.). The majority of inhibition-based biosensors for herbicide detection are mono-enzymatic. Only one enzyme is immobilized, thus giving a simple system unlike other more complex traditional biosensors for pesticide detection

coupling acetylcholinesterase (AChE) and choline oxidase (ChOx) for instance. The response time is also shorter.

Depending on the enzyme and on the inhibitor nature, different types of inhibition can occur, classified as reversible (competitive, noncompetitive, uncompetitive or mixed) or irreversible. For instance, organophosphorous pesticides are irreversible inhibitors of AChE. In this case, a reactivation step can be envisioned after inhibition to recover enzyme activity. On another hand, alkaline phosphatase (ALP) inhibition by 2,4-D is known to be reversible (non-competitive). In this case, the biosensor can be reused after a suitable washing step that removes non-covalent interactions between the enzyme and the inhibitor.

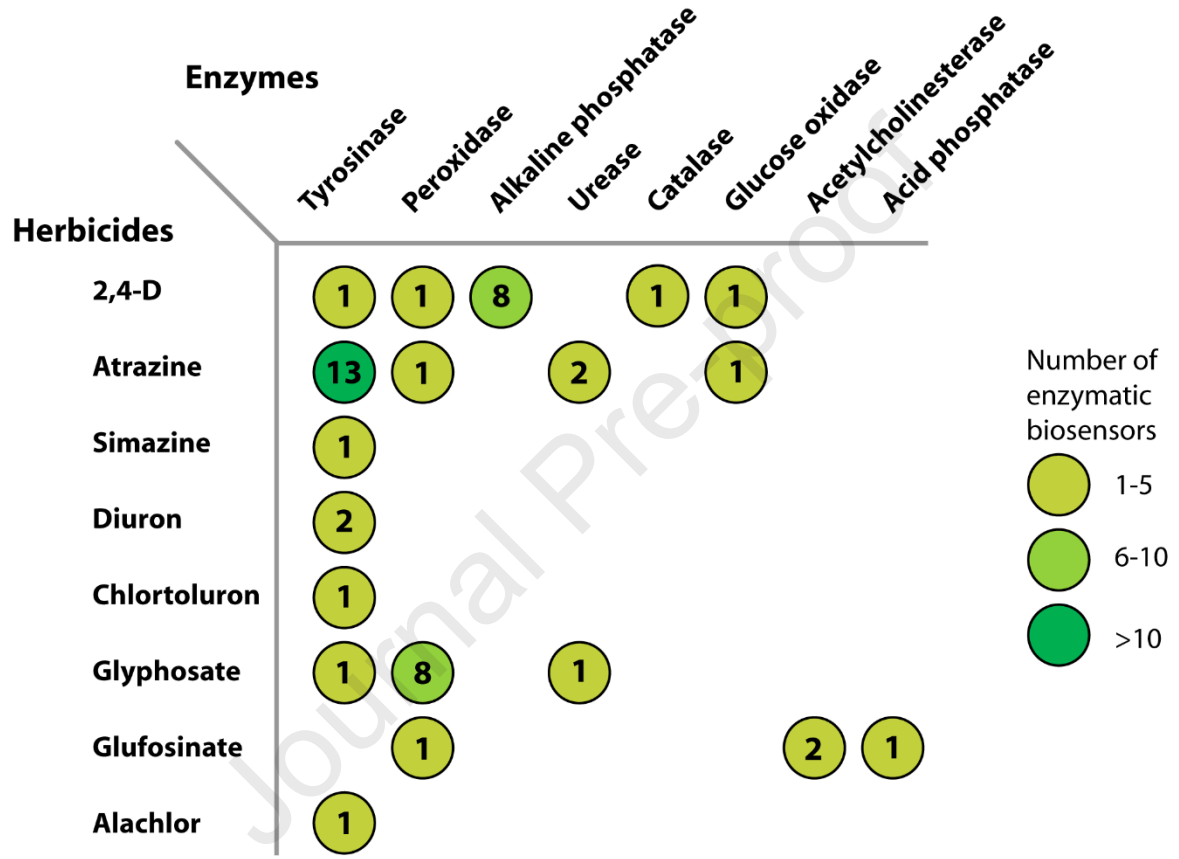

Figure 5. Main enzymes and the corresponding detected herbicide(s) in enzyme-based biosensors based on inhibition of enzyme activity. The number of identified biosensors is shown in bold.

2.1. Tyrosinase

Tyrosinase, also referred to as polyphenol oxidase (PPO) (E.C. 1.14.18. 1) is a Cu-containing oxidoreductase displaying a bifunctional activity towards phenolic substrates. In the presence of molecular oxygen, the enzyme catalyzes ortho-hydroxylation of monophenols to *o*-diphenols (monophenolase or cresolase activity) and oxidation of *o*-diphenols to *o*-quinones (diphenolase or catecholase activity) (Figure 6).

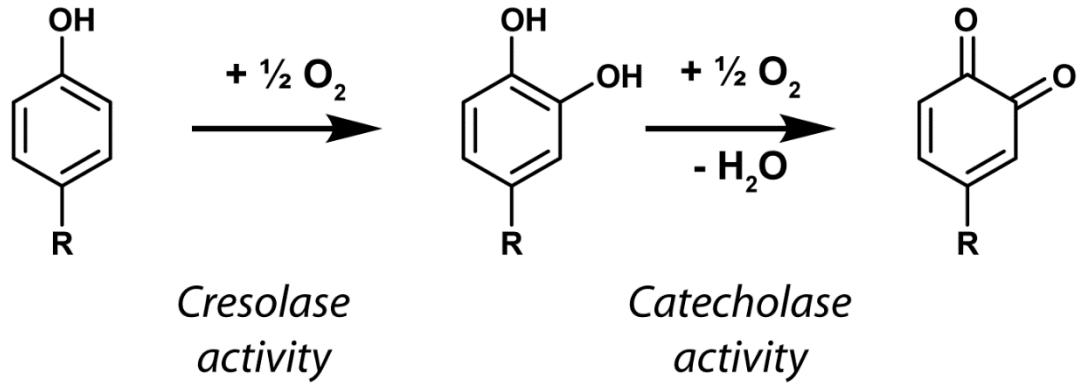

305

306 **Figure 6.** Two-step phenol oxidation into *o*-quinone catalyzed by tyrosinase.
307
308 Many biosensors based on inhibition of tyrosinase activity have been reported. Enzyme
309 activity is affected by many inhibitors such as triazine and phenylurea herbicides, but also by
310 carbamate and organophosphate insecticides (e.g., dichlorvos) as well as other pollutants
311 including photosynthetic inhibiting herbicides. Tyrosinase-based biosensors are not specific
312 to individual pesticides and are presented as warning devices. As described below, detection
313 mainly relies on monitoring quinone products by electrochemical reduction at a low potential,
314 using diphenol substrates such as catechol or dopamine (Table 3). A 30 min incubation time
315 (from 15 to 60 min) of the enzymatic biosensor with the herbicide solution is classically
316 reported before determination of percentage of inhibition and correlation to herbicide
317 concentration.
318
319 McArdle and Persaud (1993) reported the first example of an enzyme electrode for the
320 detection of atrazine based on tyrosinase (competitive) inhibition (McArdle and Persaud,
321 1993). The amperometric biosensor was based on the immobilization of tyrosinase by cross-
322 linking it with glutaraldehyde on a preformed polypyrrole film on a gold working electrode.
323 Using catechol violet as the substrate, a concentration of 5 µM (*ca.* 1 ppm) of atrazine could
324 be measured at – 0.2 V *vs*. Ag|AgCl. The biosensor was supposed to respond to other
325 herbicides inhibiting photosynthesis.

326 Besombes *et al.* (1995) described an amperometric warning device based on tyrosinase
327 entrapment in an electropolymer deposited at the surface of a glassy carbon electrode (GCE)
328 (Besombes *et al.*, 1995). Using dopamine as the substrate, the detection limit for atrazine was
329 4 µM (0.8 ppm). In addition to atrazine, the biosensor could also detect other pollutants
330 inhibiting tyrosinase activity, such as cyanide, chlorophenols and carbamate pesticides.

331 Tyrosinase (PPO) was also entrapped in electropolymerized polyethylenedioxythiophene
332 (PEDT) to design a PEDT/PPO amperometric biosensor (Védrine *et al.*, 2003). Dopamine was
333 used as a diphenolic substrate for the detection of atrazine and diuron with a modified
334 electropolymerization method to reduce polymer film thickness and minimize diffusion
335 constraints. The reduction of *o*-quinone resulting from dopamine was measured at the surface
336 of a GCE at - 0.2 V *vs*. saturated calomel electrode (SCE). Inhibition of tyrosinase in the
337 presence of atrazine (5-40 ppm, linear range) and diuron (1-30 ppm, nonlinear plot) was
338 obtained with a LOD of 1 and 0.5 ppm, respectively.

A sensitive and simple amperometric biosensor for atrazine detection was reported, after entrapment of PPO in an electropolymerized polypyrrole film on a GCE (El Kaoutit *et al.*, 2004).The enzyme electrode was used in open-circuit conditions, thus simplifying the experiments and leading to a long lifetime (90 % of the sensor response is maintained after 21 days). A second GCE was used as the working electrode. Atrazine was incubated with the enzyme electrode during 60 min prior to catechol (substrate) addition and 1,2-quinone (product) reduction was measured on the second GCE by linear sweep voltammetry (LSV). The percentage of inhibition was determined and correlated to atrazine concentration, with a linear range extending from 0.05 to 0.5 ppm of atrazine. The monitoring of atrazine in the case of highly contaminated samples seems possible.

A conductometric biosensor was developed for the detection of diuron, atrazine, desisopropylatrazine (DIA) and desethylatrazine (DEA), known as its main metabolites (Anh *et al.*, 2004). Tyrosinase was cross-linked on the electrode using glutaraldehyde. Determination of the inhibition rate after a 30-minute incubation of the biosensor with different herbicide concentrations was carried out. Before and after incubation, the tyrosinase activity was obtained in the presence of 4-chlorophenol (substrate). Low detection limits close to 1 ppb were obtained for atrazine or diuron. The linear range extended from 2.3 ppb to 2.33 ppm and from 2.15 ppb to 2.15 ppm for diuron and atrazine, respectively. As underlined by the authors, the detection limit was 100-1000 times lower than the one obtained using previously described amperometric tyrosinase biosensors.

Due to the poor water solubility of many herbicides, organic phase enzyme electrodes (OPEEs) operating in nonaqueous solvents have been proposed, especially for the detection of triazine and benzotriazine herbicides, based on competitive and reversible inhibition of tyrosinase activity (Campanella *et al.*, 2005)(Campanella *et al.*, 2006). Tyrosinase was adsorbed onto a κ-carrageenan hydrogel placed in contact with the gas permeable membrane of a Clark-type electrode. The amperometric biosensor was incubated for 15 minutes in water-saturated chloroform herbicide solution before adding phenol as substrate. The percentage of inhibition was then related to the logarithm of herbicide concentration. Linear range for atrazine, atrazine-desethyl and atraton was given as 2 µM - 200 µM and LOD as 0.5 µM (Campanella *et al.*, 2005). Propazine, simazine, terbuthylazine, azinphos-methyl and azinphos-ethyl led to a similar linear range (2 µM - 10 mM) (Campanella *et al.*, 2006). A total measurement time of 20 minutes was indicated. Detection of triazine-treated vegetal samples was also reported, with recoveries of 75-95%.

Wang *et al.* (2006) presented a conductimetric biosensor for the detection of several pesticides, including the herbicide alachlor (Wang *et al.*, 2006). Diazinon, alachlor and carbaryl were shown to inhibit mushroom tyrosinase activity. The enzyme was cross-linked in the presence of BSA and glutaraldehyde on a gold interdigitated electrode, whereas BSA was immobilized alone on a second electrode serving as the reference (blank). Conductivity variation was measured in the presence of catechol. The differential signal was determined as the difference of signal between the BSA-electrode and the BSA/tyrosinase-electrode. An incubation time of 30 minutes with each pesticide was selected. The limit of detection for alachlor was reported to be 0.15 µM. After a 4 week-storage period, the biosensor still presented over 90% activity. An early warning device is thus presented to indicate the presence of tyrosinase inhibitors. In the study, the authors did not differentiate herbicides (alachlor) from organophosphorous and carbamate insecticides (diazinon, carbaryl).

In 2008, Kim *et al.* proposed an amperometric biosensor based on mushroom tyrosinase inhibition by two herbicides (atrazine and 2,4-D), as well as a fungicide (ziram) (Kim *et al.*, 2008). Gold nanoparticles (AuNP) were deposited by a double-pulse technique on a pretreated GCE. Tyrosinase was then immobilized by the formation of a self-assembled monolayer (SAM) using 3-mercaptopropionic acid (MPA). Cyclic voltammetry (CV) measurements were conducted using catechol as a substrate before and after addition of herbicides, and inhibition of the enzyme activity was estimated by analysis of cathodic peak intensity in a continuous flow system. A linear range extending from 1 to 500 $ng.L^{-1}$ was observed for both herbicides, with detection limits of 0.35 $ng.L^{-1}$ and 0.55 $ng.L^{-1}$ for atrazine and 2,4-D, respectively. Although the flow system was not described in the publication, the biosensor displayed a good stability with minimal response loss after 10 assays, as well as only 20 % loss after 20 days of storage at 4°C.

Organophosphorous (dichlorvos) and triazine (atrazine) herbicides were also detected using amperometric biosensors based on tyrosinase inhibition (Vidal *et al.*, 2008). The enzyme activity could be modulated by electrochemically generating reduced forms of a co-immobilized charge-transfer quinonic mediator (1,2-naphtoquinone, NQ). Cross-linking with glutaraldehyde was performed before electropolymerization with *o*-phenylenediamine to form an outer protective layer. By chronocoulometry at – 600 mV *vs*. Ag|AgCl, the reagentless biosensor could detect atrazine with a linear range extending from 0.8 to 10 µM and a detection limit of 0.15 µM. Good recovery was obtained in spiked (*ca.* 90 ppb atrazine) river water samples.

Tyrosinase was also immobilized on the surface of nanomaterials (vertical growth TiO_2 nanotubes) to design a high performance amperometric biosensor for atrazine detection (Yu *et al.*, 2010) (Figure 7A). High sensitivity and stability were obtained in the presence of biocompatible nanotubes presenting highly ordered vertically aligned structures with a large surface area for enzyme adsorption before glutaraldehyde cross-linking. In the presence of *p*-cresol as the substrate, 4-methylcatechol was enzymatically produced and was oxidized in the presence of oxygen into 2-methyl,1,2-benzoquinone. Working at – 500 mV *vs*. SCE, the quinone was reduced to electro-regenerate 4-methylcatechol, resulting in amplification of the signal. The percentage of inhibition measured in the presence of atrazine could be correlated to its concentration. Detection limit as low as 0.1 ppt was achieved and a wide linear range was observed, from 0.2 ppt to 2 ppb atrazine. The system was applied for atrazine determination in soil samples. Obviously, it may also be affected by other tyrosinase inhibitors such as carbamate or organophosphorous pesticides.

Chlortoluron, a phenylurea herbicide, could be detected based on reversible tyrosinase activity inhibition (Haddaoui and Raouafi, 2015). A sensitive and disposable electrochemical enzymatic biosensor was described using a screen-printed carbon electrode (SPCE) modified with ZnO nanoparticles (NPs). The enzyme was immobilized by adsorption on ZnO NPs and cross-linking with glutaraldehyde. Tyrosinase oxidation of phenol to *o*-quinone (reduction measured at – 0.2 V *vs*. Ag|AgCl) was inhibited in the presence of the herbicide. Using a 30-minute incubation time, the linear range extended from 1 to 100 nM, with a limit of detection of 0.47 nM (*ca.* 0.1 ppb) of chlortoluron. The biosensor was used for herbicide detection in real water samples, with 93 – 115.8 % recovery. Measurements were also possible in the presence of aniline, pyrogallol or ascorbic acid. The biosensor could potentially be used for analysis of other phenylurea herbicides.

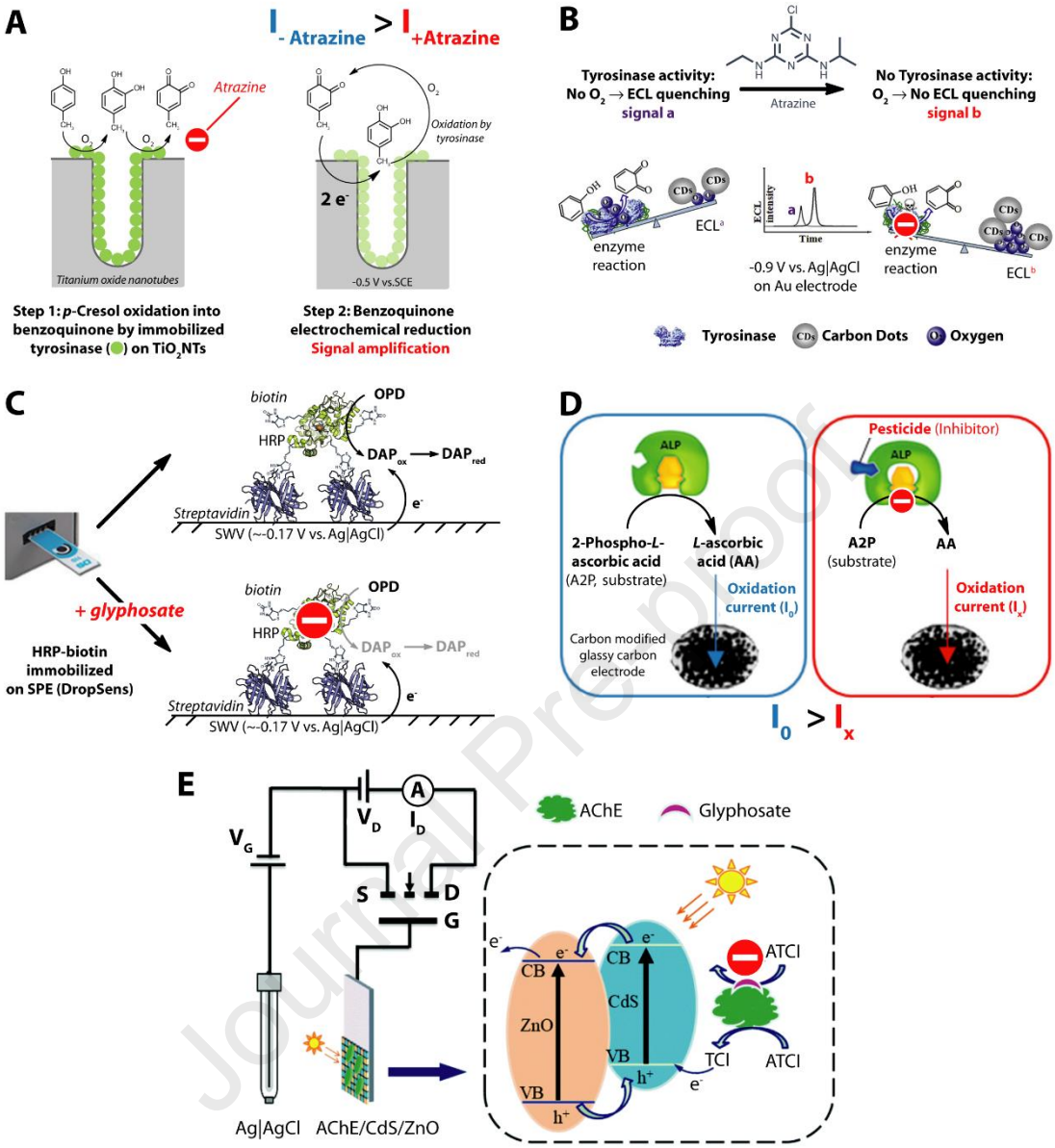

Figure 7. Examples of enzymatic biosensors showing a low limit of detection for herbicides, based on tyrosinase (**A**, modified from Yu *et al.*, 2010 ; **B**, modified from Wu *et al.*, 2019), HRP (**C**, modified from Kergaravat *et al.*, 2021), ALP (**D**, modified from Gianvittorio *et al.*, 2023) or AChE (**E**, modified from Yu *et al.*, 2021). (ATCI: acetylthiocholine iodide ; TCI: thiocholine iodide).

Guan *et al.* (2016) proposed an electrochemical biosensor based on tyrosinase inhibition by atrazine (Guan *et al.*, 2016). The enzyme was entrapped *in situ* during polymerization of 3,4-dihydroxy-L-phenylalanine (*L*-DOPA) (catalyzed by tyrosinase) on a gold electrode, and then covered with Nafion. The biosensor was used for phenol (substrate) and for atrazine (inhibitor) detection. In the presence of phenol and after a 15-minute incubation period with the herbicide, the percentage of inhibition was calculated and correlated to atrazine concentration. A linear range was observed between 50 ppb and 3 ppm and the limit of detection was given as 10 ppb. Atrazine detection was also assayed with success on spiked river water, lake water and

443 farmland water (filtered and 10 times diluted). However, this biosensor is not specific to
444 atrazine. It is also sensitive to the presence of phenol or phenolic compounds in contaminated
445 waters.

446 A tyrosinase inhibition-based biosensor was also reported by Tortolini *et al.* in 2016 for
447 atrazine detection (Tortolini *et al.*, 2016). Tyrosinase was immobilized on commercial SPCEs
448 (DropSens) modified with multi-walled carbon nanotubes (MWCNTs). The immobilization
449 method was based on UV polymerization of polyvinyl alcohol with styrylpyridinium groups
450 (PVA-SbQ). The biosensor was used for the detection of atrazine, using catechol as substrate.
451 It showed a LOD of 0.3 ppm and a linear range between 0.5 and 20 ppm. A good accuracy
452 was reported for the quantification of atrazine in supplemented lake water samples. The device
453 could be used as a complement to traditional analytical methods for atrazine detection, or as
454 a warning tool for pre-selecting contaminated samples for further analysis. However, a more
455 precise evaluation of its stability and the impact of interfering compounds is necessary.

456 In 2019, Sok and Fragoso used inhibition of tyrosinase for glyphosate detection (Sok and
457 Fragoso, 2019). The enzyme was conjugated to carbon nano-onions and covalently linked to
458 chitosan on a commercial SPCE (DropSens). *L*-DOPA was added as the substrate, thus
459 allowing amperometric detection at - 0.2 V *vs.* Ag|AgCl. Glyphosate detection could be
460 performed by reporting the percentage of inhibition *versus* glyphosate concentration, with a
461 linear range extending from 15 nM to 10 µM, and a limit of detection of 6.5 nM (1.1 ppb). The
462 biosensor underwent testing using real samples and the results showed a good correlation
463 with those obtained from a commercial ELISA. The biosensor was demonstrated to be stable
464 (82% signal intensity after 4 months at 4°C) and reusable (10% of intensity decrease after 33
465 measurements). However, no specificity studies were conducted.

466 An ultrasensitive optical biosensor involving nanomaterials was described by Wu *et al.* (Wu *et*
467 *al.*, 2019) (Figure 7B). Mesoporous biocarbon dispersions were dropped at the surface of a
468 gold electrode and further coated with tyrosinase and Nafion. The resulting electrode placed
469 in a suspension of dispersed sulfur and nitrogen co-doped carbon dots (S,N-CDs) exhibited
470 luminescence upon electrochemical reduction (below - 0.9 V vs. Ag|AgCl). The
471 electrochemiluminescence (ECL) reaction was expected to be dependent on oxygen
472 concentration. In the presence of phenol as the tyrosinase substrate, the ECL signal was
473 extinguished due to the consumption of dissolved oxygen by the enzyme. By placing the
474 electrode into an atrazine solution for 20 minutes prior to measurement, tyrosinase was
475 inhibited and the ECL signal was further recovered. This two-step system exhibited an ECL
476 signal related to the concentration of atrazine (logarithm) from 10^{-4} to 10^{-2} ppb, with a LOD of
477 8×10^{-5} ppb. No interferences were identified with 50 ppb profenofos (an organophosphorous
478 insecticide), bromoxynil (an inhibitor of PSII), malathion (a cholinesterase inhibitor), and
479 pentachlorophenol (a fungicide), which were never described as tyrosinase inhibitors. The
480 signal recovery was 94-106 % using tap, river or lake waters.
481

482 2.2. Peroxidases

483 Horseradish peroxidase (HRP) (EC 1.11.1.7) is a member of the large class of heme
484 peroxidases catalyzing the oxidation of substrates by H_2O_2. The enzyme contains iron (III)
485 protoporphyrin IX (ferriprotoporphyrin IX) as the prosthetic group. The iron is capable of

undergoing oxidation and reduction. HRP is the most commonly used enzyme, particularly because of its stability over a broad range of pH and temperature. Considering biosensors based on inhibition of HRP activity, glyphosate is the main herbicide that has been detected (Table 3, Figure 5). Experiments are performed in the presence of H_2O_2 and, eventually, a redox mediator such as hydroquinone (HQ) (Figure 8). As described hereafter, reduction currents are measured at a low operating potential, thus minimizing the risk of surface fouling and interference from electroactive species.

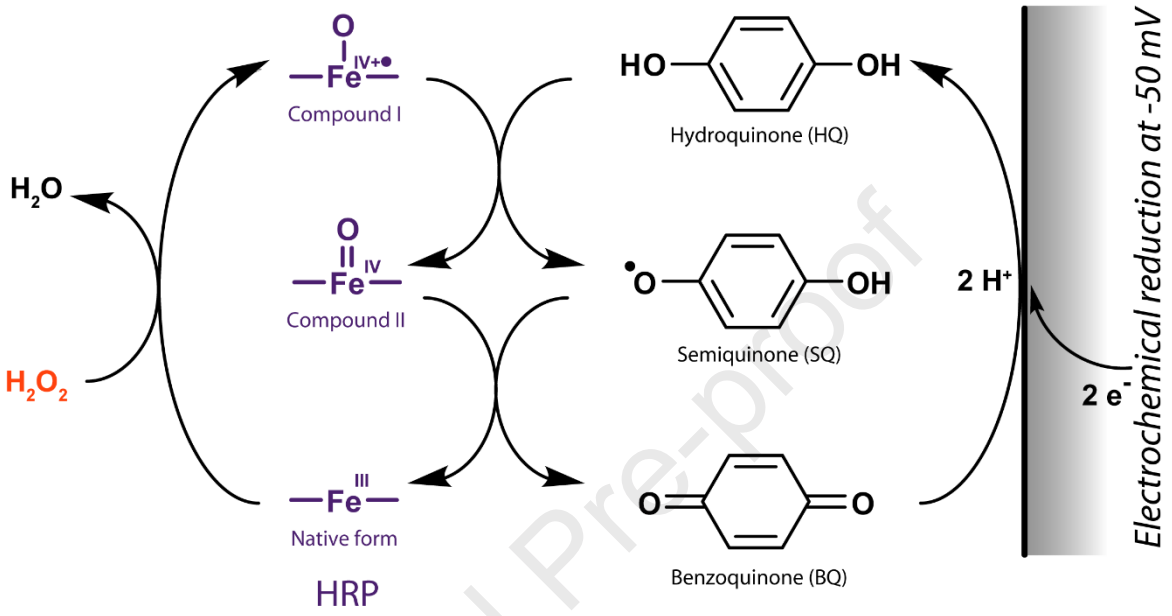

Figure 8. Peroxidase-catalyzed hydroquinone oxidation reaction showing the formation of HRP compounds I and II, as well as the intermediate semiquinone. Here, hydroquinone is regenerated from benzoquinone by electrochemical reduction (adapted from (Zambrano-Intriago *et al.*, 2023)).

Songa *et al.* (Songa *et al.*, 2009a) immobilized HRP on a gold electrode modified by electrodeposition of poly(2,5-dimethoxyaniline) doped with poly(4-styrenesulfonic acid) (PSS). In the presence of H_2O_2, the intensity of the reduction peaks (measured by CV) decreased with glyphosate due to enzyme inhibition. Glyphosate quantification was possible between 0.25 and 14 ppb. The specificity of the electrochemical biosensor and its activity on environmental samples were not assayed. The same authors also proposed the application of the biosensor for the detection of glyphosate and glufosinate in corn samples (Songa *et al.*, 2009b). A gold rotating disk electrode was used to increase sensitivity. Amperometric measurements at an applied potential of - 0.1 V *vs*. Ag|AgCl were carried out in the presence of H_2O_2. The current intensity decrease following the addition of glyphosate or glufosinate was found to be linearly related to herbicide concentrations in a range extending from 2 to 78 ppb for glyphosate and from 2 to 10 ppb for glufosinate. The matrix effect of complex samples was assessed in herbicide-spiked corn samples. Unspiked corn samples showed no inhibitory effect on HRP activity, but no systematic interference studies with exogenous compounds were carried out.

In order to detect glyphosate, Oliveira *et al.* used *atemoya* peroxidase adsorbed on modified nanoclay (Oliveira *et al.*, 2012). Carbon paste electrodes (CPEs) were then obtained by mixing

the enzyme preparation with graphite powder, MWCNTs and mineral oil. Measurements were performed in the presence of HQ and H_2O_2. The *p*-benzoquinone (BQ) reduction current was measured by square wave voltammetry (SWV). The percentage of inhibition of the peroxidase activity by glyphosate was determined after incubation of the enzyme for 2 minutes in the presence of the herbicide. It was linearly related to glyphosate concentrations (semi-logarithmic plot) between 0.1 ppm and 4.55 ppm (LOD of 30 ppb). No studies on matrix effect and specificity were conducted.

Inhibition of HRP was also used by Cahuantzi-Muñoz *et al.* to develop an amperometric biosensor for glyphosate detection, applied to maize kernels (Cahuantzi-Muñoz *et al.*, 2019). A graphite-epoxy electrode modified with MWCNTs was used as the working electrode. HRP was then immobilized on the modified electrodes by adsorption. The intensity of H_2O_2 reduction peak was measured by CV at - 0.3 V *vs*. SCE, after 5 min incubation with glyphosate before H_2O_2 addition. A wide linear range was reported for glyphosate, extending from 1.7 x 10^{-2} ppb to 1.9 ppm (semi-logarithmic plot). Detection was performed at pH 4 where herbicide-enzyme interaction is thought to be optimized. No interference from chlorpyrifos (insecticide) and starch (major component of maize) was found. Spiked corn samples were analyzed using glyphosate concentrations between 0.1 nM and 11 µM with success (recovery of 100%).

Another electrochemical biosensor for glyphosate detection based on inhibition of HRP activity was reported (Roman *et al.*, 2020). The target enzyme was immobilized by electrodeposition on a polyaniline film that was firstly electropolymerized on silicon. Amperometric measurements were performed in the presence of H_2O_2, HQ and a given glyphosate concentration, during a 20 min incubation time. Current densities were correlated with the logarithm of glyphosate concentration. The linear range extended from 16.9 ppb to 16.9 ppm and the LOD was reported as 5.44 ppb. The authors pointed out the potential of integrating their system into silicon electronic devices.

Kergaravat *et al.* reported another HRP-inhibition based electrochemical biosensor (Kergaravat *et al.*, 2021) (Figure 7C). Streptavidin was first covalently immobilized on a commercial SPCE, then HRP-biotin conjugates were added and thus immobilized thanks to streptavidin-biotin interactions. *O*-phenylenediamine (OPD) and hydrogen peroxide were used as substrates of HRP which catalyzes the dimerisation of OPD into 2,3-diaminophenazine (DAP). DAP reduction was thus measured. Inhibition of HRP resulted in decreased SWV current. The inhibition percentage was calculated and correlated with glyphosate concentrations (logarithm). A LOD of 45 $ng.L^{-1}$ and a linear range from 0.08 to 11 ppb were reported. A more sensitive bioassay (LOD of 0.085 $ng.L^{-1}$) was also reported using soluble (instead of immobilized) HRP, but it was slower, less simple and less adapted to *in field* measurements, compared to the biosensor. No interference with carbaryl, chlorpyrifos, calcium, nitrate or sulfate was found and the biosensor was validated using groundwater samples with recoveries between 79 % and 98 %. It can be underlined that the biosensor exhibited good performance without using nanomaterials.

In 2021, Kucherenko *et al.* described an amperometric biosensor based on laser-induced graphene (LIG) electrodes for atrazine monitoring by HRP inhibition (Kucherenko *et al.*, 2021). HRP was immobilized onto the LIG working electrode by glutaraldehyde cross-linking. Amperometric measurements of H_2O_2 reduction peak were performed after addition of atrazine and allowed to determine a LOD of 1.6 µM. Other common herbicides (glyphosate,

dicamba and 2,4-D) were also assayed and showed negligible interferences on atrazine sensing. It seems surprising that glyphosate did not induce measurable HRP inhibition. The presented LIG electrode platform could be a versatile base for future detection applications.

An amperometric biosensor based on covalent peroxidase immobilization on carbon nano-onions followed by cross-linking to a cyclodextrin polymer matrix on a SPCE was recently reported (Sok and Fragoso, 2021). Two phenoxy-based herbicides acting as peroxidase inhibitors, 2,4-D and 2,4,5-T, could be detected. The presence of highly conductive and biocompatible carbon nanomaterials was shown to improve sensitivity and stability of the biosensor. Amperometric detection was performed at 0 V *vs*. Ag|AgCl for reducing 3,3',5,5'-tetramethylbenzidine (TMB) that was added with H_2O_2 in the solution. The inhibition percentage increased linearly with herbicide concentrations from 0.15 to 1 µM. Detection limits were given as 10 nM (2.6 ppb) for 2,4,5-T and 23 nM (5.1 ppb) for 2,4-D. Analysis in real samples was reported, in a soil treated with 2,4-D and in a river water spiked with 2,4,5-T.

An innovative enzymatic biosensor for the electrochemical detection of glyphosate based on HRP inhibition was also recently developed (Zambrano-Intriago *et al.*, 2023). The system consisted in a PGE with HRP immobilized by entrapment (phase inversion procedure) in a MWCNT-doped polysulfone (PSF) membrane. Amperometric measurements were performed using H_2O_2 and HQ as substrate and redox mediator, respectively. A detection limit of 0.15 µM glyphosate was determined, with a linear range extending from 0.6 µM to 60 µM. The simplicity and low-cost nature of the biosensor was pointed out by the authors who also conducted an interference study by several pesticides (dimethoate, methomyl, mesosulfuron-methyl) revealing a good selectivity, with signal recoveries varying from 95.2 % to 103.5 %.

2.3. Alkaline phosphatase

Alkaline phosphatase (ALP, EC 3.1.3.1) is a metalloenzyme containing Mg^{2+} and Zn^{2+} ions in its active center and catalyzing the dephosphorylation of substrates. The enzyme is also characterized by a broad substrate range and is sensitive to a wide variety of inhibitors, such as pesticides and heavy metals. Alkaline phosphatase has been used in several biosensors devoted to 2,4-D detection based on its reversible non-competitive inhibition (Gianvittorio *et al.*, 2023). In reported biosensors, the enzyme catalyzes the hydrolysis of the phosphoester linkage within substrates such as 3-indoxyl phosphate, glucose-6-phosphate or ascorbic acid-2-phosphate (A2P) (Table **3**). The most recent reports are based on A2P as the ALP substrate, thus producing ascorbic acid that can be detected by electrochemical oxidation, as shown hereafter:

$$\text{Ascorbic acid-2-phosphate} \xrightarrow{ALP} \text{Ascorbic acid} + HPO_4^{2-}$$

$$\text{Ascorbic acid} \xrightarrow{Oxidation} \text{Dihydroascorbic acid} + 2\,H^+ + 2e^-$$

In 2000, Botrè *et al.* used a bi-enzymatic inhibition biosensor based on the combined catalytic activity of alkaline phosphatase (ALP) and glucose oxidase (GOx) for the detection of 2,4-D (Botrè *et al.*, 2000). Glucose-6-phosphate (G6P) was used as an ALP substrate to generate glucose, further oxidized by glucose oxidase to form H_2O_2, itself detected by amperometry on a platinum electrode poised at +0.65 V *vs*. Ag|AgCl. ALP and GOx were immobilized on

cellulose acetate and nylon membranes, respectively, using polyazetidine prepolymer (PAP). The membranes were then placed on the platinum electrode. 2,4-D was detected by measuring the current decrease in the presence of 0.5 mM G6P. A 45 nM detection limit and a linear range from 68 nM to 19 µM were obtained. Measurements with environmental samples were not reported.

The same authors later reported an amperometric monoenzymatic biosensor based on inhibition of ALP activity for the detection of 2,4-D and malathion (an organophosphorous insecticide) (Mazzei *et al.*, 2004). In the presence of 3-indoxyl phosphate, hydrogen peroxide is enzymatically produced and can be detected as previously described. Linear range extended from 1.5 to 60 ppb and LOD was given as 0.5 ppb. The authors mentioned that the biosensor is a promising tool for rapid detection of 2,4-D and malathion, but also related environmental pollutants acting as ALP inhibitors.

Also based on ALP inhibition, Shyuan *et al.* reported an amperometric biosensor for the detection of several toxicants: 2,4-D and 2,4,5-T herbicides (Shyuan *et al.*, 2008), carbofuran and endosulfan insecticides, and heavy metals. The chlorophenoxyacetic acid herbicides showed the highest inhibition degree of ALP that was entrapped in a silica / chitosan film deposited on SPCE. The percentage of inhibition was related to herbicide concentration, with a 15-min incubation time, using A2P as the substrate and detecting ascorbic acid oxidation. The linear range was 1 - 60 ppb and LOD was 0.5 and 0.8 ppb for 2,4-D and 2,4,5-T, respectively. The authors underlined the higher specificity of electrochemical immunosensors compared to the present one but also mentioned their complexity of fabrication and the low sensitivity and high LOD (40 and 50 ppb). The enzymatic biosensor could be used as a disposable screening device for water toxicity.

Loh *et al.* (2008) reported a disposable electrochemical biosensor based on ALP and biocompatible Fe_3O_4 NPs that improved the sensitivity towards 2,4-D (Loh *et al.*, 2008). Immobilization was performed by entrapment in a sol-gel silica / chitosan matrix on a SPCE. In the presence of A2P, 2,4-D could be detected after a 15 min incubation time, thus giving a linear range extending from 0.5 to 30 ppb and a detection limit of 0.3 ppb. Heavy metals could also be detected, but at 1000 times higher concentrations. High recoveries were observed for 2,4-D spiked water samples from a rice field (complex matrix). A good correlation was obtained with HPLC after solid-phase extraction.

In 2016, Bollela *et al.* also proposed a biosensor based on ALP inhibition for the detection of 2,4-D (ascorbic acid electrochemical oxidation) (Bollella *et al.*, 2016). Better results were obtained when ALP was entrapped in PVA-SbQ rather than covalently immobilized on a MWCNT-modified SPE *via* N-(3-dimethylaminopropyl)-N′-ethylcarbodiimide (EDC) and N-hydroxysuccinimide (NHS). LOD was given as 1 ppb of 2,4-D, with a linear response observed between 2.1 and 110 ppb after 20 minutes incubation. Spiked lake water samples were also tested with satisfying results, but a small matrix effect was detected (> 90% recovery). However, no specificity assays were conducted. The biosensor was also considered reusable, with a 30% signal decrease after 12 measurements.

Enzymatic inhibition-based reusable biosensors using ALP immobilized on GCE modified with nanomaterials were recently reported (Gianvittorio *et al.*, 2023) (Figure 7D). The enzyme was cross-linked with BSA and glutaraldehyde on a mixture of MWCNTs and electrochemically

reduced graphene oxide (ERGO) whose synergic effect led to increased sensitivity and decreased potential. In the presence of A2P as a substrate and 2,4-D as a non-competitive inhibitor, ascorbic acid was detected by CV (ascorbic acid oxidation peak at +0.3 V vs. SCE). After a 10 min incubation time, the linear range extended from 0.04 to 24 nM of 2,4-D (semi-logarithmic plot). The biosensor could be reused, after a 30 min washing step in Triton X-100 (pH 8). Pesticides other than 2,4-D such as malathion or parathion could also be detected at nanomolar concentrations.

2.4. Urease

Urease (EC 3.5.1.5) is known as the first purified and crystallized enzyme. It is a nickel-containing metalloenzyme, catalyzing the following reaction:

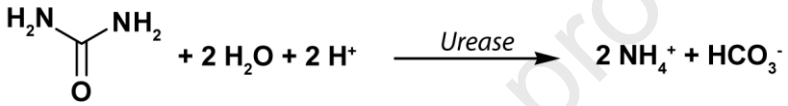

Different types of compounds are known to inhibit urease activity, such as heavy metal ions or several pesticides including herbicides. Electrochemical biosensors for herbicide detection based on the inhibition of urease that have been reported in the literature are either potentiometric (ion-selective membrane) or silicon-type (semiconductor-based) enzyme-modified field-effect biosensors such as enzyme-field-effect transistors (ENFETs) or enzyme-modified capacitive field-effect biosensors (ENFEC) (Table 3).

A capacitive field-effect biosensor based on urease inhibition was reported for atrazine detection (Braham *et al.*, 2013). Fe_3O_4 NPs combined with cationic and anionic polyelectrolytes were chosen as suitable materials for enzyme immobilization and glutaraldehyde was used as cross-linking agent. In the presence of urea, the ENFEC system was characterized by a detection limit of 0.13 µM (28 ppb) atrazine and a linear range extending from 10^{-2} to 10^{-7} M.

In 2016, Cao *et al.* described a biosensor consisting of a highly sensitive graphene-based liquid gated field effect transistor (GFET) for atrazine detection (Cao *et al.*, 2016). The GFET device consisted of 19 coupled interdigitated source and drain platinum electrodes on a silicium wafer, and a platinum wire top gate electrode. Urease was immobilized on the GFET sensor by glutaraldehyde vapor cross-linking and variations of the drain-source current as a function of the gate voltage were recorded to evaluate the inhibition of urease by atrazine. The differential current was found to be linearly related to atrazine concentrations ranging from 2.10^{-4} ppb to 20 ppb, with a limit of detection as low as 0,05 ppt. The authors claimed that the performance of the sensor was linked to the graphene-based ENFET configuration and enhanced by the chemical vapor deposition method used for thin graphene layer synthesis. The electron transfer properties of this kind of graphene still remain to be studied.

In their 2018 work, Vaghela *et al.* reported a potentiometric biosensor for glyphosate detection based on urease conjugation with AuNPs further entrapped in an agarose-guar gum matrix (Vaghela *et al.*, 2018). Ammonium ions were produced by urease in the presence of urea. The biosensor thus used a potentiometric detection with a commercial ammonium-selective electrode. The percentage of inhibition was correlated to the logarithm of glyphosate concentrations and revealed a linear relationship between 0.5 and 50 ppm, with a LOD of 0.5 ppm. A good selectivity was noticed by testing responses to dichlorvos, dimethoate, 2,4-D, hexaconazole and paraquat. Biosensors were also validated on glyphosate-spiked water samples. Surprisingly, no inhibition was observed in the presence of atrazine (unknown concentration) elsewhere described as an urease inhibitor.

2.5. Other enzymes

Acetolactate synthase (ALS, EC 4.6.3.8) is implicated in valine, leucine and isoleucine biosynthetic pathways in plants, bacteria, fungi and algae. Sulfonylurea and imidazolinone herbicides are known inhibitors of ALS (Table 1). In 1996, Seki *et al.* used the ALS II isoenzyme expressed in *E. coli* and immobilized in PVA-SbQ on an oxygen electrode (Seki *et al.*, 1996). Micromolar concentrations of imazaquin, sulfometuron methyl, thifensulfuron methyl and chlorsulfuron were shown to decrease the enzyme oxygen-consuming activity in the presence of pyruvate as the substrate, after a 30-min incubation period with the herbicides. Stability and sensitivity remained to be improved.

In 2010, glucose oxidase (EC 1.1.3.4) was adsorbed on aligned carbon nanotubes (CNTs) on a copper electrode to design an electrochemical biosensor for atrazine detection (Yang *et al.*, 2010). Measurements by SWV were performed after a 7-min incubation time. The current response (peak at *ca.* -0.5 V *vs*. SCE) decreased with increasing atrazine concentrations, due to inhibition of the enzyme activity. A linear range was observed between 5.8 x 10^{-7} M and 4.22 x 10^{-5} M of atrazine, with a detection limit of 3.9 x 10^{-8} M (8.4 ppb). Other glucose oxidase inhibitors such as Pb^{2+} and Cu^{2+} heavy metal ions were shown to interfere in the detection of the herbicides. Good recovery was obtained in filtered wastewater samples spiked with micromolar atrazine concentrations.

Catalase (EC 1.11.1.6) is inhibited by 2,4 D in wheat and other plants. To design a biosensor for 2,4-D detection, Liu *et al.* (Liu *et al.*, 2016) immobilized the enzyme in hierarchical porous calcium phosphate microspheres further entrapped in chitosan at the surface of a GCE. Amperometric measurements in a flow injection system were obtained with an applied potential of -0.35 V *vs*. Ag|AgCl for the reduction of H_2O_2. 2,4-D was found to be competitive to H_2O_2. Percentage of inhibition led to two linear regions: 30-300 nM and 300-3000 nM. The LOD was found to be 15 nM (3.3 ppb). No interferences were found with several molecules or ions present in environmental samples such as glucose, citric acid, prometryn, cycloxydim, sethoxydim, forchlorfenuron, Fe^{3+} or Mg^{2+}. Structural analogues of 2,4-D (e.g. 2,4-dichlorophenylacetic acid and 2,4-dichlorobenzoic acid) were found to interfere at concentration of 0.3 µM. Interestingly, after 2,4-D reversible inhibition, the signal could be fully recovered by washing. The biosensor was stable over one month at 4°C and recoveries of 97-103% were obtained using real samples.

Acetylcholinesterase (AChE) is often used for insecticide detection due to its inhibition by organophosphorous and carbamate compounds. Glyphosate is an organophosphorous

pesticide which can also inhibit AChE. Liu *et al.* (2020) immobilized AChE and choline oxidase (ChOx) on reduced graphene oxide NPs on a GCE, in the presence of luminol, AuNPs, *L*-Cys and Cu(II) (Liu *et al.*, 2020). The coupled enzyme system produced H_2O_2 in the presence of acetylcholine. Cu(II) was used for its peroxidase-mimicking function. After one hour incubation of the biosensor with glyphosate, H_2O_2 detection was performed by ECL of luminol, using CV between 0 and 0.7 V *vs*. Ag|AgCl, Two suppression processes occurred: inhibition of AChE activity and complexation between Cu(II) and glyphosate which resulted in Cu(II) desorption from the electrode surface, giving rise to a lower optical signal measured at *ca.* 0.55 V *vs.* Ag|AgCl. The authors reported a LOD of 0.5 nM and a linear range from 1 nM to 1 µM (semi-logarithmic plot). The biosensor was successfully assayed in environmental matrices (lake and river water) and the results showed a good correlation with those obtained by ion chromatography. No interference was detected in the presence of deltamethrin, acridine, chlorpyrifos or carbendazim.

Another very sensitive biosensor based on AChE activity inhibition was described for glyphosate detection (Yu *et al.*, 2021) (Figure 7E). CdS and ZnO particles were used as photoactive materials on the surface of which the enzyme was entrapped in chitosan. The enzymatic photoelectrochemical FET used light as an excitation source thus generating photo-drain current in the presence of thiocholine produced from acetylthiocholine. With a 9 min incubation time with glyphosate, the photocurrent decrease was correlated to logarithmic glyphosate concentration in a linear range extending from 1.7×10^{-7} ppb to 1.7×10^{-3} ppb and a very low detection limit of 6.4×10^{-8} ppb was reported. A partial interference from imidacloprid and carbaryl was mentioned. The device was applied in vegetable samples with good recoveries.

Indirect glyphosate detection based on acid phosphatase (ACP) inhibition was reported (Butmee *et al.*, 2021). The amperometric biosensor was based on enzyme immobilization by glutaraldehyde cross-linking on a SPCE modified with AgNPs decorated with electrochemically reduced graphene oxide. Phenyl phosphate was used as the ACP substrate and glyphosate as a reversible competitive inhibitor. This disposable early warning device, suitable for on-field analysis, used nanomaterials for signal enhancement (*via* acceleration of the electron transfer process) as the ACP activity is reduced. The current densities were correlated with glyphosate concentrations, with two linear ranges: 0.05 – 0.5 ppm and 0.5 – 22 ppm. The detection limit was 0.015 ppm. Good recovery measurements (95.6 – 104.7 %) on spiked water samples were reported. Ultra high performance liquid chromatography (UHPLC) was also used as a comparative standard method to validate the biosensor.

2.6. Microfluidic paper-based analytical devices (µPADs)

Microfluidic paper-based user-friendly devices have recently been developed for eco-designed environmental monitoring, mainly for heavy metal ions, insecticide and fungicide detection (Kung *et al.*, 2019)(Colozza *et al.*, 2021). Paper has been shown to be a suitable material for electrochemical sensing, simplifying analysis of complex real samples that can be performed without previous treatment or further reagent addition, thus giving rise to reagentless detection. As described above (Table 3), µPADs based on inhibition of ALP, tyrosinase or HRP have been developed for 2,4-D, atrazine or glyphosate detection, respectively.

In 2019, Arduini *et al.* proposed an origami paper-based platform for paraoxon (an insecticide), 2,4-D and atrazine detection based on butyrylcholinesterase, ALP and tyrosinase inhibition, respectively (Arduini *et al.*, 2019). The device was composed of groups of three paper pads, with enzymes and substrates separately immobilized by adsorption (drop casting) on two of the paper pads whereas the third pads included carbon black-modified SPEs. For chronoamperometric measurements, the device was folded as an origami, superimposing all three zones. Pesticides could be quantified by relating the concentration to the inhibition percentage. A linear range could be observed between 100 to 600 ppb for 2,4-D and 10 to 100 ppb for atrazine. Limits of detection of 2 ppb (atrazine) or 50 ppb (2,4-D) were determined. The same group continued to develop a paper-based platform in 2022 (Caratelli *et al.*, 2022) with the design of a flower-like origami paper-based device for pesticide detection in aerosol phase. Paraoxon and 2,4-D were detected by the same enzymatic inhibitions as in their previous work, while glyphosate was also tested using HRP inhibition. Separate flower-like paper pads were pre-loaded with the selected enzyme, exposed to the pesticide solutions, and then slipped between a substrate pad and an electrode pad. Chronoamperometry measurements were performed with a smartphone-assisted potentiostat, improving the miniaturization of the device and its on-site usability. Reported detection performances for paraoxon and 2,4-D were similar to those obtained in their previous study, while glyphosate concentrations as low as 10 ppb were detected, with a linear range between 50 and 150 ppb. A selectivity study was also performed against eventual interfering species (lead, atrazine, lindane), which resulted in low inhibition (3-7% range). A paper-based ready-to-use electrochemical biosensing device was recently described by the same authors for the fast and smart detection of glyphosate in human urine (Moro *et al.*, 2023). Interference from uric acid was overcome by integrating sample treatment (pH-driven precipitation) into a paper strip. The paper origami biosensing strategy was based on inhibition of HRP activity and the use of TMB as substrate (Figure 9). A commercial portable potentiostat connected to a laptop was used to perform chronoamperometry measurements. A total time of analysis of 10 minutes was reported, including 5-min and 2-min incubation times with the HRP and the TMB pads, respectively. Glyphosate could be detected with a linear range extending from 100 to 700 ppb and LOD of 75 ppb. The authors pointed out a high score of sustainability (whiteness) of the paper-based microfluidic screening device, higher than that of the HPLC-MS reference method.

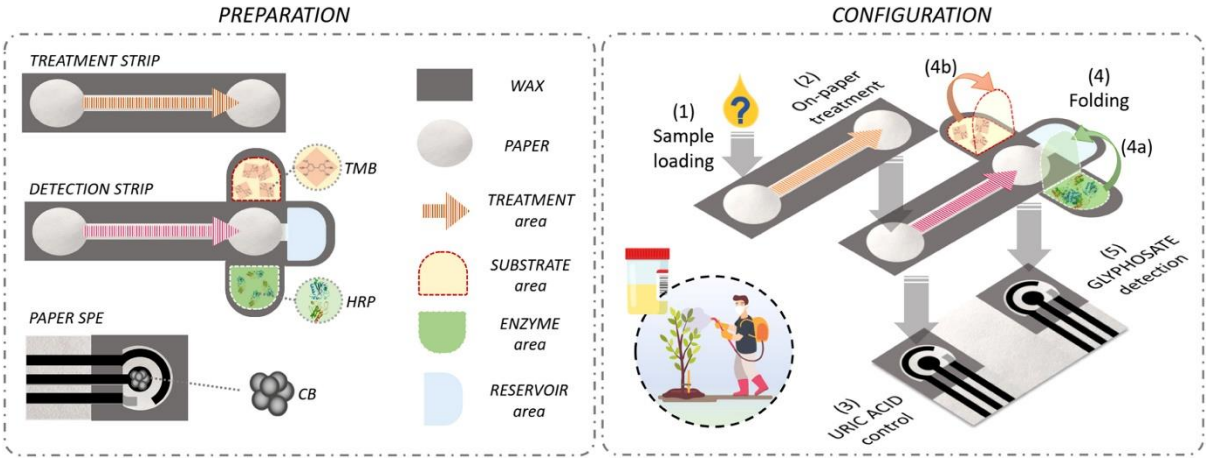

Figure 9. Paper-based origami biosensing of glyphosate in urine. Reproduced with permission from (Moro *et al.*, 2023). Copyright (2023) Elsevier.

2.7. Direct detection

Only few enzymatic biosensors based on direct detection have been reported in the literature compared to highly described inhibition-based biosensors for herbicide detection. Two main direct detection systems have been described: *signal-on* systems using herbicide as the enzymatic substrate and systems based on specific interactions.

Glutathione transferase isoenzyme GST-I from maize (zea mays) was used by Andreou *et al.* in order to detect atrazine (Andreou and Clonis, 2002). The sensing layer was located at the end of an optical fiber linked to a portable dual optical fiber spectrometer. GST was immobilized in the presence of BSA and glutaraldehyde on a polyvinylidene fluoride membrane, in order to enhance stability. This active membrane was used in combination with silica gel entrapping bromocresol green used as a pH indicator. GST catalyzes the conjugation of glutathione with atrazine, thus producing H^+ which can be monitored by the rate of absorbance decrease at 625 nm, in correlation with color change of the entrapped pH indicator. A LOD of 0.85 µM (181 ppb) and a linear range from 2.52 to 125 µM were reported. Surprisingly, no interference was detected with carbaryl and alachlor. This biosensor was validated by spiking drinking water samples and groundwater (81 - 115 % recoveries).

Laccase from *Trametes versicolor* was also used as a recognition element in amperometric biosensors for 2,4-D detection (Sezgintrk *et al.*, 2010). Laccase was entrapped in gelatin before cross-linking with glutaraldehyde, on the surface of a dissolved oxygen probe allowing measurement of the decrease of dissolved oxygen concentration. The linear range for 2,4-D detection extended from 1.1 - 4.4 ppb. The limitation of the system is related to the specificity of the laccase enzyme that is also active towards other phenolic compounds.

Glyphosate detection was also recently performed using glycine oxidase (GlyOx) co-immobilized with FAD by cross-linking with glutaraldehyde on an electrode produced by LIG decorated with PtNPs (Johnson *et al.*, 2022). By applying + 0.6 V *vs*. Ag|AgCl as the potential to detect the enzymatically-produced H_2O_2, a linear range was obtained from 1.7 ppm to 44 ppm glyphosate, with a limit of detection of 0.5 ppm. Negligible interference from other herbicides (atrazine, dicamba, 2,4-D), organophosphorous insecticides or neonicotinoids was observed. Recovery tests performed in river water samples spiked with glyphosate were validated. The low-cost amperometric device with a response time of 150 s was thought to be applicable for rapid in-field measurements.

Atomic force spectroscopy (AFS) methodology could be promising for herbicide detection, as shown by Leite's group. For instance, nanobiosensors based on atomic force microscopy (AFM) tip functionalization with a recombinant acetolactate synthase (ALS) were presented for metsulfuron-methyl detection (Da Silva *et al.*, 2013).This herbicide is a well-known ALS inhibitor (Table 1). A muscovite mica substrate was functionalized with 1 mM metsulfuron-methyl. Force curves were acquired and the adhesion force values were shown to be significantly higher when the AFM tip was enzymatically modified, resulting from enzyme-herbicide specific interaction. As mentioned by the authors, ALS can be inhibited by three classes of herbicides: not only sulfonylureas, but also imidazolinones and triazolopyrimidines. In the same way, atrazine could be detected by using an AFM cantilever nanobiosensor based on immobilized tyrosinase-herbicide interaction (Martinazzo *et al.*, 2018). A low cost tyrosinase extracted from banana was used for cantilever functionalization. The enzymatic cantilever

voltage was monitored as a function of atrazine concentration. A limit of detection of 7.8 ppb was obtained. No dynamic range was given. Glyphosate could also be detected by AFM, using peroxidase functionalized cantilevers (Muenchen *et al.*, 2018). A low cost peroxidase extract from zucchini was used, thus leading to a limit of detection of 28 ppb glyphosate by measuring cantilever deflection (voltage) *vs*. logarithm of glyphosate concentration. It can be noticed that the detection of herbicides based on mechanical transducers is performed without enzyme substrate addition.

3. Whole cell-based biosensors

In plants' chloroplasts and cyanobacteria, thylakoid membranes are responsible for light-dependent photosynthesis, oxidizing water to O_2, generating NADPH and indirectly ATP. The photosynthetic electron transport (PET) chain comprises two photosystems: photosystem I (PSI) and photosystem II (PSII) (Figure 10). PSII contains A-chlorophyll, a photosynthetic pigment able to absorb photons and use their energy to excite electrons produced by water oxidation. PSII is also composed of a reaction center formed by a heterodimer of two homologous proteins D1 and D2 (Figure 10B). The transport of excited electrons from the water oxidizing complex (Oxygen-Evolving Complex, OEC) through PSII involves two quinone molecules, Q_A and Q_B, which bind D2 and D1 at sites located on the outer side of the membrane, facing the stroma. Q_A is the initial electron acceptor molecule, which becomes reduced when the D1/D2 heterodimer is excited by light and remains linked with the D2 protein. The Q_B plastoquinone is a mobile redox species linked to D1, which can receive electrons from Q_A and be released from the PSII, allowing electrons to be transferred to the rest of the photosynthetic chain.

Photosynthetic herbicides inhibiting photosynthesis at PS II belong to two HRAC classes: 5 (D1 Serine 264 binders) and 6 (D1 Histidine 215 binders) (Table 1). They bind with the Q_B site of the D1 protein in PS II, thus competing with the native plastoquinone and interfering with the electron transport. PS I is also known to be the inhibitory target of herbicides from the 22 HRAC herbicide group. Unlike PS II inhibitors, PS I inhibitors do not block electron flow but rather divert electrons that react with oxygen, thus forming toxic oxygen radicals and finally, the ultra-reactive hydroxyl radicals. As shown on Figure 10, paraquat is known to inhibit the PSI whereas atrazine and diuron are known to inhibit the PSII.

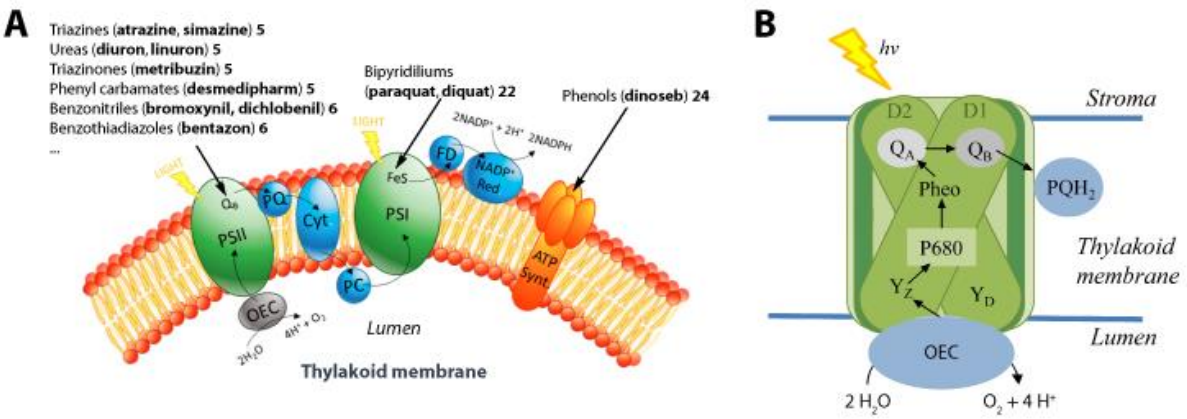

Figure 10. Photosynthetic transport chain in the thylakoid membrane showing the action site of selective herbicides (numbers refer to groups of herbicides acting on photosynthesis) (A), and simplified PS II structure showing the Q_A and Q_B sites (B). (Figures have been modified from (Tucci *et al.*, 2019a) and (Zharmukhamedov *et al.*, 2022)).

Consequently, photosynthetic organisms can be used as recognition elements in herbicide biosensors. Among them, microalgae have been widely used, due to their rapid growth rate and easy culture conditions. The use of whole cells as recognition elements guarantees good device stability, as well as the presence of all the elements needed to analyze photosynthesis disturbances. Two major detection methods are used: electrochemical or optical. The first one is based either on the oxygen production during light exposition or on the electrons produced by the photosynthetic system, and can be performed with the addition of redox mediator compounds, optimizing the electron transfer between the photosynthetic reaction sites and the surface of electrodes. On the other hand, optical detection refers to A-chlorophyll fluorescence measurements. When the light is absorbed by A-chlorophyll, the excess energy is partially re-emitted in the form of fluorescence. In the presence of PSII-inhibiting herbicides, energy cannot be transferred into the photosynthetic chain, resulting in greater energy dissipation in the form of increased A-chlorophyll fluorescence.
Therefore, whole cell-based biosensors mostly rely on inhibitory mechanisms, resulting in a lack of specificity for a large majority of microalgae biosensors described so far, owing to the diversity of pollutants affecting the microalgae metabolism. Whole cell-based biosensors for herbicide detection, based either on microalgae or on bacteria immobilization, are presented in Table 4 and described hereafter.

Table 4. Whole cell-based biosensors for herbicide detection, based either on microalgae or on bacteria immobilization.

Herbicide	Organism	Principle	Immobilization method	Detection	LOD (ppm or ppb)	Linear range (ppm or ppb)	Reference
Microalgae							
atrazine, isoproturon, propanil, bromoxynil	*Chlorella vulgaris*	PSII inhibition	adsorption	amperometry	< 100 ppb	nd	(Pandard and Rawson, 1993)
atrazine	*Scenesdesmus subspicatus*	PSII inhibition	adsorption on filter paper and entrapment in calcium alginate	fluorescence	ppb range	10 - 50 ppb	(Frense *et al.*, 1998)

diuron, atrazine, simazine, alachlor, glyphosate	*Chlorella vulgaris*	PSII inhibition	adsorption on microfiber filter	fluorescence	1.1 ppb atrazine, 0.2 ppb simazine, 0.02 ppb diuron, 1.3 ppm alachlor, 338 ppm glyphosate	nd	(Naessens *et al.*, 2000)
diuron, isoproturon , atrazine, simazine, DNOC	*Chlorella vulgaris*	PSII inhibition	adsorption on microfiber filter	fluorescence	0.25 ppb atrazine, 0.5 ppb simazine, 0.025 ppb diuron/isoproturon, 5 ppb DNOC	nd	(Védrine *et al.*, 2003)
AMPA, diuron	*Dunaliella tertiolecta ,Paeodactylum tricornutum*	external membrane esterase inhibition	Self-assembly monolayer (SAM)	conductometry	10 ppb AMPA, 10 ppb diuron	0.01 - 1 ppm	(Durrieu *et al.*, 2011)
atrazine, DCMU (diuron)	*Chlorella vulgaris*	PSII inhibition	entrapment in calcium alginate or polyion complex	amperometry	216 ppb atrazine (alginate), 11 ppb atrazine (polyion complex)	nd	(Shitanda *et al.*, 2005)
atrazine, DCMU (diuron)	*Chlorella vulgaris*	PSII inhibition	entrapment in calcium alginate	amperometry	216 ppb atrazine	nd	(Shitanda *et al.*, 2009)
diuron	*Chlorella vulgaris*	PSII inhibition	silica gel	fluorescence	1 ppb	nd	(Nguyen-Ngoc and Tran-Minh, 2007)
simazine, atrazine, propazine, terbuthylazine, linuron, 2,4-D	*Dictyosphaerium chlorelloides, Scenedesmus sp., Scenedesmus intermedius*	PSII inhibition	sol-gel membranes (Na silicate-glycerol) entrapment	fluorescence	3.6 ppb simazine	19 - 860 ppb simazine	(Peña-Vázquez *et al.*, 2009)
atrazine,	*Chlorella*	PSII	magnetic	amperome	151 ppm	194 - 1.6 x	(Zamalee

propazine	*pyrenoidosa*	inhibition	NPs-functionalized cells immobilized by an external magnet	try	atrazine, 92 ppm propazine	10^4 ppm atrazine 138 ppm - 2.8 x 10^4 ppm propazine	va *et al.*, 2011)
atrazine, diuron	*Chlamydomonas reinhardtii*	PSII inhibition	entrapment in Nafion	fluorescence	0.11 ppb atrazine, 0.12 ppb diuron	nd	(Scognamiglio *et al.*, 2012)
atrazine, diuron, prometryn	*Chlamydomonas reinhardtii*	PSII inhibition	entrapment in Nafion	fluorescence	0.11 ppb atrazine, 0.11 ppb diuron, 0.075 ppb prometryn	nd	(Scognamiglio *et al.*, 2013)
linuron, simazine	*Chlamydomonas reinhardtii*	PSII inhibition	alginate entrapment	amperometry	1.5 ppb linuron, 18.1 ppb simazine	nd	(Husu *et al.*, 2013)
atrazine, simazine, diuron	*C. vulgaris* in symbiosis with paramecia *(T. pyriformis)*	PSII inhibition	entrapment in calcium alginate	fluorescence	0.4 ppb diuron, 0.9 ppb atrazine, 1.6 ppb simazine	nd	(Turemis *et al.*, 2018)
atrazine	*Chlamydomonas reinhardtii*	PSII inhibition	entrapment in calcium alginate	Amperometry	0.22 ppb	21.6 ppb - 1.1 ppm	(Attaallah *et al.*, 2020)
atrazine, terbutylazine, diuron	*Chlamydomonas reinhardtii*	PSII inhibition	entrapment in calcium alginate	amperometry and fluorescence	0.43 ppb atrazine (electrochemical), 1.1 x 10^{-3} ppb atrazine (fluorescence)	21.6 ppb - 1.4 ppm atrazine (electrochemical), 2.2 - 43.1 ppb atrazine (fluorescence)	(Antonacci *et al.*, 2021)
atrazine (nanoencapsulated)	*Chlamydomonas reinhardtii*	PSII inhibition	entrapment in calcium alginate	Fluorescence	1 x 10^{-3} ppb	0,11 - 43 ppb	(Scognamiglio *et al.*, 2019)
atrazine (nanoen	*Chlamydomonas*	PSII inhibition	entrapment in calcium	Amperometry	0.2 ppb	21.6 ppb - 1.1	(Antonacci *et al.*,

capsulated)	*reinhardtii*		alginate			ppm	2023)
simazine	*Dictyosphaerium chlorelloides*	PSII inhibition	adsorption in porous silicone polymer	Fluorescence	12 ppb	50 - 800 ppb	(Haigh-Flórez *et al.*, 2014)
atrazine	*Chlorella vulgaris*	PSII inhibition	entrapment in alginate/silica hydrogel	imaging PAM-fluorometry	nd	nd	(Pannier *et al.*, 2014)
atrazine	*Scenedesmus acutus, Monoraphidium contortum*	PSII inhibition	entrapment in calcium alginate	Amperometry	23.7 ppb	-	(Boron *et al.*, 2020)
atrazine	*Scenedesmus obliquus*	PSII inhibition	algae biofilm onto graphite felt electrode	MFC current reduction	nd	nd	(Gonzalez Olias *et al.*, 2019)
Bacteria							
atrazine, linuron, metoxuron, ioxynil	cyanobacteria (*Synechococcus*)	PSII inhibition	adsorption in porous alumina filter disks or entrapment in calcium alginate	amperometry	nd	nd	(Rawson *et al.*, 1989)
atrazine, diuron	cyanobacteria (*Synechococcus sp.*)	PSII inhibition	entrapment in calcium alginate	amperometry	nd	nd	(Preuss and Hall, 1995)
2,4-D	bacteria (*Pseudomonas putida*)	metabolic oxygen consumption	entrapment in gelatin then cross-linking with glutaraldehyde	amperometry	nd	2.2 - 13.3 ppm (Clark electrode), 4.4 - 17.7 ppm (SPCE)	(Odaci *et al.*, 2009)
atrazine	bacteria (*P. sp.* ADP and *C. michiganese* ATZ1) expressing atrazine chlorohydrolase	pH variations (acidification) due to the reaction products	entrapment in calcium alginate	fluorescence (pH-sensitive optical probe)	1 ppb	1 - 100 ppb	(Das and Reardon, 2012)

atrazine, diuron	cyanobacteria *(Anabaena variabilis)*	PSII inhbition	entrapment in calcium alginate	amperometry	5 / 13.8 ppb atrazine (mediator in solution/entrapped), 0.7 / 1.4 ppb diuron (mediator in solution/entrapped)	5 ppb - 1 ppm / 13.8 ppb - 3.7 ppm atrazine (mediator in solution/entrapped) 0.7 - 105 ppb / 1.4 - 350 ppb diuron (mediator in solution/entrapped)	(Tucci *et al.*, 2019b)
atrazine, diuron, paraquat	cyanobacteria *(Synechocystis PCC6803 wt)*	PSII inhbition	adsorption on paper screen printed electrodes	amperometry	nd	nd	(Tucci *et al.*, 2019a)
atrazine	bacteria (*E. coli, S.oneidensis, M.capsulatus*)	reduction of insulating properties	poly L-Lys binding	CV, impedance spectroscopy	nd	nd	(Hisham Abu-Ali *et al.*, 2019) (H. Abu-Ali *et al.*, 2019)
diuron, glyphosate	cyanobacteria *(A. flos-aquae)*	PSII inhibition	entrapment in calcium alginate	amperometry	nd	nd	(Le Gall *et al.*, 2021)
atrazine	Anaerobic bacterial consortium (sludge from a wastewater treatment plant)	PSII inhibition	bacteria biofilm onto untreated carbon electrode	MFC current reduction	0.05 ppm	0.05 - 3 ppm	(Chouler and Di Lorenzo, 2019)

(MFC: Microbial Fuel Cell; PAM: pulse amplitude modulated ; nd: not determined)

3.1. Algae

An optical biosensor based on immobilized algae was reported (Frense *et al.*, 1998). *Scenesdesmus subspicatus* cells were adsorbed on a filter paper before alginate covering, then placed on the surface of an optical probe. Atrazine concentrations from 10 to 50 ppb could be measured by monitoring chlorophyll fluorescence induction upon herbicide treatment. With a response time of about 10 minutes, this device could be used for a simple estimation of the toxic load in water samples.

Another optical biosensor was described in 2000 by Naessens *et al.* (Naessens *et al.*, 2000) and later in 2003 (Védrine *et al.*, 2003). *Chlorella vulgaris* microalgae were immobilized by adsorption on a microfiber filter and placed in a flow system, close to the tip of an optical fiber bundle connected to a fluorometer. Fluorescence induction upon illumination and herbicide treatment was monitored, and detection limits for reversible PSII-inhibiting herbicides such as atrazine, simazine or diuron were reported as 5, 1 or 0.1 nM, respectively (Naessens *et al.*, 2000), or 0.25, 0.5 or 0.025 ppb, respectively (Védrine *et al.*, 2003). A phenolic herbicide, dinitro-*o*-cresol (DNOC), mainly acting as an irreversible uncoupler of oxidative phosphorylation and photophosphorylation, could also be detected, with a detection limit of 5 ppb (Védrine *et al.*, 2003). Alachor and glyphosate could also be detected, with detection limits of 5 µM and 0.1 mM, respectively, although their mechanisms of action on photosynthesis are not yet clear (Naessens *et al.*, 2000). These early-warning systems could be used as alarms to monitor seasonal variation of photosynthetic herbicides in aquatic media.

Later in 2011, the same group or consortium proposed a conductometric algae-based biosensor (Durrieu *et al.*, 2011). Cells of *Dunaliella tertiolecta* and *Paeodactylum tricornutum* marine microalgae were deposited on an epoxy resin sensitive surface placed between two interdigitated gold electrodes on a ceramic substrate. Cell monolayers were obtained by the self assembly monolayer (SAM) technique consisting of 3-mercaptopropionic acid (MPA) grafting on electrodes, followed by algae deposition. Measurements were based on detection of variations in conductivity of the sensitive area, linked to the ionic species produced by the activity of external membrane esterase(s). Diuron and AMPA (the main photodegradation product of glyphosate) were detected through their ability to inhibit the esterase activity, by comparison with untreated controls. Both herbicides were detected as low as 43 nM for diuron and 90 nM for AMPA, after 24 h incubation, with linear ranges extending up to values in the µM order. The authors noted the qualitative nature of these biosensors and the necessity to take into account possible interferences of other elements in environmental samples.

Chlorella vulgaris algae were also immobilized in calcium-alginate hydrogel on an indium tin oxide (ITO) electrode surface (Shitanda *et al.*, 2005). The oxygen production by algal photosynthesis was measured by chronoamperometry (- 0.7 V *vs.* Ag|AgCl) under illumination. The percentage of current decreased upon injection of DCMU (diuron) and atrazine was reported *vs.* herbicide concentration. A detection limit of 1 µM for atrazine was determined. Due to calcium-alginate hydrogel swelling, algae were finally immobilized within two layers of a poly(L-lysine)-PSS complex at the surface of the electrode. Despite a decrease in reduction current by one order of magnitude, steady state was reached within 5 sec upon illumination and stable inhibition was obtained after 200 s (0.25-100 µM). The LOD for atrazine decreased to 0.05 µM. The polyion-based biosensor also displayed an enhanced stability, with 80% response retained after 1 week storage at 4°C. The authors emphasized that the biosensor displayed a time-response much smaller (200 sec) than sensors based on the measurement of chlorophyll fluorescence at this time (14 h), and that other pollutants (toluene, benzene) could be detected with the sensor.

The same group later reported an amperometric screen-printed algal biosensor based on oxygen measurements (Shitanda *et al.*, 2009). For algal immobilization on the working electrode, a mixture (ink) including whole *Chlorella vulgaris* cells, MWCNTs and sodium alginate was screen-printed on the surface of a SPCE. A $CaCl_2$ gelling solution was used for FIA measurements, performed in a dark box. By application of a potential of - 0.7 V *vs*. Ag|AgCl and by periodic red light illumination by a red LED, atrazine and DCMU could be detected. The inhibition ratio of the oxygen reduction current was reported *vs.* herbicide concentrations.

Detection limit of 1 µM for atrazine was obtained, that is the same as the one the authors previously reported by directly depositing the algal cells in an alginate gel on an ITO electrode (Shitanda *et al.*, 2005). Both systems were compact and disposable, suitable for on-site monitoring. A better detection limit of 0.2 µM was reported by immobilizing the cells on a Clark oxygen electrode (Pandard and Rawson, 1993) that is not compact compared to the other devices. The biosensor based on a screen-printed algal ink was shown to be the more rapid, in correlation with the low algal film thickness.

Another optical biosensor based on chlorophyll fluorescence detection in *Chlorella vulgaris* was reported in 2007 (Nguyen-Ngoc and Tran-Minh, 2007). Algal cells were entrapped in a porous translucent silica gel obtained by a sol-gel process involving aqueous precursors. The translucent membranes could be placed directly in contact with the optical fibers. The immobilized algal cells were shown to keep over 95% of their initial activity after a 5 week-storage period. Diuron could be detected with a limit of detection of 1 ppb, mentioned as lower than the one reported with bioassays (Conrad *et al.*, 1993).

A fluorescent-based biosensor for the detection of simazine was proposed by Peña-Vázquez *et al.* (Peña-Vázquez *et al.*, 2009). Three microalgal species, *Dictyosphaerium chlorelloides* (*D.c.*), *Scenedesmus sp.* (*S.s.*) and *Scenedesmus intermedius* (*S.i.*) were entrapped in sol-gel membranes gelified on a glass disc. Silica gels provide a biocompatible environment to the cells, are chemically and thermally stable in aqueous environments and the size and the nature of the pore can be tailored. Their natural transparency is also advantageous for the immobilization of photosynthetic organisms as well as for optical measurement. Glass discs were placed at the extremity of an optical fiber itself incorporated into a flow cell chamber. Fluorescence was measured under darkness/illumination cycles. Under increasing concentrations of simazine (from 0.5 ppb to 10 ppm), photosynthesis was inhibited thus leading to an increase of fluorescence after 30 minutes allowing quantification of the herbicide. Using *D.c.* as the algae providing the broader dynamic range (19-860 ppb) and lower LOD (3.6 ppb) for simazine, the biosensor was assayed with other photosynthetic herbicides (atrazine, propazine, terbuthylazine, linuron), all giving similar results and showing that the biosensor was suitable to detect (without selectivity) a broad range of herbicides. On the other hand, a non-photosynthetic herbicide like 2,4-D could not be detected. Similar experiments conducted with a *D.c.* strain resistant to simazine but sensitive to other herbicides allowed to discriminate several herbicides within a single sample, thus opening up leads for improving the selectivity of the devices.

Algae immobilization in hydrogels or polymers is usually time-consuming and/or impairs the viability of the cells. To circumvent this, Zamaleeva *et al.* functionalized *Chlorella pyrenoidosa* microalgae with magnetic nanoparticles stabilized by poly(allylamine hydrochloride) before immobilization at the surface of a SPE using an external magnet (Zamaleeva *et al.*, 2011). Under these conditions, the viability of the cells was not affected. Photocurrent could be detected under daylight illumination cycles by covering the electrode with an opaque lid for 30 s. Ferricyanide was used as a mediator, under an applied potential of - 600 mV *vs*. pseudo-Ag|AgCl, for an amperometric detection. The percentage of the current inhibition in the presence of atrazine or propazine was used to quantify the response. Linear range was from 0.9 to 74 mM for atrazine and from 0.6 to 120 mM for propazine, and LOD were found to be 0.7 mM and 0.4 mM, respectively. The same electrode could be used at least 10 times for repeated deposition of magnetically functionalized algae.

Between 2012 and 2023, several studies describing the development of optical and electrochemical whole cell-based biosensors for herbicide detection were reported by a consortium linked to the Institute of Crystallography of the National Research Council (CNR) of Italy, in Monterotondo (Rome, Italy). These biosensors are presented in the following paragraphs. These authors also reported some of the few studies focusing on biosensors for the detection of nanoencapsulated herbicides, which are presented at the end of this section.

An automatic portable biosensor array for the simultaneous detection of several endocrine disruptor chemicals, among which triazine and urea herbicides, was reported by Scognamiglio *et al.* (Scognamiglio *et al.*, 2012). To recognize a wide range of chemical classes, several biosensing elements were integrated with an amperometric or an optical (fluorescent) detection in a six independent sensing cell format. For atrazine and diuron, wild-type and mutant strains of photosynthetic *Chlamydomonas reinhardtii* algae cells were immobilized on graphite SPEs. Fluorescence measurements were performed, thus leading to a detection limit of 0.5 nM for atrazine and diuron. The same authors later reported the use of the same kind of integrated biosensing platform for food analysis purposes, using gold microelectrode arrays (Scognamiglio *et al.*, 2013). Low detection limits were reported for atrazine (0.5 nM), prometryn (0.31 nM) and diuron (0.48 nM). The aim of these works is to design a biosensing screening tool able to reveal several analytes simultaneously, components and contaminants. The real-time parallel monitoring of multiple compounds is performed rapidly, with low cost and using low sample volume.

Immobilized *Chlamydomonas reinhardtii* algae cells were also used by Husu *et al.* to detect linuron and simazine (Husu *et al.*, 2013). Algae cells were immobilized by alginate entrapment directly on a commercial MWCNT-modified SPE (DropSens). Red light (650 nm) illumination pulses were used to induce photosynthetic oxygen production, leading to cathodic reduction currents measured at - 0.7 V *vs.* Ag|AgCl by amperometry. The biosensor was then used to evaluate PSII inhibition by the herbicides, which were detected at limits of 6 nM and 90 nM, respectively. However, specificity and matrix effects were not evaluated. The biosensor showed an interesting stability over 10 days (90% of initial activity) but a relatively fast sensitivity decrease afterwards (75% after 20 days, 20 % after 40 days).

An automatic system including an optical biosensor based on the symbiotic association of microalgae (*Chorella vulgaris*) and paramecia (*Tetrahymena pyriformis*) was then reported for marine monitoring of water contaminants (Turemis *et al.*, 2018). The symbiotic strain resistant to marine water salinity was entrapped in calcium alginate and integrated in a flow system. Fluorescence measurements correlated to PSII inhibition by herbicides. Six tests could be simultaneously performed, under LED illumination. Detection limits for simazine, atrazine and diuron were 1.55, 0.89 and 0.39 ppb, respectively. Measurements of marine water samples spiked with herbicides showed a good correlation with those obtained by LC-MS. A fast (10 min) pre-screening of toxic contaminants in seawater samples could be performed. The authors compared their results with other optical or electrochemical microalgae based biosensors and bioassays. High sensitivity, and short detection times were emphasized, as well as the use of real seawater samples instead of buffers.

The consortium recently reported an amperometric algae-based biosensor for detection of atrazine (Attaallah *et al.*, 2020) (Figure 11A). Atrazine induced a decrease of molecular oxygen concentration by interacting with photosynthetic electron transport. Carbon black (CB) nanomaterial deposited on a SPE was used to detect the light-induced oxygen evolution. CB

was supposed to enhance the C*. reinhardtii* CC125 algal loading and to increase the electron transfer. Algae were entrapped in calcium alginate on a CB-modified SPE, thus providing a biocompatible environment. Repeated cycles of 30 s light excitation with red LEDs and 10 min dark in the presence of different atrazine concentrations were performed. The herbicide could be detected with a low detection limit (1 nM) and a linear range extending from 0.1 to 5 µM. Suitability in a real sample from surface river water was also achieved. Obviously, the algae-based system suffers from a lack of specificity and could be used as an on/off alarm for environmental analysis.

An innovative algae-based dual electro-optical biosensor was reported in 2021 (Antonacci *et al.*, 2021). *Chlamydomonas reinhardtii* cells were immobilized by alginate entrapment on paper-based SPEs modified with CB nanomaterials (pCB-SPEs). A portable dual electro-optical transducer prototype was developed for the project (Biosensor srl.). The device included a LED system allowing algae illumination at 650 nm and subsequent measurement of fluorescence emission at 680 nm. Chlorophyll autofluorescence increase (due to photosynthetic energy dissipation after PSII inhibition) following illumination and herbicide treatment was used for detection, as well as chronoamperometric measurements of photosynthetic O_2 reduction. A large collection of *C. reinhardtii* genetic variants was tested to identify the optimal strain to use as the recognition element in the dual electro-optical biosensor. Triazine (atrazine and terbutylazine) and ureic (diuron) herbicide classes were detected. The authors pointed out the sensitivity differences between optical and electrochemical detection methods, with the first leading to a detection limit of 5 pM (1.1×10^{-3} ppb) with a linear range from 10 to 200 nM, while the latter showed a linear response in the 0.1 to 6.6 µM range, with a detection limit of 2 nM (0.43 ppb) for atrazine. The novelty of the transducer prototype, as well as its use for a systematic study of *C. reinhardtii* strains in a low-cost and sustainable format was nevertheless underlined by the authors.

The use of nanoencapsulated atrazine was described by Oliveira *et al.* and enabled the application of lower dosages of the herbicide, without any loss of efficiency, thus providing environmental benefits (Oliveira *et al.*, 2015). Therefore, in a more recent study, Scognamiglio *et al.* (Scognamiglio *et al.*, 2019) described, together with the previously mentioned authors, the development of the first algal bioassay for nanoformulated herbicide (in poly ε-caprolactone) detection based on an optical paper-based system (Figure 11B). Wild-type *Chlamydomonas reinhardtii* algae cells were entrapped in agar hydrogel on a paper support. This work is the first reported bioassay focusing on the detection of nanoformulated herbicides, which are increasingly being used in smart agriculture (smart delivery systems). Recently, the same authors reported an eco-designed algal biosensor for detecting zein-encapsulated atrazine (Antonacci *et al.*, 2023). *Chlamydomonas reinhardtii* UV 180 mutants were entrapped in calcium alginate on carbonized lignin SPEs and integrated into a photo-electrochemical transducing system. Reduction of oxygen produced by cell photosynthesis under illumination was measured at - 0.8 V *vs*. Ag|AgCl. Linear range extended from 0.1 to 5 µM and LOD was given as 0.9 nM (0.2 ppb). No interference was observed from different compounds among which paraoxon, arsenic, bisphenol A or copper. Good recovery (106 %) was obtained in wastewater samples.

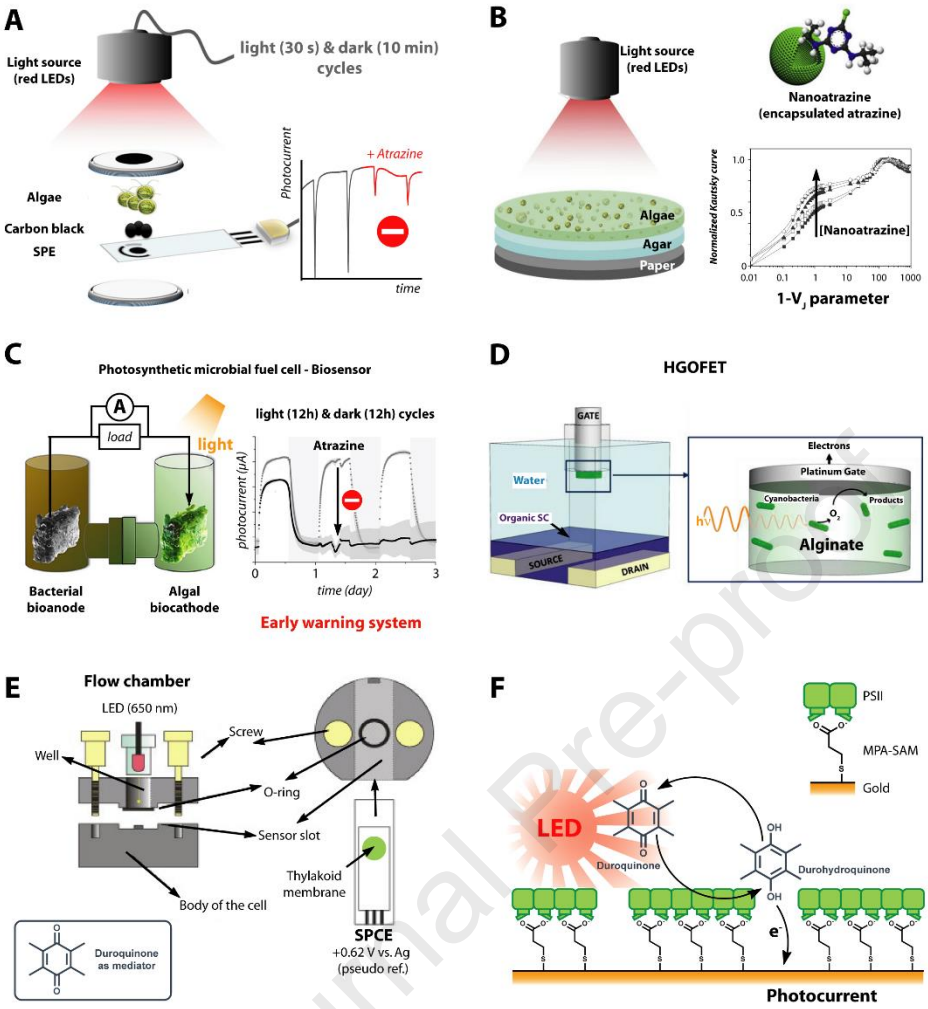

Figure 11. Examples of whole cell-based biosensors based on algae (**A**, modified from Attallah *et al.*, 2020 ; **B**, modified from Scognamiglio *et al.*, 2019 ; **C**, modified from Gonzalez Olias *et al.*, 2019), bacteria (**D**, modified from Le Gall *et al.*, 2021), thylakoids (**E**, modified from Bettazzi *et al.*, 2007) or BBY particles (**F**, modified from Bhalla & Zazubovich, 2011).

Apart from the work of this Italian group, other algae-based biosensors are described in the literature. Haigh-Flórez *et al.* proposed an optical microalgae biosensor for the detection of simazine with improved specificity (Haigh-Flórez *et al.*, 2014). The device was based on the monitoring of photosynthetic activity of *Dictyosphaerium chlorelloides* cells by luminescent O_2 detection, and comprised a dual-head fiber-optic measuring chamber with two separate compartments. Simazine-sensitive and simazine-resistant *D. chlorelloides* strains were obtained, and each was immobilized in a compartment of the measuring chamber by adsorption in porous silicone polymer disks. Photosynthetic O_2 detection was achieved by the use of a polymeric film containing an O_2-sensing RD3 dye. The biosensor was used for simazine detection, with an increased specificity due to differential inhibition of photosynthetic O_2 production by the sensitive and resistant strains. Specificity was confirmed by using a control herbicide (isoproturon), for which both strains showed comparable sensitivity. Quantitative analysis resulted in a simazine detection limit of 12 ppb, over a linear range from 50 to 800 ppb. This work is one of the few examples of studies focused on improving the

specificity of algae-based herbicide biosensors, while also valuing the balance between sensitivity and durability.

In 2014, a study by Pannier *et al.* demonstrated the feasibility of microalgae immobilization in alginate/silica hybrid hydrogels for the design of cell-based sensors (Pannier *et al.*, 2014). Cells of *Chlorella vulgaris* microalgae were deposited onto a cationically modified glass substrate and encapsulated in an alginate hydrogel thin film reinforced by a gelation process based on amino-functionalized silica sol. The obtained hybrid hydrogel displayed improved stability and mechanical properties compared to traditional Ca^{2+}-based hydrogels, particularly for long term storage of the immobilized cells. Photosynthesis inhibition by atrazine was monitored by analyzing chlorophyll *a* fluorescence, using imaging pulse amplitude modulated-fluorometry (imaging-PAM). The detection limit and linear range were not determined, but an EC_{50} for photosynthesis of 0.11 ppm after 1h exposure to atrazine was observed. The authors underlined the stability and versatility of this encapsulation method, as a promising tool for further cell-based biosensors design.

In 2020, Boron *et al.* described a biosensor based on the interaction of alginate and microalgae with polyelectrolyte-surfactant matrix modified SPEs (Boron *et al.*, 2020). In this work, *Scenedesmus acutus* and *Monoraphidium contortum* microalgae were used for atrazine detection. Oxygen concentration was monitored by electrochemistry with a three-electrodes system composed of polyallylamine, dodecylsulfate and MWCNTs-modified SPEs. The algae suspension was immobilized on the electrode and in a flow cell, by inclusion in alginate hydrogel. The presence of atrazine was then detected by chronoamperometry (0.5 V *vs*. Ag|AgCl) under illumination. A detection limit of 0.11 µM (23.7 ppb) was determined, in particular using *M. contortum* cells which demonstrated the highest sensitivity. The device remained stable at room temperature for 5 months, and also allowed successful atrazine measurements in river water samples with heavy sediment load. This work showed that a variety of microalgae can be used for herbicide detection. Although chlorophyll content of both used strains was characterized, the question of the influence of these particular microalgae species on the specificity of the biosensor is essential, and no studies were carried out with potential interfering compounds.

A photosynthetic microbial fuel cell (MFC) sensor using an algae-assisted cathode was recently described for the first time for atrazine detection (Gonzalez Olias *et al.*, 2019) (Figure 11C). The cathode (graphite felt) modified with *Scenedesmus obliquus* microalgae served as a self-powered dissolved oxygen probe. The cathode chamber operated under light/dark 12h/12h cycles with LED lights. The current output generated during the 12h-light period correlated with the dissolved oxygen in the catholyte. In the presence of atrazine, inhibition of the light-induced oxygen produced by the algal cells occurred, thus leading to a decrease of the current output. Atrazine concentrations from 0.1 ppb to 10 ppm were tested and shown to modify the signal but no correlation between them could be established. Such systems could be used as early warnings of herbicide pollution in water. A low reproducibility was thought to be due to an uneven response of the algae to the herbicide. The response time was in the range of hours, due to mass transfer limitations. Further work is still needed to improve the system.

3.2. Bacteria

In an early work, Rawson *et al.* (Rawson *et al.*, 1989) developed a mediated amperometric biosensor using the cyanobacterium *Synechococcus* as a recognition element for the detection of herbicides. The cells were either adsorbed on porous alumina membranes or entrapped in desiccated calcium alginate beads. Although the former method provided better sensitivity, the latter was chosen because it was relevant to design a portable, easy-to-handle biosensor. Photosynthetic electron transfer (PET) of the cells upon illumination was monitored using potassium ferricyanide as an electron mediator and a porous graphite electrode mounted in a flow cell. The rate of mediator reduction was proportional to the rate of PET-induced NADPH production at the plasma membrane of intact cells. No limit of detection was described, but a 50% inhibition of PET was achieved within 20 minutes using concentration ranging from 125 to 350 ppb of herbicides from urea (linuron, metoxuron), nitrile (ioxynil) and triazine (atrazine) families. This work is one of the first studies to focus on the development of a biosensor taking into account the ease of use of the recognition element, and its potential portability in an online, real-time monitoring system.
The same group later described another amperometric biosensor in which *Chlorella vulgaris* microalgae cells were adsorbed on porous alumina filter disks and immobilized onto a teflon-covered carbon oxygen electrode (Pandard and Rawson, 1993). This setup was used in a flow cell to detect atrazine, isoproturon and propanil within 30 minutes, due to their inhibitory activity on photosynthetic oxygen synthesis. LODs below 100 ppb were observed for atrazine and isoproturon, while propanil was more rapidly detected, albeit with lower sensitivity.

Preuss and Hall (Preuss and Hall, 1995) described in 1995 the immobilization of *Synechococcus sp.* cyanobacteria onto calcium alginate film at the surface of a GCE covered by a dialysis membrane. Diaminodurene (DAD) was used as a redox mediator between the reduced plastoquinone B (Q_BH_2 PSII) or PSI and the electrode polarized at 0.2 V *vs*. SCE, under dark/light illumination. The biosensor was first used to study the binding of atrazine and diuron on the photosystems. It was found that atrazine is competitive to Q_B only in the light period while diuron binding is independent of the light cycle and follows a noncompetitive mechanism for Q_B on D1. Kinetic analysis, based on models for soluble enzymes, allowed to determine an apparent K_I of 29 ppb (0.13 µM) for atrazine but not for diuron, whose value was too small to be accurately determined. Although this biosensor was analyzed as a homogenous system (whole algae was resumed to the D1 protein and no mass transfer limitations were considered), this seminal work showed the potential of biosensors for the determination of kinetic parameters and for identification or comparison of herbicide mechanisms.

In 2009, amperometric microbial biosensors for 2,4-D detection were reported (Odaci *et al.*, 2009). Adapted *Pseudomonas putida* cells were immobilized by entrapment in gelatin before cross-linking with glutaraldehyde. The cells were deposited either on a SPCE or on the membrane of a Clark oxygen electrode. Oxygen consumption due to the metabolic activity of bacteria was monitored by chronoamperometry at - 0.7 V *vs*. printed Ag|AgCl. The linear range for 2,4-D concentrations extended from 10 to 60 µM (2.2 – 13.3 ppm) with the Clark electrode and from 20 to 80 µM (4.4 – 17.7 ppm) with the SPCE. A total measurement time of 200 seconds appeared advantageous with the carbon electrode, compared to 10 minutes using the oxygen electrode. No clear link between 2,4-D exposure and oxygen consumption was described by the authors. Moreover, and despite the system's simplicity and ease of use, responses were also obtained with several compounds such as phenol and derivatives, glucose, ethanol or methanol, thus pointing out the lack of specificity.

Das and Reardon designed an optical biosensor based on immobilization of bacterial cells (*Pseudomonas sp.* ADP and *Clavibacter michiganese* ATZ1) expressing atrazine chlorohydrolase (AtzA) and entrapped in calcium alginate, on the tip of an optical fiber covered by a pH-sensitive fluoresceinamine layer (Das and Reardon, 2012). In the presence of atrazine (or s-triazine herbicides), H^+ was produced as a product of the atrazine dechlorination reaction catalyzed by AtzA, thus leading to acidification of the medium and modification of fluorescence intensity. A detection limit close to 1 ppb was obtained and the linear range extended from 1 to 100 ppb (*C. michiganese*) or 125 ppb (*P. sp.*). Continuous and real time measurements could be performed with a soil column continuously fed with atrazine. As this system relies on the formation of an enzymatic product, it is one of the very few "signal-on" biosensors reported. It offers an undeniable advantage in terms of specificity over other inhibition-based systems.

In 2019, Tucci *et al.* proposed an interesting amperometric herbicide biosensor based on the direct monitoring of photocurrent of *Anabaena variabilis* cyanobacteria (Tucci *et al.*, 2019b). The cells were immobilized on carbon felt electrodes by encapsulation in an alginate hydrogel. Photocurrent generation upon illumination and direct extracellular electron transfer was monitored by CV, using *p*-benzoquinone (BQ) as a redox mediator in the electrolyte. BQ was shown to enhance the electron transfer between purple photosynthetic bacteria and the surface of an electrode (Grattieri *et al.*, 2019), and the authors tested the possibility to directly entrap this mediator in the alginate polymer. In this configuration, higher concentrations of BQ were used and activated carbon was added to ensure the electrical conductivity of the alginate matrix. In both cases (encapsulated and unencapsulated BQ), the biosensor was used for atrazine and diuron detection by amperometrically measuring (at + 0.5 V *vs.* SCE) the photocurrent reduction due to the PSII inhibitory effect of the two herbicides. Mediator encapsulation led to a 2- to 3-fold loss of sensitivity (LOD increased from 5 ppb (0.023 µM) to 13.8 ppb (0.064 µM) for atrazine, and from 0.7 ppb (0.03 µM) to 1.4 ppb (0.06 µM) for diuron, probably due to the presence of activated carbon) and to a broadening of the linear range, particularly at high concentrations. This study presents one of the few examples of whole-cell bacterial amperometric biosensors based on direct photocurrent measurements, in which the use of a redox mediator has been optimized, offering useful insight for future developments. However, the lack of specificity remains the main disadvantage of the proposed system. Later in 2019, the same authors described a novel photo-bioelectrochemical biosensor for herbicide detection, operating this time in the absence of any artificial electron mediator (Tucci *et al.*, 2019a). In this work, a biofilm of *Synechocystis* PCC6803 *wt* cyanobacteria was immobilized by adsorption on paper-based SPEs. These electrodes were obtained by coating filter paper with 7 layers of single-walled carbon nanotube (SWCNT) ink and one titanium nanolayer. The three electrodes system (platinum counter electrode and Ag|AgCl reference electrode) allowed the direct measurement of photocurrent by chronoamperometry at + 0.4 V *vs*. Ag|AgCl, under illumination. A decrease in photocurrent was observed after addition of 10.7 µM atrazine or 0.5 µM diuron in the medium. On the other hand, the presence of 0.7 µM paraquat led to a current increase, which can be explained by the herbicide's capacity to act as a redox mediator between the cells and the electrode. Moreover, cytotoxic compounds (formaldehyde, heavy metals, other kinds of herbicides) also caused photocurrent decrease. Despite the absence of sensitivity determination (LOD, linear range) and an inherent lack of specificity, this work illustrates the possibility of designing mediator-free amperometric detection systems based on bacterial whole cells. As redox mediators are often toxic and increase operating costs, their absence could be beneficial.

In 2019, Abu-Ali *et al.* also described the use of three types of bacteria (*Escherichia coli*, *Shewanella oneidensis* and *Methylococcus capsulatus*) in a sensor array for detection of water pollutants, including atrazine (together with heavy metals and petrochemicals) (H. Abu-Ali *et al.*, 2019). Optical methods (optical density, fluorescence microscopy and flow cytometry) and CV were used on bacterial suspensions to correlate bacterial concentration with optical and electrical properties (more specifically conductivity). Bacteria were then immobilized on gold SPEs coated with poly L-Lysine, and CV measurements were carried out, to identify patterns in the reduction of the three bacterial strains' insulating properties linked to pollutant-induced damage. Atrazine was detectable in the mM range, and the authors emphasized the possibility of using pattern recognition methods to identify pollutants. This study was continued and extended in the same year, by using the same approach on a wider range of pollutants and by adding impedance spectroscopy measurements (Hisham Abu-Ali *et al.*, 2019). Atrazine was detectable in the µM range this time. Pollutants could be identified and quantified to some extent, by analyzing the sensor array data using an artificial neural network (ANN) program.

In 2021, Le Gall *et al.* described, in a proof-of-concept study, the feasibility of herbicide detection using hydrogel-gated organic field-effect transistors (HGOFET) (Le Gall *et al.*, 2021) (Figure 11D). In this work, the authors designed an HGOFET consisting of a Pt gate electrode and two source and drain Au electrodes separated by water acting as a dielectric material and interfaced with an organic semiconductor layer made of poly(DPP-DTT). Alginate-entrapped *Anabaena flos-aquae* cyanobacteria were immobilized on the gate electrode and, upon illumination, produced oxygen which was locally reduced into water on the Pt surface. This low reduction current was then amplified as a source-drain current of several orders of magnitude higher intensity (µA range). After herbicide treatment (diuron or glyphosate at 10 µM each for 1 h), the photosynthetic drain current generated by the cyanobacteria showed a significant decrease, with a greater sensitivity for diuron compared to glyphosate. This work needs to be further developed with quantitative data for LOD and linear range determination, and it should be expanded to a wider range of herbicides, but it offers a promising alternative for herbicide biosensor design.

Consortia of microorganisms were used to design a membrane-free microbial fuel cell (MFC) sensitive to formaldehyde and atrazine (Chouler and Di Lorenzo, 2019). The use of mixed anaerobic consortia simplified practical applications compared to the use of pure species. The MFC chamber was equipped with two untreated carbon electrodes, the cathode being exposed to air. Both electrodes were connected to an external load of 1 kΩ, and artificial wastewater containing a mixed culture of bacteria from an anaerobic sludge was used to develop a biofilm at the anode surface for 7 days. The MFC operated at alkaline pH (12) because this pH favors the cathodic reaction. When assayed as a biosensor for atrazine during a 30-minute exposure time, the current density (expressed as the variation of the normalized current) dropped linearly from 0.05 ppm (LOD) to 0.3 ppm atrazine, with an average response time of 9 min. The recovery time of the biosensor (*e.g.* the time necessary to recover initial current density after atrazine treatment) was *ca.* 29 min. This low cost MFC is effective for real-time water quality control but probably lacks selectivity toward herbicides due to the nature of the bacterial consortia. Nevertheless, it presents a fast response in complex media (artificial wastewater) suitable for on-line applications.

4. Organelles and subcellular components

4.1. Thylakoids and chloroplasts

An alternative approach to whole cell-based biosensors for the detection of photosynthetic herbicides has been proposed in various studies by isolating organelles (chloroplasts), subcellular components (thylakoids) or even PSII particles. In all these approaches, amperometry is the preferred detection method, and the use of cellular or subcellular element preparations enables close coupling between the biosensing element and the transducer (electrode), which improves sensitivity.

Biosensors reported in the literature are mainly based on thylakoid membranes rather than chloroplasts. The short lifespan of isolated thylakoids needs to be taken into account, highlighting the importance of the immobilization process for biosensor stability. More recent biofuel cell examples are also considered. Table 5 presents the different organelle- and subcellular element-based biosensors for herbicide detection reported in the literature.

Table 5. Organelle- and subcellular element-based biosensors for herbicide detection.

Herbicide	Organelle	Principle	Immobilization method	Detection	LOD (ppm or ppb)	Linear Range (ppm or ppb)	Reference
Thylakoids and chloroplasts							
diuron, atrazine	thylakoid membranes from spinach leaves	PSII inhibition	entrapment in PVA-SbQ	amperometry	5 ppb diuron 43 ppb atrazine	nd	(Rouillon *et al.*, 1995)
diuron, bromoxynil, triazines (atrazine, cyanazine, hexazinone, metribuzin)	thylakoid membranes from spinach leaves	PSII inhibition	cross-linking with glutaraldehyde-BSA	amperometry	10 ppb atrazine, 5 ppb cyanazine 8 ppb hexazinone, 10 ppb metribuzin, 10 ppb diuron, 2 ppm bromoxynil	10 ppb - 1 ppm triazines	(Laberge *et al.*, 1999)
paraquat, diuron, prometryn, ametryn, atrazine	thylakoid membranes from spinach leaves	Inhibition of H_2O_2 scavenging by thylakoids	entrapment in PVA-SbQ	amperometry	0.25 ppb paraquat, 0.42 ppb diuron, 3.4 ppb	0.26 - 38.6 ppb paraquat, 2.33 - 70 ppb	(Li *et al.*, 2005)

					prometryn, 10 ppb ametryn, 0.54 ppb atrazine	diuron, 8.6 ppb - 12 ppm atrazine	
diuron, atrazine, ioxynil	thylakoid membranes from spinach leaves	PSII inhibition	cross-linking with glutaraldehyde	amperometry	1.3 ppb diuron, 2.8 ppb atrazine, 2.1 ppb ioxynil	nd	(Bettazzi *et al.*, 2007)
diuron, triazines (atrazine, simazine, terbuthylazine, desethylterbutilazine)	thylakoid membranes from spinach leaves, *S. vulgaris* wild-type and atrazine resistant mutant	PSII inhibition	cross-linking with glutaraldehyde-BSA or entrapment in gelatin	amperometry	4 ppb diuron, 5 ppb atrazine, 8 ppb simazine, 6 ppb terbuthylazine, 5 ppb desethylterbuthylazine	nd	(Touloupakis *et al.*, 2005)
diuron, linuron	thylakoid membranes from spinach leaves (*S. oleracea*)	PSII inhibition	laser-induced forward transfer (LIFT)	amperometry	2 ppb diuron, 1 ppb linuron	nd	(Touloupakis *et al.*, 2012)
diuron, terbuthylazine, metribuzin	thylakoid membranes from pea plants (*P. sativum*)	PSII inhibition	adsorption on carbon paper working electrode	amperometry	*ca.* 0.1 ppm	nd	(Lettieri *et al.*, 2022)
diuron, atrazine, bromacil	thylakoid membranes from spinach leaves (*S. oleracea*)	PSII inhibition	adsorption on carbon paper electrodes	amperometry (biofuel cell)	0.37 ppb atrazine, 0.21 ppb bromacil, 0.1 ppb diuron	up to 12 ppb atrazine, up to 16 ppb bromacil, up to 14 ppb diuron	(Rasmussen and Minteer, 2013)
diuron	chloroplasts from spinach leaves (S. oleracea)	PSII inhibition	ethylene glycol diglycidyl ether (EGDGE) cross-linking	amperometry (biofuel cell)	23.3 ppb	23.3 ppb - 0.23 ppm	(Grattieri *et al.*, 2020)

Isolated PSII complex or other reaction centres							
diuron, atrazine, simazine, ioxynil, bromoxynil, dinoseb	isolated PSII paricles from a thermophilic cyanobacterium	PSII inhibition	encapsulation with a dialysis membrane	amperometry	0.12 ppb diuron, 0.43 ppb atrazine	nd	(Kobliz ek *et al.*, 1998)
diuron, atrazine, simazine	isolated PSII paricles from a thermophilic cyanobacterium	PSII inhibition	cross-linking with glutaraldehyde	amperometry	0.23 ppb diuron, 0.43 ppb atrazine, 0.8 ppb simazine	nd	(Koblíž ek *et al.*, 2002)
diuron	Isolated *Synechococcus bigranulatus* PSII particles	PSII inhibition	adsorption on polySBQ	amperometry	0.16 ppb	nd	(Maly *et al.*, 2005)
diuron, atrazine, isoproturon	PSII complex from a thermophilic cyanobacterium	PSII inhibition	cross-linking with glutaraldehyde	amperometry	0.23 ppb diuron, 0.35 ppb atrazine, 2 ppb isoproturon	nd	(Masojídek *et al.*, 2011)
diuron	PSII complex from a thermophilic cyanobacterium	PSII inhibition	cross-linking with glutaraldehyde	amperometry	nd	0.23 - 23.3 ppb diuron	(Krejci *et al.*, 2011)
atrazine	BBY particles	PSII inhibition	covalence on carboxylated SAM	amperometry	0.25 ppb	nd	(Bhalla and Zazubovich, 2011)
atrazine, terbutryn	*Rhodobacter sphaeroides* reaction centre	reaction centre inhibition	adsorption	amperometry	1.9 ppb terbutryn, 10.8 ppb atrazine	nd	(Swainsbury *et al.*, 2014)

(nd: not determined).

Rouillon *et al.* described in 1995 an amperometric biosensor using thylakoid membranes isolated from spinach leaves as recognition elements (Rouillon *et al.*, 1995). The biosensor was composed of a microelectrochemical cell using a Pt working electrode, where the membranes were immobilized in PVA-SbQ. Upon white light illumination, H_2O_2 was produced and reoxidized at the working electrode, generating photocurrent measured at a potential of 0.65 V (*vs*. Ag|AgCl). The photocurrent inhibition induced by diuron and atrazine was monitored, and allowed detection of both herbicides at concentrations as low as 20 nM and 200 nM, respectively. The results were compared with non-immobilized thylakoids, which showed significantly lower sensitivities. Another biosensor using spinach leaves thylakoids was proposed by the same group or consortium (Laberge *et al.*, 1999). After extraction, the membranes were immobilized in an albumin-glutaraldehyde cross-linked matrix leading to enhanced stability. Using a microelectrochemical cell and under illumination, measurement of the photocurrent was performed on Pt electrodes. Inhibition of the photocurrent by a relatively large range of herbicides was monitored, amongst which photosynthetic inhibitors like triazines (atrazine, cyanazine, hexazinone, metribuzin), diuron or bromoxynil. Non-photosynthetic inhibitors like 2,4-D were also tested. Photosynthetic inhibitors displayed limits of detection, as low as 5 ppb for cyanazine, together with a detection range ranging from 5 ppb to 1 ppm. The authors point out the advantage of the screening tool developed for pollutants that specifically target photosynthetic processes.

A very similar biosensor based on thylakoid membranes isolated from spinach leaves was later described in 2005 (Li *et al.*, 2005). The membranes were immobilized on platinum electrodes using PVA-SbQ. Herbicide detection was achieved by measuring the inhibition of the oxidative current due to hydrogen peroxide scavenging by the thylakoid's enzymes (ascorbate peroxidase, dehydroascorbate reductase and glutathione reductase). The inhibition caused by paraquat, diuron and triazines (atrazine, ametryn, prometryn) was studied, with a detection limit in the nM range for paraquat and diuron, and in the 10 nM range for triazines. The immobilized thylakoid membranes showed an interesting stability over time, retaining 89.5% and 50% activity after 2 and 6 months of storage at - 20°C, respectively.

Thylakoid membranes from spinach leaves were also immobilized at the surface of a SPCE by cross-linking using a mixture of BSA and glutaraldehyde (Bettazzi *et al.*, 2007) (Figure 11E). The biosensor was placed in a flow cell chamber containing buffer and duroquinone as an electron acceptor from oxygen. Under illumination at 650 nm, duroquinone was reduced and further reoxidized at the electrode surface (at + 0.62 V *vs.* Ag pseudoreference) leading to a peak current proportional to PSII activity. The biosensor was sensitive to diuron from 2.3 to 233 ppb with a sigmoidal behavior and a LOD of 1.3 ppb.

Several biosensors based on immobilized thylakoids were proposed between 2005 and 2012 by the consortium linked to the Institute of Crystallography of the National Research Council (CNR) of Italy, whose studies on microalgal whole-cell biosensors are described in the present review (see 2.2.1). These works propose innovative approaches for thylakoid immobilization methods and herbicide subclass discrimination, and they are presented in the following paragraphs**.**

Thylakoids from several organisms (*Spinacia oleracea*, *Senecio vulgaris* and *Senecio vulgaris* mutant resistant to atrazine) showing different sensitivities to herbicides were used to design a multiplex biosensor in 2005 (Touloupakis *et al.*, 2005). Thylakoids were immobilized at the

surface of a graphite SPE within glutaraldehyde-BSA or gelatin, the latter being placed in a flow-cell cell under LED illumination at 650 nm, giving rise to independant biosensors. Photocurrent intensity is recorded over time using duroquinone as an electron mediator. With *Spinacia oleracea* thylakoids immobilized in BSA-glutaraldehyde, LOD ranging from 12.7 nM to 41 nM for atrazine, diuron, terbuthylazine, desethylterbuthylazine and simazine were obtained. A low sensitivity to phenolic-type herbicides (dinoseb, ioxynil, bromoxynil) was noticed. With gelatin immobilization, the sensor is sensitive to phenolic compounds. This is attributed to differential diffusion of herbicides within the immobilization matrix. Noticeably, thylakoids from the *Senecio vulgaris* mutants are inhibited by diuron and linuron (urea-type herbicides), but they are only slightly inhibited by phenolic-type herbicides (when immobilized in gelatine) and not at all by tested triazines. Therefore, the use of an electrochemical array of immobilized thylakoids allows for the differentiation between sub-classes of herbicides. The assay was applied to detect the presence of total herbicides in real river samples (Po river, Italy) allowing to detect the total herbicide content in the nM range after sample preparation (concentration and dilution steps). An optical biosensor based on an array of PSII mutants was also reported (Giardi *et al.*, 2005). Fluorescence measurements were used for detection of herbicide subclasses (such as urea, diamine, triazine or dinitrophenol compounds) in river water. Thylakoids from various organisms (*Spinacia olearacea, Amaranthus retroflexus, Senecio vulgaris* and *Solanum Nigrum* wild-type or mutants selected from atrazine treated soil) were immobilized either by cross-linking with glutaraldehyde-BSA or by entrapment in gelatin. Inhibition of PSII fluorescence activity led to the detection of herbicides in river water at concentrations in the nM to µM range. An interesting innovation in this biosensor resides in the use and comparison of specific immobilized thylakoid membranes from wild-type and herbicide-resistant organisms, which allowed identification of herbicide subclasses. The same consortium also proposed in 2012 a photosynthetic biosensor, based on isolated thylakoid membranes from spinach (*Spinacea oleracea*) leaves, for the chronoamperometric detection of herbicides on gold SPE (Touloupakis *et al.*, 2012). The detection method was based on PSII inhibition. However, particular attention was paid to the immobilization of thylakoid membranes, with the use of laser-induced forward transfer (LIFT). Briefly, this method relies on the irradiation by a pulsed laser of a 40-nm titanium laser-absorbing layer, previously deposited on quartz plates. Thylakoid solutions were drop-casted on the titanium layer and the light-matter interaction of the laser with the absorbing layer caused the fast ejection of droplets of biological material onto a target substrate (the working electrode surface), placed in close vicinity. After optimizing the LIFT process and the SPE material, the authors obtained continuous layers of thylakoids, showing strong junctions with the electrodes. These systems were used for the detection of diuron and linuron, with detection limits of 8 nM (2 ppb) and 4 nM (1 ppb) respectively. The LIFT technology allowed the use of a much lower amount of photosynthetic material, with a higher photocurrent signal, and an excellent signal-to-noise ratio.

Thylakoid membranes were also recently used in 2022 by Lettieri *et al.* in the design of a simple electrochemical biosensor for the detection of photosynthetic herbicides of different chemical families, namely diuron, terbuthylazine and metribuzin (Lettieri *et al.*, 2022). The thylakoid membranes were immobilized by drop-casting and subsequent adsorption on unmodified carbon paper working electrodes. Mediatorless chronoamperometric measurements of PSII photocurrent inhibition by increasing concentrations of herbicides were performed. The authors reported LOD close to 0.5 µM (0.1 ppm) for the studied herbicides,

and also observed an interesting stability of up to 120 days at - 80 °C. They emphasized sustainability and low-cost of the biosensor.

Recent works reported photosynthetic biofuel cells for the detection of herbicides. Chloroplasts or thylakoids are immobilized at the anode allowing oxygen production under illumination. The electrical circuit is closed by a (bio)cathode catalyzing oxygen reduction. The overall system is a self-powered biosensor using only oxygen and water as substrates, both regenerated during the catalytic cycle (Figure 12).

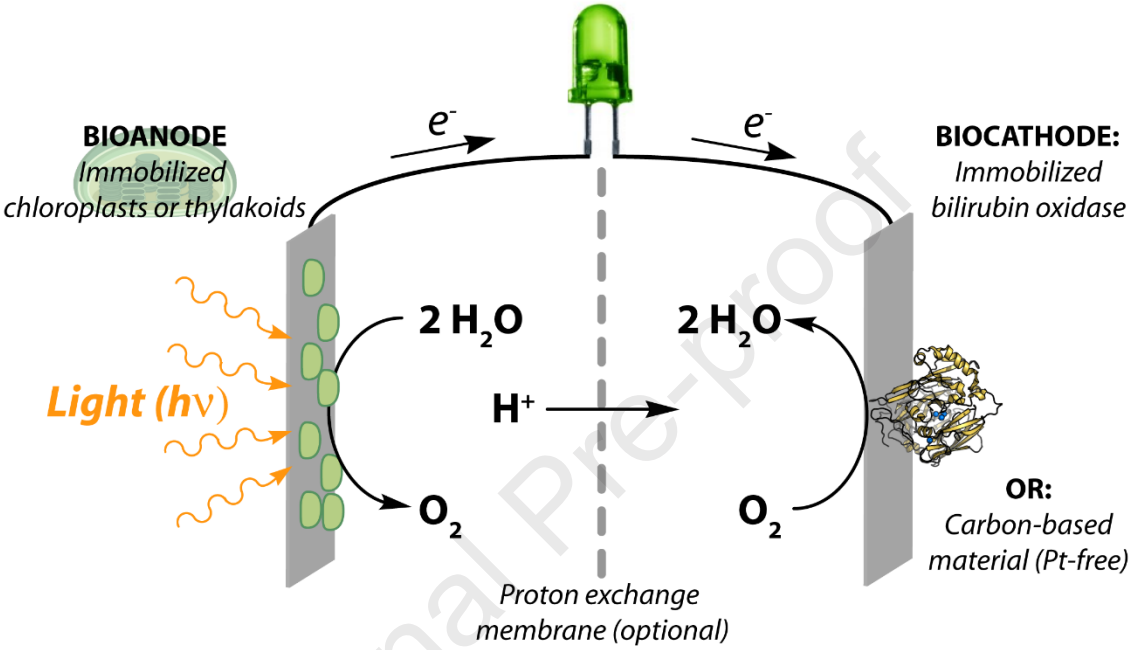

Figure 12. Biofuel cell operating with immobilized organelles (chloroplasts or thylakoid membranes) at the anode allowing oxygen production under illumination. Current generation in the electrical circuit (symbolized as a green LED) allows water production with or without immobilizing a copper oxidase (bilirubin oxidase) at the cathode.

In 2013, Rasmussen & Minteer developed a biosolar cell incorporating thylakoid membranes and used it for the detection of atrazine, bromacil and diuron (Rasmussen and Minteer, 2013). Thylakoid membranes from spinach chloroplasts were immobilized by adsorption on a carbon paper bioanode, which was coupled to an air-breathing platinum cathode (Figure 12). Under illumination, the bioanode catalyzed water oxidation into O_2 thus allowing direct electron transfer with the electrode and amperometric detection. Since the photoelectrocatalytic activity generates reactive oxygen species, catalase was also added for stabilization of the bioanode. The presence of photosynthesis-inhibiting herbicides in the biosolar cell resulted in a decrease in the measured current proportional to the herbicide concentration. LODs of 0.37 ppb, 0.21 ppb, 0.1 ppb and linear ranges extending up to 12 ppb, 16 ppb and 14 ppb were reported for atrazine, bromacil and diuron, respectively. This study describes an interesting concept of a self-powered biosolar cell-based herbicide sensor capable of direct photoelectrocatalysis. The authors underlined the system's lack of specificity for photosynthesis inhibiting-herbicides, making the device an alarm rather than a detection tool.

Another efficient photobiofuel cell was recently reported as a self-powered biosensor for photosynthesis-inhibiting pesticide detection (Masi *et al.*, 2020).The anode (a highly porous

gold electrode, hPG) was functionalized with spinach thylakoid membranes whereas the cathode (a buckypaper composed of compressed MWCNTs) was modified with bilirubin oxidase catalyzing the thylakoid (including PS II)-produced O_2 reduction and water production (Figure 12). The system thus mimics plant photosynthesis and respiration processes. In this system, no external artificial redox mediator was used. The electrical power was generated only from light absorption without consumption of any material. Photobioanodes were first incubated in a pesticide solution for 1.5 hours, before assembling the biofuel cell and then they were irradiated with light for 20 minutes before power output determination. In the presence of a commercial pesticide, Weed B Gon containing 2,4-D, a linear relationship was obtained between the produced power and Weed B Gon concentration, from 0.5 to 10 % v/v and the limit of detection was given as 0.15 % v/v. The authors do not explain the detection of group 4 herbicides (Weed B Gon composed of 2,4-D, dicamba and mesoprop mixture) acting as auxin mimics rather than inhibitors of the photosynthetic systems. The biofuel cell should be applied to other herbicides or pollutants affecting photosynthesis.

A rare biosensor based on intact chloroplasts was described by Grattieri *et al.* (Grattieri *et al.*, 2020). In intact chloroplasts, all the necessary enzymes are already present, ensuring enhanced stability and preventing catalase addition. Spinach chloroplasts were cross-linked on a carbon paper electrode using EGDGE, in order to obtain a bio-photoanode outperforming regular (non EGDGE-treated) anodes with a five-fold increase in photocurrent generation. The photoanode was then employed in a biosolar cell with an air-breathing activated carbon-based (Pt-free) cathode, for the self-powered detection of diuron. PSII inhibition by diuron was monitored under illumination, by amperometric measurement of the decrease in current density following herbicide addition, with a detection limit of 0.1 µM (23.3 ppb) and a linear range of 0.1-1 µM. In this work, the use of intact chloroplasts allowed for a simplified and cost-effective electrode architecture, with improved stability due to the presence of all the necessary enzymes responsible for photoprotection mechanisms.

4.2. Isolated PSII complex or other reaction centers

Once isolated from their natural environment, after a time- and cost-consuming extraction procedure, photosynthetic subcomponents suffer from unstability, particularly upon illumination. Immobilization on the transducer surface is thus crucial to obtain stable biosensors, with a good shelflife. As described hereafter and as shown in Table 5, several methods have been proposed in the literature, mainly for PSII particle immobilization. Adsorption or glutaraldehyde cross-linking have mainly been used. In the different systems, duroquinone was classically used as the mediator.

An amperometric biosensor for PSII-inhibiting herbicide detection was reported in 1998 (Koblizek *et al.*, 1998). Isolated PSII particles from the thermophilic cyanobacterium *Synechococcus elongatus* were immobilized under a dialysis membrane on a Clark oxygen electrode placed in a flow system, under illumination. In the presence of triazine-, urea-, and phenolic-type herbicides, release of oxygen was inhibited and could be measured. Detection limits of 0.5 nM and 2 nM were obtained for diuron and atrazine, respectively. Simazine, ioxynil, bromoxynil and dinoseb limits of detection were significantly higher. Good stability, reusability and regeneration of the biosensor were underlined by the authors. To assure mass production of the biosensors, Koblizek *et al.* (Koblížek *et al.*, 2002) immobilized PSII particles on graphite SPEs resulting in a biosensor that is specific to phenylurea and triazine herbicides,

but insensitive to phenolic ones. After partial purification of PSII from the thermophilic cyanobacterium *Synechococcus elongatus*, immobilization on the electrode surface was better achieved by cross-linking with glutaraldehyde in the presence of BSA. Compared to other biosensors based on chloroplasts or thylakoids, only ~10^{-11} moles of PSII were necessary. The electrode was placed in a flow cell under illumination by a photodiode (at 650 nm) in the presence of duroquinone as an artificial electron acceptor. Photoreduction of the mediator was detected by amperometry. The authors emphasized that silver ions (Ag^{+}) are inhibitors of the PSII. Therefore, the reference electrode should be placed after the working one in terms of the flow. The biosensor half-life was 24 h. Diuron (phenylurea), atrazine and simazine could be detected with LOD of 1 nM (0.23 ppb), 2 nM (0.43 ppb) and 4 nM (0.8 ppb), respectively. The same group proposed in 2005 another approach for the design of mediatorless PSII inhibition-based biosensors (Maly *et al.*, 2005). Working gold electrodes were functionalized with an electrodeposited conductive layer of poly-mercapto-*p*-benzoquinone (polySBQ). PSII particles isolated from the thermophilic cyanobacteria *Synechococcus bigranulatus* were then adsorbed on the polySBQ-covered electrodes and amperometric measurements of PSII activity were realized upon illumination by red LEDs (650 nm), the conductive polySBQ layer acting as a mediator between the immobilized PSII particles and the gold electrode. The detection of diuron by inhibition of PSII activity was studied and a detection limit of 0.7 nM (0.16 ppb) was reported. The authors underlined the biosensor's rapid response and its improved sensitivity compared to other published PSII-based biosensors, although the functionalized electrodes displayed a relatively poor reusability. Detection of photosynthetic herbicides based on isolated PSII complexes or on algae was also reported by the same authors in 2011 (Masojídek *et al.*, 2011). A comparison was performed between an amperometric biosensor based on PSII immobilization and a standard algal growth inhibition bioassay using intact algal cells. The PSII complex was isolated from a thermophilic cyanobacterium and immobilized on the surface of a Pt SPE by cross-linking with glutaraldehyde. Duroquinone was added as an artificial electron acceptor, in a flow system. Light pulses were applied, leading to a decrease of the signal during the illumination period in the presence of herbicides, due to the blocked electron transfer between the PSII complex and duroquinone. Diuron, atrazine and isoproturon concentration could be determined with detection limits of 1 nM (0.23 ppb), 1.6 nM (0.35 ppb) and 9.9 nM (2 ppb) with the biosensor and 110, 100 and 400 nM with the bioassay, respectively. Duration of measurements was also shorter with the biosensor (1 h compared to 72 h with the bioassay). The same group reported improvement of the biosensor sensitivity, with diuron that could be detected in a linear range extending from 1 to 100 nM (0.23 – 23.3 ppb), using the principle of synchronous detection (Krejci *et al.*, 2011).

Bhalla and Zazubovich proposed to immobilize BBY particles (PS-II enriched membrane fragments) by covalence on a carboxylated SAM at the surface of a gold SPE (Bhalla and Zazubovich, 2011) (Figure 11F). The reoxidation of the soluble duroquinol (reduced duroquinone) mediator was obtained as a photocurrent on the gold electrode. Compared to BBY particles immobilized in glutaraldehyde-BSA, which have been used previously by others, a lower current background was obtained and current intensity was 1.3 times higher. The response time decreased significantly from 20 minutes to less than 1 minute after illumination. Picric acid (proposed as a nitrophenolic herbicide based on its chemical structure) and atrazine were chosen as target herbicides. After a preconditioning phase of 10 min in the dark, the photocurrent was measured after an illumination of 10 sec. A sigmoidal decay response curve was used to determine the LOD for picric acid and atrazine, which were found to be 157

nM (36 ppb) and 1.15 nM (0.25 ppb), respectively. Interestingly, the non-selective early warning device could be reused after regeneration (washing), with a half-life of 24 h after storage at 4°C. It could also be stored at - 80°C without loss of activity.

As an alternative to PSII, the purple bacterium *Rhodobacter sphaeroides* reaction centre could also be used to develop biosensors for herbicide detection (Swainsbury *et al.*, 2014). This latter is relatively robust and generates photocurrent which is inhibited by atrazine and terbutryn (triazines), but not by phenylurea herbicides (such as diuron). Purified reaction centres were adsorbed on a gold electrode surface poised at – 100 mV *vs*. SCE. Photocurrent generation attenuation measured by chronoamperometry under appropriate illumination was correlated to herbicide concentration. Detection limits were close to 8 nM (1.9 ppb) and 50 nM (10.8 ppb) for terbutryn and atrazine, respectively. The authors indicated that the detection limit obtained in their work is higher than the one generally reported with PSII reaction centre (1 or 2 nM atrazine, close to the maximum admissible concentration in drinking water in the EU) but lower than the one reported in other works with the same purple bacterial reaction centres. Sensitivity needs to be improved, for instance through protein engineering. Nevertheless, the *Rhodobacter sphaeroides* reaction centre is natively selective for triazine herbicides whereas PSII is not very selective.

5. Tissues

As presented afterwards, plant tissue-based biosensors reported for herbicide detection are based on potato or apple, known for their high content in PPO. Atrazine detection could thus be performed, based on inhibition of PPO activity. Such biosensors present a long lifetime (high stability) but a low sensitivity.

A plant tissue based amperometric biosensor was reported by Mazzei *et al.* (1995) for determination of atrazine (Mazzei *et al.*, 1995). A thin slice of potato (*Solanum tuberosum*) tissue containing PPO was deposited on a Clark oxygen electrode. After a 20 min incubation time in the presence of the herbicide, the percentage of enzyme activity inhibition could be correlated to atrazine concentrations with a linear range extending from 20 to 130 µM (4.3 - 28 ppm) and a detection limit of 10 µM (2.2 ppm). Organophosphorous and carbamate pesticides did not interfere. The lifetime of the biosensor was 8-14 days and was improved by washing the sensor's tip between measurements. Contrary to biosensors based on the immobilization of purified enzymes, the tissue-based biocatalytic layer can be easily changed and gives rise to a so-called "partially disposable" system. Detection of spiked samples of flowing water containing atrazine was also validated.

Another tissue-based amperometric biosensor was reported in 2008 (Majidi *et al.*, 2008). An apple tissue also containing PPO activity was immobilized in a silica sol-gel / carbon paste matrix. The percentage of inhibition was determined by measuring the current response to dopamine at 400 mV *vs*. SCE, in the presence of atrazine. A linear range between 10 µM and 100 µM (2.2 - 22 ppm) was observed, with a detection limit of 5.5 µM (1.2 ppm). Inhibition of atrazine was shown to be competitive. The response current of the biosensor decreased to 20 % after 50 days. The lifetime was not specified.

6. Conclusion

Biosensors have become promising and important modern tools for the detection of environmental pollutants such as herbicides. As underlined in a recent review (Arkhypova *et al.*, 2023), it is important to keep in mind that biosensors can complement traditional analytical methods. They can be used as rapid and low-cost early warning screening devices, signaling the eventual presence of toxic substances in a sample. If necessary, more sensitive, time-consuming and costly conventional chromatographic and mass spectrometry methods can then be used.

Biosensors suffer from low selectivity and are mainly intended for on-site alarm systems capable of detecting classes of compounds, well suited to screening analysis. Simple pre-treatment of sample by solid phase extraction column could improve the selectivity, by separating heavy metals from pesticides for instance, before analysis. Nevertheless, limiting the number of steps required for analysis remains the preferred option.

Figure 13 presents the repartition of enzyme- and photosynthesis-based biosensors according to the herbicide group detected. Structures of the most detected herbicides are also presented. It can be noticed that the most detected herbicides belong to the group 5, triazines (5t, such as atrazine) and ureas (5u, such as diuron), representing more than 60 % of the total detected herbicides. These pesticides are photosynthetic herbicides that inhibit PS II. Apart from the highly represented group 5, the main other detected herbicides belong to groups 4 (auxin mimics, such as 2,4-D) and 9 (glyphosate). The photosynthetic group 22 (acting on PSI, such as paraquat) is also well represented (6 %).

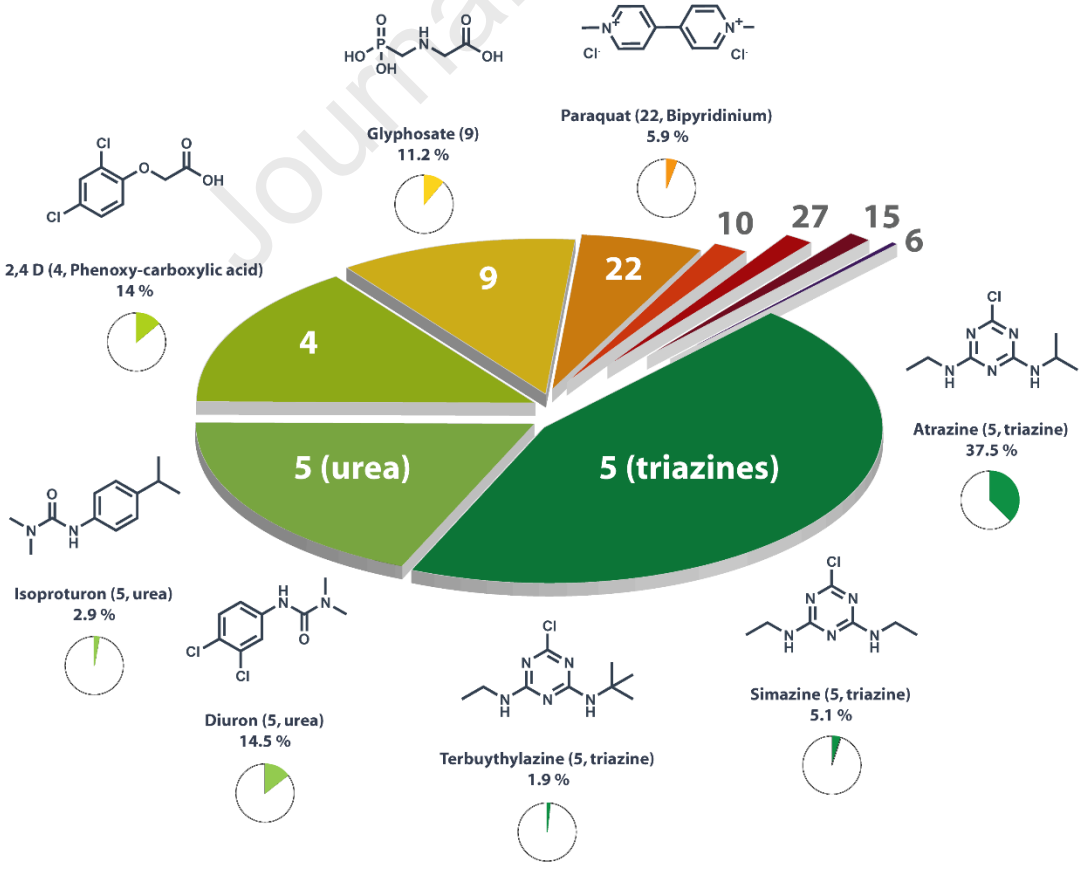

Figure 13. Repartition of the number of published biosensors by herbicide group (HRAC classification). The structures of the most studied herbicides (>1.9 %) are provided with the percentage of biosensors depicted as a pie chart. Data are obtained from the Web of Science (2023, july, 28th) using the following request: “enzyme or oxidase or peroxidase or tyrosinase or urease or phosphatase or whole cell or algae or alga or algal or bacteria or bacterial or thylakoids or PSII or photosystem” AND “biosensor” AND “herbicide or atrazine or simazine or terbuthylazine or bromoxynil or prometryne or mesotrione or sulcotrione or diuron or DCMU or linuron or chlorotoluron or chlortoluron) or isoproturon or 2,4-D or MCPA or dicamba or bromacil or glyphosate or glufosinate or alachlor or paraquat”.

Atrazine can be used as an example, in order to compare enzymatic and photosynthetic biosensors. The detection limits obtained with sub-cellular systems or with whole-cell systems are rather high. Only one recent report based on fluorescence detection and including CB nanomaterials with algae could reach a 1 ppt LOD (Scognamiglio *et al.*, 2019). On the other hand, tyrosinase-based biosensors could reach 0.1 ppt LOD using AuNPs (Kim *et al.*, 2008) or TiO_2 nanotubes (Yu *et al.*, 2010) or even less than 0.1 ppt using mesoporous biocarbon and carbon dot ECL (Wu *et al.*, 2019) or graphene-based FETs (Cao *et al.*, 2016). Enzymatic biosensors thus appear as more sensitive to atrazine than photosynthesis biosensors. In addition, nanomaterials are classically used to improve the sensitivity, and many nanomaterial-based (bio)sensors are described in the literature, as recently reviewed for the detection of glyphosate for instance (Zúñiga *et al.*, 2022).

Recent advances in the biosensor field include the development of nanozymes. Nanozymes are non biological nanomaterials behaving as enzymes whose development began in 2014 (Lin *et al.*, 2014)(Huang *et al.*, 2019) and is still in progress. These low-cost nanomaterial-based artificial enzyme mimics (mainly peroxidase and oxidase mimics) do not suffer from the well-known instability issues associated with the use of enzymes. However, they exhibit low catalytic activity, poor substrate selectivity and potential toxicity. As reported in a recent review dealing with detection of pesticides using nanozymes (Naveen Prasad *et al.*, 2021), pesticides can inhibit or modify nanozyme activity. Glyphosate detection has recently been detected by using an organic compound-based peroxidase-mimicking nanozyme (Lee and Kamruzzaman, 2023). This system is based on a relatively non-specific inhibition mechanism in which glyphosate is adsorbed onto the nanozyme, blocking its activity. Atrazine detection using nanozymes has also recently been described, with a sensor in which atrazine traps a redox dye by establishing hydrogen bonds, preventing its oxidation and the generation of a colorimetric signal (Boruah and Das, 2020). These studies highlight the need to improve the specificity of herbicide detection systems based on nanozymes.

As recently mentioned by Mazuryk *et al* (Mazuryk *et al.*, 2023), conventional (bio)sensors will soon be replaced by smart material-based (bio)sensors including smartphone-integrated (bio)sensors for instance. Indeed, miniaturized biosensor platforms capable of collecting and transmitting data *via* smartphones or other wireless devices should simplify analysis and increase system portability. In this respect, several modern lab-in-a-syringe devices have recently been described. Smartphone-based colorimetric and fluorescent dual-mode detection was reported for organophosphorous pesticides including glyphosate, with a bioassay based on AChE inhibition (Wei *et al.*, 2021). A portable paper-based lab-in-a-syringe device was also recently described for 2,4-D detection (Tong *et al.*, 2023). In this study, cascade reactions starting with the inhibition of alkaline phosphatase by 2,4-D were constructed, ending with the

modification of the color of several fluorescent probes (blue, yellow and red emission systems), which could be analyzed *via* a smartphone application.

Biosensors for herbicide or pesticide detection are not always used for the analysis of real samples. When they do, the detection is mainly performed in environmental matrices and without systematic validation by the regulatory HPLC-MS techniques. Bioaccumulation in animal tissues and hazardous effects on living organisms should be carefully considered. That is the reason why application in biological fluids needs to be further explored, as recently underlined by Fama *et al.* (Fama *et al.*, 2023). This would also constitute an opportunity to establish links with the considerable advances that have been made in the field of medical biosensors.

Based on the work presented in this review, biosensor devices have undergone significant evolution in recent decades. However, their use for on-field environmental monitoring still lags behind their use in medical applications. In environment area, the potential market remains to be established and further initiatives are needed to develop more reliable devices, which could accelerate the small-scale detection of pesticides, and offer opportunities for significant commercial exploitation. Most of biosensors for herbicide detection are in the proof-of-concept state. Versatility has been proven, with interchangeable biorecognition elements and detection of a broad spectrum of compound classes. These early warning devices present some advantages, as they are reliable and sensitive, able to detect variable environmental samples by respecting the legislation directives. The limited stability of the bioelement still acts as a brake on the commercial development of environmental biosensors. On-field stability, operating lifetime and reusability are of critical importance and represent a real challenge, hampering their current exploitation and marketability. Development of miniaturized, multi-biosensors and the use of nanomaterials continues to draw much research effort. The major developments focus on enhancing sensitivity and stability. Less attention is devoted to improving the stability of enzymes, which continues to be a bottleneck in the development of biosensors. Solutions might be the use of enzymes from extremophiles or genetically modified enzymes and interaction between enzymes and nanomaterials. Specificity could also be improved to detect a given herbicide. Miniaturized and small portable automatic biosensors for on-site alarm devices can be designed by using modern technologies and incorporating some low-cost and pocket-size portable potentiostats or fluorometers available on the market. The use of intelligent instrumentation, electronics, and multivariate signal processing methods such as chemometrics and artificial neural networks could be useful.

7. References

Abu-Ali, Hisham, Nabok, A., Smith, T.J., 2019. Electrochemical inhibition bacterial sensor array for detection of water pollutants: artificial neural network (ANN) approach. Anal. Bioanal. Chem. 411, 7659–7668. https://doi.org/10.1007/s00216-019-01853-8

Abu-Ali, H., Nabok, A., Smith, T.J., Al-Shanawa, M., 2019. Development of a Novel Electrochemical Inhibition Sensor Array Based on Bacteria Immobilized on Modified Screen-Printed Gold Electrodes for Water Pollution Detection. Bionanoscience 9, 345–355. https://doi.org/10.1007/s12668-019-00619-x

Andreou, V.G., Clonis, Y.D., 2002. Novel fiber-optic biosensor based on immobilized glutathione S-transferase and sol-gel entrapped bromcresol green for the determination

of atrazine. Anal. Chim. Acta 460, 151–161. https://doi.org/10.1016/S0003-2670(02)00250-7

Anh, T.M., Dzyadevych, S. V., Van, M.C., Renault, N.J., Duc, C.N., Chovelon, J.M., 2004. Conductometric tyrosinase biosensor for the detection of diuron, atrazine and its main metabolites. Talanta 63, 365–370. https://doi.org/10.1016/j.talanta.2003.11.008

Antonacci, A., Attaallah, R., Arduini, F., Amine, A., Giardi, M.T., Scognamiglio, V., 2021. A dual electro-optical biosensor based on Chlamydomonas reinhardtii immobilised on paper-based nanomodified screen-printed electrodes for herbicide monitoring. J. Nanobiotechnology 19, 1–13. https://doi.org/10.1186/s12951-021-00887-4

Antonacci, A., Frisulli, V., Carvalho, L.B., Fraceto, L.F., Miranda, B., De Stefano, L., Johanningmeier, U., Giardi, M.T., Scognamiglio, V., 2023. An All-Green Photo-Electrochemical Biosensor Using Microalgae Immobilized on Eco-Designed Lignin-Based Screen-Printed Electrodes to Detect Sustainable Nanoherbicides. Int. J. Mol. Sci. 24, 1–12. https://doi.org/10.3390/ijms241210088

Arduini, F., Cinti, S., Caratelli, V., Amendola, L., Palleschi, G., Moscone, D., 2019. Origami multiple paper-based electrochemical biosensors for pesticide detection. Biosens. Bioelectron. 126, 346–354. https://doi.org/10.1016/j.bios.2018.10.014

Arkhypova, V., Soldatkin, O., Soldatkin, A., Dzyadevych, S., 2023. Electrochemical Biosensors Based on Enzyme Inhibition Effect. Chem. Rec. 202300214. https://doi.org/10.1002/tcr.202300214

Attaallah, R., Antonacci, A., Mazzaracchio, V., Moscone, D., Palleschi, G., Arduini, F., Amine, A., Scognamiglio, V., 2020. Carbon black nanoparticles to sense algae oxygen evolution for herbicides detection: Atrazine as a case study. Biosens. Bioelectron. 159. https://doi.org/10.1016/j.bios.2020.112203

Besombes, J.L., Cosnier, S., Labbé, P., Reverdy, G., 1995. A biosensor as warning device for the detection of cyanide, chlorophenols, atrazine and carbamate pesticides. Anal. Chim. Acta 311, 255–263. https://doi.org/10.1016/0003-2670(94)00686-G

Bettazzi, F., Laschi, S., Mascini, M., 2007. One-shot screen-printed thylakoid membrane-based biosensor for the detection of photosynthetic inhibitors in discrete samples. Anal. Chim. Acta 589, 14–21. https://doi.org/10.1016/j.aca.2007.02.062

Bhalla, V., Zazubovich, V., 2011. Self-assembly and sensor response of photosynthetic reaction centers on screen-printed electrodes. Anal. Chim. Acta 707, 184–190. https://doi.org/10.1016/j.aca.2011.09.020

Bollella, P., Fusco, G., Tortolini, C., Sanzò, G., Antiochia, R., Favero, G., Mazzei, F., 2016. Inhibition-based first-generation electrochemical biosensors: Theoretical aspects and application to 2,4-dichlorophenoxy acetic acid detection. Anal. Bioanal. Chem. 408, 3203–3211. https://doi.org/10.1007/s00216-016-9389-z

Boron, I., Juárez, A., Battaglini, F., 2020. Portable Microalgal Biosensor for Herbicide Monitoring. ChemElectroChem 7, 1623–1630. https://doi.org/10.1002/celc.202000210

Boruah, P.K., Das, M.R., 2020. Dual responsive magnetic Fe3O4-TiO2/graphene nanocomposite as an artificial nanozyme for the colorimetric detection and photodegradation of pesticide in an aqueous medium. J. Hazard. Mater. 385, 121516. https://doi.org/10.1016/j.jhazmat.2019.121516

Botrè, C., Botrè, F., Mazzei, F., Podestà, E., 2000. Inhibition-based biosensors for the detection of environmental contaminants: Determination of 2,4-dichlorophenoxyacetic acid. Environ. Toxicol. Chem. 19, 2876–2881. https://doi.org/10.1002/etc.5620191204

Braham, Y., Barhoumi, H., Maaref, A., 2013. Urease capacitive biosensors using functionalized magnetic nanoparticles for atrazine pesticide detection in environmental samples. Anal. Methods 5, 4898–4904. https://doi.org/10.1039/c3ay40579f

Butmee, P., Tumcharern, G., Songsiriritthigul, C., Durand, M.J., Thouand, G., Kerr, M., Kalcher, K., Samphao, A., 2021. Enzymatic electrochemical biosensor for glyphosate detection based on acid phosphatase inhibition. Anal. Bioanal. Chem. 413, 5859–5869. https://doi.org/10.1007/s00216-021-03567-2

Cahuantzi-Muñoz, S.L., González-Fuentes, M.A., Ortiz-Frade, L.A., Torres, E., Ţălu, Ş., Trejo, G., Méndez-Albores, A., 2019. Electrochemical Biosensor for Sensitive

Quantification of Glyphosate in Maize Kernels. Electroanalysis 31, 927–935. https://doi.org/10.1002/elan.201800759

Campanella, L., Bonanni, A., Martini, E., Todini, N., Tomassetti, M., 2005. Determination of triazine pesticides using a new enzyme inhibition tyrosinase OPEE operating in chloroform. Sensors Actuators, B Chem. 111–112, 505–514. https://doi.org/10.1016/j.snb.2005.03.082

Campanella, L., Dragone, R., Lelo, D., Martini, E., Tomassetti, M., 2006. Tyrosinase inhibition organic phase biosensor for triazinic and benzotriazinic pesticide analysis (part two). Anal. Bioanal. Chem. 384, 915–921. https://doi.org/10.1007/s00216-005-0175-6

Cao, T.T., Nguyen, V.C., Nguyen, H.B., Bui, H.T., Vu, T.T., Phan, N.H., Phan, B.T., Hoang, L., Bayle, M., Paillet, M., Sauvajol, J.L., Phan, N.M., Tran, D.L., 2016. Fabrication of few-layer graphene film based field effect transistor and its application for trace-detection of herbicide atrazine. Adv. Nat. Sci. Nanosci. Nanotechnol. 7. https://doi.org/10.1088/2043-6262/7/3/035007

Caratelli, V., Fegatelli, G., Moscone, D., Arduini, F., 2022. A paper-based electrochemical device for the detection of pesticides in aerosol phase inspired by nature: A flower-like origami biosensor for precision agriculture. Biosens. Bioelectron. 205, 114119. https://doi.org/10.1016/j.bios.2022.114119

Chouler, J., Di Lorenzo, M., 2019. Pesticide detection by a miniature microbial fuel cell under controlled operational disturbances. Water Sci. Technol. 79, 2231–2241. https://doi.org/10.2166/wst.2019.207

Colozza, N., Caratelli, V., Moscone, D., Arduini, F., 2021. Paper-based devices as new smart analytical tools for sustainable detection of environmental pollutants. Case Stud. Chem. Environ. Eng. 4, 100167. https://doi.org/10.1016/j.cscee.2021.100167

Congur, G., 2021. Electrochemical investigation of the interaction of 2,4-D and double stranded DNA using pencil graphite electrodes. Turkish J. Chem. 45, 600–615. https://doi.org/10.3906/kim-2011-56

Conrad, R., Büchel, C., Wilhelm, C., Arsalane, W., Berkaloff, C., Duval, J.C., 1993. Changes in yield of in-vivo fluorescence of chlorophyll a as a tool for selective herbicide monitoring. J. Appl. Phycol. 5, 505–516. https://doi.org/10.1007/BF02182509

Da Silva, A.C.N., Deda, D.K., da Róz, A.L., Prado, R.A., Carvalho, C.C., Viviani, V., Leite, F.L., 2013. Nanobiosensors based on chemically modified AFM probes: A useful tool for metsulfuron-methyl detection. Sensors (Switzerland) 13, 1477–1489. https://doi.org/10.3390/s130201477

Das, N., Reardon, K.F., 2012. Fiber-Optic Biosensor for the Detection of Atrazine: Characterization and Continuous Measurements. Anal. Lett. 45, 251–261. https://doi.org/10.1080/00032719.2011.633192

Delprat, N., Martins, L.O., Blum, L.J., Aymard, C.M.G., Leca-Bouvier, B., Octobre, G., Doumèche, B., 2023. Biosensors and Bioelectronics User-friendly one-step disposable signal-on bioassay for glyphosate detection in water samples. Biosens. Bioelectron. 241, 1–11. https://doi.org/10.1016/j.bios.2023.115689

Délye, C., Jasieniuk, M., Le Corre, V., 2013. Deciphering the evolution of herbicide resistance in weeds. Trends Genet. 29, 649–658. https://doi.org/10.1016/j.tig.2013.06.001

Döring, J., Rettke, D., Rödel, G., Pompe, T., Ostermann, K., 2019. Surface functionalization by hydrophobin-EPSPS fusion protein allows for the fast and simple detection of glyphosate. Biosensors 9. https://doi.org/10.3390/bios9030104

Durrieu, C., Guedri, H., Fremion, F., Volatier, L., 2011. Unicellular algae used as biosensors for chemical detection in Mediterranean lagoon and coastal waters. Res. Microbiol. 162, 908–914. https://doi.org/10.1016/j.resmic.2011.07.002

El Kaoutit, M., Bouchta, D., Zejli, H., Izaoumen, N., Temsamani, K.R., 2004. A simple conducting polymer-based biosensor for the detection of atrazine. Anal. Lett. 37, 1671–1681. https://doi.org/10.1081/AL-120037595

Euzet, P., Giardi, M.T., Rouillon, R., 2005. A crosslinked matrix of thylakoids coupled to the

fluorescence transducer in order to detect herbicides. Anal. Chim. Acta 539, 263–269. https://doi.org/10.1016/j.aca.2005.02.077

Fama, F., Feltracco, M., Moro, G., Barbaro, E., Bassanello, M., Gambaro, A., Zanardi, C., 2023. Pesticides monitoring in biological fluids: Mapping the gaps in analytical strategies. Talanta 253, 123969. https://doi.org/10.1016/j.talanta.2022.123969

Fang, L., Liao, X., Jia, B., Shi, L., Kang, L., Zhou, L., Kong, W., 2020. Recent progress in immunosensors for pesticides. Biosens. Bioelectron. 164, 112255. https://doi.org/10.1016/j.bios.2020.112255

Frense, D., Müller, A., Beckmann, D., 1998. Detection of environmental pollutants using optical biosensor with immobilized algae cells. Sensors Actuators, B Chem. 51, 256–260. https://doi.org/10.1016/S0925-4005(98)00203-2

Gianvittorio, S., Gualandi, I., Tonelli, D., 2023. ALP-Based Biosensors Employing Electrodes Modified with Carbon Nanomaterials for Pesticides Detection. Molecules 28. https://doi.org/10.3390/molecules28041532

Giardi, M.T., Guzzella, L., Euzet, P., Rouillon, R., Esposito, D., 2005. Detection of herbicide subclasses by an optical multibiosensor based on an array of photosystem II mutants. Environ. Sci. Technol. 39, 5378–5384. https://doi.org/10.1021/es040511b

Gonzalez Olias, L., Cameron, P.J., Di Lorenzo, M., 2019. Effect of Electrode Properties on the Performance of a Photosynthetic Microbial Fuel Cell for Atrazine Detection. Front. Energy Res. 7, 1–11. https://doi.org/10.3389/fenrg.2019.00105

Grattieri, M., Chen, H., Minteer, S.D., 2020. Chloroplast biosolar cell and self-powered herbicide monitoring. Chem. Commun. 56, 13161–13164. https://doi.org/10.1039/d0cc03787g

Grattieri, M., Rhodes, Z., Hickey, D.P., Beaver, K., Minteer, S.D., 2019. Understanding Biophotocurrent Generation in Photosynthetic Purple Bacteria. ACS Catal. 9, 867–873. https://doi.org/10.1021/acscatal.8b04464

Guan, Y., Liu, L., Chen, C., Kang, X., Xie, Q., 2016. Effective immobilization of tyrosinase via enzyme catalytic polymerization of L-DOPA for highly sensitive phenol and atrazine sensing. Talanta 160, 125–132. https://doi.org/10.1016/j.talanta.2016.07.003

Haddaoui, M., Raouafi, N., 2015. Chlortoluron-induced enzymatic activity inhibition in tyrosinase/ZnO NPs/SPCE biosensor for the detection of ppb levels of herbicide. Sensors Actuators, B Chem. 219, 171–178. https://doi.org/10.1016/j.snb.2015.05.023

Haigh-Flórez, D., De la Hera, C., Costas, E., Orellana, G., 2014. Microalgae dual-head biosensors for selective detection of herbicides with fiber-optic luminescent O2 transduction. Biosens. Bioelectron. 54, 484–491. https://doi.org/10.1016/j.bios.2013.10.062

Huang, Y., Ren, J., Qu, X., 2019. Nanozymes: Classification, Catalytic Mechanisms, Activity Regulation, and Applications. Chem. Rev. 119, 4357–4412. https://doi.org/10.1021/acs.chemrev.8b00672

Husu, I., Rodio, G., Touloupakis, E., Lambreva, M.D., Buonasera, K., Litescu, S.C., Giardi, M.T., Rea, G., 2013. Insights into photo-electrochemical sensing of herbicides driven by Chlamydomonas reinhardtii cells. Sensors Actuators, B Chem. 185, 321–330. https://doi.org/10.1016/j.snb.2013.05.013

Jiang, X., Li, D., Xu, X., Ying, Y., Li, Y., Ye, Z., Wang, J., 2008. Immunosensors for detection of pesticide residues. Biosens. Bioelectron. 23, 1577–1587. https://doi.org/10.1016/j.bios.2008.01.035

Johnson, Z.T., Jared, N., Peterson, J.K., Li, J., Smith, E.A., Walper, S.A., Hooe, S.L., Breger, J.C., Medintz, I.L., Gomes, C., Claussen, J.C., 2022. Enzymatic Laser-Induced Graphene Biosensor for Electrochemical Sensing of the Herbicide Glyphosate. Glob. Challenges 6, 2200057. https://doi.org/10.1002/gch2.202200057

Kergaravat, S. V., Fabiano, S.N., Soutullo, A.R., Hernández, S.R., 2021. Comparison of the performance analytical of two glyphosate electrochemical screening methods based on peroxidase enzyme inhibition. Microchem. J. 160. https://doi.org/10.1016/j.microc.2020.105654

Kim, G.Y., Shim, J., Kang, M.S., Moon, S.H., 2008. Preparation of a highly sensitive enzyme

electrode using gold nanoparticles for measurement of pesticides at the ppt level. J. Environ. Monit. 10, 632–637. https://doi.org/10.1039/b800553b

Koblížek, M., Malý, J., Masojídek, J., Komenda, J., Kučera, T., Giardi, M.T., Mattoo, A.K., Pilloton, R., 2002. A biosensor for the detection of triazine and phenylurea herbicides designed using Photosystem II coupled to a screen-printed electrode. Biotechnol. Bioeng. 78, 110–116. https://doi.org/10.1002/bit.10190

Koblizek, M., Masojidek, J., Komenda, J., Kucera, T., Pilloton, R., Mattoo, A.K., Giardi, M.T., 1998. A sensitive photosystem II-based biosensor for detection of a class of herbicides. Biotechnol. Bioeng. 60, 664–669. https://doi.org/10.1002/(SICI)1097-0290(19981220)60:6<664::AID-BIT3>3.0.CO;2-B

Krejci, J., Ondruch, V., Maly, J., Stofik, M., Krejcova, D., Vranova, H., 2011. High sensitivity biosensor measurement based on synchronous detection. J. Photochem. Photobiol. B Biol. 102, 192–199. https://doi.org/10.1016/j.jphotobiol.2010.12.003

Kucherenko, I.S., Chen, B., Johnson, Z., Wilkins, A., Sanborn, D., Figueroa-Felix, N., Mendivelso-Perez, D., Smith, E.A., Gomes, C., Claussen, J.C., 2021. Laser-induced graphene electrodes for electrochemical ion sensing, pesticide monitoring, and water splitting. Anal. Bioanal. Chem. 413, 6201–6212. https://doi.org/10.1007/s00216-021-03519-w

Kung, C. Te, Hou, C.Y., Wang, Y.N., Fu, L.M., 2019. Microfluidic paper-based analytical devices for environmental analysis of soil, air, ecology and river water. Sensors Actuators, B Chem. 301, 126855. https://doi.org/10.1016/j.snb.2019.126855

Laberge, D., Chartrand, J., Rouillon, R., Carpentier, R., 1999. In vitro phytotoxicity screening test using immobilized spinach thylakoids. Environ. Toxicol. Chem. 18, 2851–2858. https://doi.org/10.1002/etc.5620181228

Le Gall, J., Vasilijević, S., Battaglini, N., Mattana, G., Noël, V., Brayner, R., Piro, B., 2021. Algae-functionalized hydrogel-gated organic field-effect transistor. Application to the detection of herbicides. Electrochim. Acta 372. https://doi.org/10.1016/j.electacta.2021.137881

Lee, D.H., Kamruzzaman, M., 2023. Organic compound-based nanozymes for agricultural herbicide detection. Nanoscale 15, 12954–12960. https://doi.org/10.1039/d3nr02025h

Lettieri, S., Battaglino, B., Sacco, A., Saracco, G., Pagliano, C., 2022. A green and easy-to-assemble electrochemical biosensor based on thylakoid membranes for photosynthetic herbicides detection. Biosens. Bioelectron. 198, 113838. https://doi.org/10.1016/j.bios.2021.113838

Li, J., Wei, X., Peng, T., 2005. Fabrication of herbicide biosensors based on the inhibition of enzyme activity that catalyzes the scavenging of hydrogen peroxide in a thylakoid membrane. Anal. Sci. 21, 1217–1222. https://doi.org/10.2116/analsci.21.1217

Lin, Y., Ren, J., Qu, X., 2014. Catalytically active nanomaterials: A promising candidate for artificial enzymes. Acc. Chem. Res. 47, 1097–1105. https://doi.org/10.1021/ar400250z

Liu, F., Zhong, A., Xu, Q., Cao, H., Hu, X., 2016. Inhibition of 2,4-Dichlorophenoxyacetic Acid to Catalase Immobilized on Hierarchical Porous Calcium Phosphate: Kinetic Aspect and Electrochemical Biosensor Construction. J. Phys. Chem. C 120, 15966–15975. https://doi.org/10.1021/acs.jpcc.5b12559

Liu, H., Chen, P., Liu, Z., Liu, J., Yi, J., Xia, F., Zhou, C., 2020. Electrochemical luminescence sensor based on double suppression for highly sensitive detection of glyphosate. Sensors Actuators, B Chem. 304, 127364. https://doi.org/10.1016/j.snb.2019.127364

Loh, K.S., Lee, Y.H., Musa, A., Salmah, A.A., Zamri, I., 2008. Use of Fe3O4 nanoparticles for enhancement of biosensor response to the herbicide 2,4-dichlorophenoxyacetic acid. Sensors 8, 5775–5791. https://doi.org/10.3390/s8095775

Majdinasab, M., Daneshi, M., Louis Marty, J., 2021. Recent developments in non-enzymatic (bio)sensors for detection of pesticide residues: Focusing on antibody, aptamer and molecularly imprinted polymer. Talanta 232, 122397. https://doi.org/10.1016/j.talanta.2021.122397

Majidi, M.R., Asadpour-Zeynali, K., Gholizadeh, S., 2008. Sol-gel-derived biosensor based

on plant tissue: The inhibitory effect of atrazine on polyphenol oxidase activity for determination of atrazine. J. Chinese Chem. Soc. 55, 522–528. https://doi.org/10.1002/jccs.200800077

Maly, J., Masojidek, J., Masci, A., Ilie, M., Cianci, E., Foglietti, V., Vastarella, W., Pilloton, R., 2005. Direct mediatorless electron transport between the monolayer of photosystem II and poly(mercapto-*p*-benzoquinone) modified gold electrode - New design of biosensor for herbicide detection. Biosens. Bioelectron. 21, 923–932. https://doi.org/10.1016/j.bios.2005.02.013

Martinazzo, J., Muenchen, D.K., Brezolin, A.N., Cezaro, A.M., Rigo, A.A., Manzoli, A., Hoehne, L., Leite, F.L., Steffens, J., Steffens, C., 2018. Cantilever nanobiosensor using tyrosinase to detect atrazine in liquid medium. J. Environ. Sci. Heal. - Part B Pestic. Food Contam. Agric. Wastes 53, 229–236. https://doi.org/10.1080/03601234.2017.1421833

Marty, J.L., Mionetto, N., Noguer, T., Ortega, F., Roux, C., 1993. Enzyme sensors for the detection of pesticides. Biosens. Bioelectron. 8, 273–280. https://doi.org/10.1016/0956-5663(93)85007-B

Masi, M., Bollella, P., Riedel, M., Lisdat, F., Katz, E., 2020. Photobiofuel cell with sustainable energy generation based on micro/nanostructured electrode materials. ACS Appl. Energy Mater. 3, 9543–9549. https://doi.org/10.1021/acsaem.0c02169

Masojídek, J., Souček, P., Máchová, J., Frolík, J., Klem, K., Malý, J., 2011. Detection of photosynthetic herbicides: Algal growth inhibition test vs. electrochemical photosystem II biosensor. Ecotoxicol. Environ. Saf. 74, 117–122. https://doi.org/10.1016/j.ecoenv.2010.08.028

Mazuryk, J., Klepacka, K., Kutner, W., Sharma, P.S., 2023. Glyphosate Separating and Sensing for Precision Agriculture and Environmental Protection in the Era of Smart Materials. Environ. Sci. Technol. https://doi.org/10.1021/acs.est.3c01269

Mazzei, F., Botrè, F., Lorenti, G., Simonetti, G., Porcelli, fernando, Scibona, G., Botrè, C., 1995. Plant tissue electrode for the determination of atrazine. Anal. Chim. Acta 316, 79–82. https://doi.org/10.1016/0003-2670(95)00343-X

Mazzei, F., Botrè, F., Montilla, S., Pilloton, R., Podestà, E., Botrè, C., 2004. Alkaline phosphatase inhibition based electrochemical sensors for the detection of pesticides. J. Electroanal. Chem. 574, 95–100. https://doi.org/10.1016/j.jelechem.2004.08.004

McArdle, F.A., Persaud, K.C., 1993. Development of an enzyme-based biosensor for atrazine detection. Analyst 4, 419–423. https://doi.org/10.1039/AN9931800419

Moro, G., Fama, F., Colozza, N., Gambaro, A., Bassanello, M., Arduini, F., Zanardi, C., 2023. A paper-based device for glyphosate electrochemical detection in human urine: A case study to demonstrate how the properties of the paper can solve analytical issues. Green Anal. Chem. 7, 100076. https://doi.org/10.1016/j.greeac.2023.100076

Muenchen, D.K., Martinazzo, J., Brezolin, A.N., de Cezaro, A.M., Rigo, A.A., Mezarroba, M.N., Manzoli, A., de Lima Leite, F., Steffens, J., Steffens, C., 2018. Cantilever Functionalization Using Peroxidase Extract of Low Cost for Glyphosate Detection. Appl. Biochem. Biotechnol. 186, 1061–1073. https://doi.org/10.1007/s12010-018-2799-y

Naessens, M., Leclerc, J.C., Tran-Minh, C., 2000. Fiber optic biosensor using Chlorella vulgaris for determination of toxic compounds. Ecotoxicol. Environ. Saf. 46, 181–185. https://doi.org/10.1006/eesa.1999.1904

Nageib, A.M., Halim, A.A., Nordin, A.N., Ali, F., 2023. Recent Applications of Molecularly Imprinted Polymers (MIPs) on Screen-Printed Electrodes for Pesticide Detection. J. Electrochem. Sci. Technol. 14, 1–14. https://doi.org/10.33961/jecst.2022.00654

Naveen Prasad, S., Bansal, V., Ramanathan, R., 2021. Detection of pesticides using nanozymes: Trends, challenges and outlook. TrAC - Trends Anal. Chem. 144, 116429. https://doi.org/10.1016/j.trac.2021.116429

Nguyen-Ngoc, H., Tran-Minh, C., 2007. Fluorescent biosensor using whole cells in an inorganic translucent matrix. Anal. Chim. Acta 583, 161–165. https://doi.org/10.1016/j.aca.2006.10.005

Odaci, D., Sezgintürk, M.K., Timur, S., Pazarlioğlu, N., Pilloton, R., Dinçkaya, E., Telefoncu,

A., 2009. Pseudomonas putida based amperometric biosensors for 2,4-D detection. Prep. Biochem. Biotechnol. 39, 11–19. https://doi.org/10.1080/10826060802589460

Oliveira, G.C., Moccelini, S.K., Castilho, M., Terezo, A.J., Possavatz, J., Magalhães, M.R.L., Dores, E.F.G.C., 2012. Biosensor based on atemoya peroxidase immobilised on modified nanoclay for glyphosate biomonitoring. Talanta 98, 130–136. https://doi.org/10.1016/j.talanta.2012.06.059

Oliveira, H.C., Stolf-Moreira, R., Martinez, C.B.R., Grillo, R., De Jesus, M.B., Fraceto, L.F., 2015. Nanoencapsulation enhances the post-emergence herbicidal activity of atrazine against mustard plants. PLoS One 10, 1–12. https://doi.org/10.1371/journal.pone.0132971

Pandard, P., Rawson, D.M., 1993. An amperometric algal biosensor for herbicide detection employing a carbon cathode oxygen electrode. Environ. Toxicol. Water Qual. 8, 323–333. https://doi.org/10.1002/tox.2530080309

Pannier, A., Soltmann, U., Soltmann, B., Altenburger, R., Schmitt-Jansen, M., 2014. Alginate/silica hybrid materials for immobilization of green microalgae Chlorella vulgaris for cell-based sensor arrays. J. Mater. Chem. B 2, 7896–7909. https://doi.org/10.1039/c4tb00944d

Peña-Vázquez, E., Maneiro, E., Pérez-Conde, C., Moreno-Bondi, M.C., Costas, E., 2009. Microalgae fiber optic biosensors for herbicide monitoring using sol-gel technology. Biosens. Bioelectron. 24, 3538–3543. https://doi.org/10.1016/j.bios.2009.05.013

Phopin, K., Tantimongcolwat, T., 2020. Pesticide aptasensors—state of the art and perspectives. Sensors (Switzerland) 20, 1–40. https://doi.org/10.3390/s20236809

Podola, B., Melkonian, M., 2005. Selective real-time herbicide monitoring by an array chip biosensor employing diverse microalgae. J. Appl. Phycol. 17, 261–271. https://doi.org/10.1007/s10811-005-4945-5

Preuss, M., Hall, E.A.H., 1995. Mediated herbicide inhibition in a PET biosensor. Anal. Chem. 67, 1940–1949. https://doi.org/10.1021/ac00109a006

Prudkin-Silva, C., Lanzarotti, E., Álvarez, L., Vallerga, M.B., Factorovich, M., Morzan, U.N., Gómez, M.P., González, N.P., Acosta, Y.M., Carrizo, F., Carrizo, E., Galeano, S., Lagorio, M.G., Juárez, Á.B., Ithuralde, R.E., Romero, J.M., Urdampilleta, C.M., 2021. A cost-effective algae-based biosensor for water quality analysis: Development and testing in collaboration with peasant communities. Environ. Technol. Innov. 22, 101479. https://doi.org/10.1016/j.eti.2021.101479

Raman Suri, C., Boro, R., Nangia, Y., Gandhi, S., Sharma, P., Wangoo, N., Rajesh, K., Shekhawat, G.S., 2009. Immunoanalytical techniques for analyzing pesticides in the environment. TrAC - Trends Anal. Chem. 28, 29–39. https://doi.org/10.1016/j.trac.2008.09.017

Rasmussen, M., Minteer, S.D., 2013. Self-powered herbicide biosensor utilizing thylakoid membranes. Anal. Methods 5, 1140–1144. https://doi.org/10.1039/c3ay26488b

Rawson, D.M., Willmer, A.J., Turner, A.P.F., 1989. Whole-cell biosensors for environmental monitoring. Biosens. 4 4, 299–311. https://doi.org/10.1177/002029408902200604

Rocaboy-Faquet, E., Noguer, T., Romdhane, S., Bertrand, C., Dayan, F.E., Barthelmebs, L., 2014. Novel bacterial bioassay for a high-throughput screening of 4-hydroxyphenylpyruvate dioxygenase inhibitors. Appl. Microbiol. Biotechnol. 98, 7243–7252. https://doi.org/10.1007/s00253-014-5793-5

Roman, R.L., Nagi, L., Silva, L.L., Fernandes, S.C., de Mello, J.M.M., Magro, J.D., Fiori, M.A., 2020. Monocrystalline silicon/polyaniline/horseradish peroxidase enzyme electrode obtained by the electrodeposition method for the electrochemical detection of glyphosate. J. Mater. Sci. Mater. Electron. 31, 9443–9456. https://doi.org/10.1007/s10854-020-03484-7

Rouillon, R., Sole, M., Carpentier, R., Marty, J.L., 1995. Immobilization of thylakoids in polyvinylalcohol for the detection of herbicides. Sensors Actuators B. Chem. 27, 477–479. https://doi.org/10.1016/0925-4005(94)01645-X

Sassolas, A., Blum, L.J., Leca-Bouvier, B.D., 2011. Optical detection systems using immobilized aptamers. Biosens. Bioelectron. 26, 3725–3736.

https://doi.org/10.1016/j.bios.2011.02.031
Scognamiglio, V., Antonacci, A., Arduini, F., Moscone, D., Campos, E.V.R., Fraceto, L.F., Palleschi, G., 2019. An eco-designed paper-based algal biosensor for nanoformulated herbicide optical detection. J. Hazard. Mater. 373, 483–492. https://doi.org/10.1016/j.jhazmat.2019.03.082
Scognamiglio, V., Pezzotti, I., Pezzotti, G., Cano, J., Manfredonia, I., Buonasera, K., Arduini, F., Moscone, D., Palleschi, G., Giardi, M.T., 2012. Towards an integrated biosensor array for simultaneous and rapid multi-analysis of endocrine disrupting chemicals. Anal. Chim. Acta 751, 161–170. https://doi.org/10.1016/j.aca.2012.09.010
Scognamiglio, V., Pezzotti, I., Pezzotti, G., Cano, J., Manfredonia, I., Buonasera, K., Rodio, G., Giardi, M.T., 2013. A new embedded biosensor platform based on micro-electrodes array (MEA) technology. Sensors Actuators, B Chem. 176, 275–283. https://doi.org/10.1016/j.snb.2012.09.101
Seki, A., Ortéga, F., Marty, J.L., 1996. Enzyme sensor for the detection of herbicides inhibiting acetolactate synthase. Anal. Lett. 29, 1259–1271. https://doi.org/10.1080/00032719608001479
Sezgintrk, M.K., Odaci, D., Pazarliolu, N., Pilloton, R., Dinçkaya, E., Telefoncu, A., Timur, S., 2010. Construction and comparison of trametes versicolor laccase biosensors capable of detecting xenobiotics. Artif. Cells, Blood Substitutes, Biotechnol. 38, 192–199. https://doi.org/10.3109/10731191003776777
Sharma, A., Kumar, V., Shahzad, B., Tanveer, M., Sidhu, G.P.S., Handa, N., Kohli, S.K., Yadav, P., Bali, A.S., Parihar, R.D., Dar, O.I., Singh, K., Jasrotia, S., Bakshi, P., Ramakrishnan, M., Kumar, S., Bhardwaj, R., Thukral, A.K., 2019. Worldwide pesticide usage and its impacts on ecosystem. SN Appl. Sci. 1, 1–16. https://doi.org/10.1007/s42452-019-1485-1
Shitanda, I., Takada, K., Sakai, Y., Tatsuma, T., 2005. Compact amperometric algal biosensors for the evaluation of water toxicity. Anal. Chim. Acta 530, 191–197. https://doi.org/10.1016/j.aca.2004.09.073
Shitanda, I., Takamatsu, S., Watanabe, K., Itagaki, M., 2009. Amperometric screen-printed algal biosensor with flow injection analysis system for detection of environmental toxic compounds. Electrochim. Acta 54, 4933–4936. https://doi.org/10.1016/j.electacta.2009.04.005
Shyuan, L.K., Heng, L.Y., Ahmad, M., Aziz, S.A., Ishak, Z., 2008. Evaluation of pesticide and heavy metal toxicity using immobilized enzyme alkaline phosphatase with an electrochemical biosensor. Asian J. Biochem. https://doi.org/10.3923/ajb.2008.359.365
Sok, V., Fragoso, A., 2021. Carbon Nano-Onion Peroxidase Composite Biosensor for Electrochemical Detection of 2,4-D and 2,4,5-T. Appl. Sci. 11, 6889. https://doi.org/10.3390/app11156889
Sok, V., Fragoso, A., 2019. Amperometric biosensor for glyphosate based on the inhibition of tyrosinase conjugated to carbon nano-onions in a chitosan matrix on a screen-printed electrode. Microchim. Acta 186. https://doi.org/10.1007/s00604-019-3672-6
Songa, E.A., Arotiba, O.A., Owino, J.H.O.O., Jahed, N., Baker, P.G.L.L., Iwuoha, E.I., 2009a. Electrochemical detection of glyphosate herbicide using horseradish peroxidase immobilized on sulfonated polymer matrix. Bioelectrochemistry 75, 117–123. https://doi.org/10.1016/j.bioelechem.2009.02.007
Songa, E.A., Somerset, V.S., Waryo, T., Baker, P.G.L., Iwuoha, E.I., 2009b. Amperometric nanobiosensor for quantitative determination of glyphosate and glufosinate residues in corn samples. Pure Appl. Chem. 81, 123–139. https://doi.org/10.1351/PAC-CON-08-01-15
Sun, C., Liu, M., Sun, H., Lu, H., Zhao, G., 2019. Immobilization-free photoelectrochemical aptasensor for environmental pollutants: Design, fabrication and mechanism. Biosens. Bioelectron. 140. https://doi.org/10.1016/j.bios.2019.111352
Swainsbury, D.J.K., Friebe, V.M., Frese, R.N., Jones, M.R., 2014. Evaluation of a biohybrid photoelectrochemical cell employing the purple bacterial reaction centre as a biosensor for herbicides. Biosens. Bioelectron. 58, 172–178.

https://doi.org/10.1016/j.bios.2014.02.050
Tong, X., Wang, T., Cao, Y., Cai, G., Shi, S., Jiang, Q., Guo, Y., 2023. Multi-emitting fluorescent system–assisted lab-in-a-syringe device for on-site and background-free detection of 2,4-dichlorophenoxyacetic acid. Food Front. 1–9. https://doi.org/10.1002/fft2.273
Tortolini, C., Bollella, P., Antiochia, R., Favero, G., Mazzei, F., 2016. Sensors and Actuators B : Chemical Inhibition-based biosensor for atrazine detection 224, 552–558.
Touloupakis, E., Boutopoulos, C., Buonasera, K., Zergioti, I., Giardi, M.T., 2012. A photosynthetic biosensor with enhanced electron transfer generation realized by laser printing technology. Anal. Bioanal. Chem. 402, 3237–3244. https://doi.org/10.1007/s00216-012-5771-7
Touloupakis, E., Giannoudi, L., Piletsky, S.A., Guzzella, L., Pozzoni, F., Giardi, M.T., 2005. A multi-biosensor based on immobilized Photosystem II on screen-printed electrodes for the detection of herbicides in river water. Biosens. Bioelectron. 20, 1984–1992. https://doi.org/10.1016/j.bios.2004.08.035
Tucci, M., Bombelli, P., Howe, C.J., Vignolini, S., Bocchi, S., Schievano, A., 2019a. A storable mediatorless electrochemical biosensor for herbicide detection. Microorganisms 7, 1–14. https://doi.org/10.3390/microorganisms7120630
Tucci, M., Grattieri, M., Schievano, A., Cristiani, P., Minteer, S.D., 2019b. Microbial amperometric biosensor for online herbicide detection: Photocurrent inhibition of Anabaena variabilis. Electrochim. Acta 302, 102–108. https://doi.org/10.1016/j.electacta.2019.02.007
Turemis, M., Silletti, S., Pezzotti, G., Sanchís, J., Farré, M., Giardi, M.T., 2018. Optical biosensor based on the microalga-paramecium symbiosis for improved marine monitoring. Sensors Actuators, B Chem. 270, 424–432. https://doi.org/10.1016/j.snb.2018.04.111
Vaghela, C., Kulkarni, M., Haram, S., Aiyer, R., Karve, M., 2018. A novel inhibition based biosensor using urease nanoconjugate entrapped biocomposite membrane for potentiometric glyphosate detection. Int. J. Biol. Macromol. 108, 32–40. https://doi.org/10.1016/j.ijbiomac.2017.11.136
Védrine, C., Leclerc, J.C., Durrieu, C., Tran-Minh, C., 2003. Optical whole-cell biosensor using Chlorella vulgaris designed for monitoring herbicides. Biosens. Bioelectron. 18, 457–463. https://doi.org/10.1016/S0956-5663(02)00157-4
Vidal, J.C., Bonel, L., Castillo, J.R., 2008. A modulated tyrosinase enzyme-based biosensor for application to the detection of dichlorvos and atrazine pesticides. Electroanalysis 20, 865–873. https://doi.org/10.1002/elan.200704115
Wang, X., Chen, L., Xia, S., Zhu, Z., Zhao, J., Chovelon, J.M., Renau, N.J., 2006. Tyrosinase biosensor based on interdigitated electrodes for herbicides determination. Int. J. Electrochem. Sci. 1, 55–61. https://doi.org/10.20964/1020055
Wei, D., Wang, Y., Zhu, N., Xiao, J., Li, X., Xu, T., Hu, X., Zhang, Z., Yin, D., 2021. A Lab-in-a-Syringe Device Integrated with a Smartphone Platform: Colorimetric and Fluorescent Dual-Mode Signals for On-Site Detection of Organophosphorus Pesticides. ACS Appl. Mater. Interfaces 13, 48643–48652. https://doi.org/10.1021/acsami.1c13273
Wu, Y., Chen, Y., Zhang, S., Zhang, L., Gong, J., 2019. Bifunctional S, N-Codoped carbon dots-based novel electrochemiluminescent bioassay for ultrasensitive detection of atrazine using activated mesoporous biocarbon as enzyme nanocarriers. Anal. Chim. Acta 1073, 45–53. https://doi.org/10.1016/j.aca.2019.04.068
Yang, Q., Qu, Y., Bo, Y., Wen, Y., Huang, S., 2010. Biosensor for atrazin based on aligned carbon nanotubes modified with glucose oxidase. Microchim. Acta 168, 197–203. https://doi.org/10.1007/s00604-009-0272-x
Yu, J., Lin, J., Li, J., 2021. A photoelectrochemical sensor based on an acetylcholinesterase-CdS/ZnO-modified extended-gate field-effect transistor for glyphosate detection. Analyst 146, 4595–4604. https://doi.org/10.1039/d1an00797a
Yu, Z., Zhao, G., Liu, M., Lei, Y., Li, M., 2010. Fabrication of a novel atrazine biosensor and its subpart-per-trillion levels sensitive performance. Environ. Sci. Technol. 44, 7878–

7883. https://doi.org/10.1021/es101573s
Zamaleeva, A.I., Sharipova, I.R., Shamagsumova, R. V., Ivanov, A.N., Evtugyn, G.A., Ishmuchametova, D.G., Fakhrullin, R.F., 2011. A whole-cell amperometric herbicide biosensor based on magnetically functionalised microalgae and screen-printed electrodes. Anal. Methods 3, 509–513. https://doi.org/10.1039/c0ay00627k
Zambrano-Intriago, L.A., Amorim, C.G., Araújo, A.N., Gritsok, D., Rodríguez-Díaz, J.M., Montenegro, M.C.B.S.M., 2023. Development of an inexpensive and rapidly preparable enzymatic pencil graphite biosensor for monitoring of glyphosate in waters. Sci. Total Environ. 855, 158865. https://doi.org/10.1016/j.scitotenv.2022.158865
Zharmukhamedov, S.K., Shabanova, M.S., Rodionova, M. V., Huseynova, I.M., Karacan, M.S., Karacan, N., Aşık, K.B., Kreslavski, V.D., Alwasel, S., Allakhverdiev, S.I., 2022. Effects of Novel Photosynthetic Inhibitor [CuL2]Br2 Complex on Photosystem II Activity in Spinach. Cells 11. https://doi.org/10.3390/cells11172680
Zúñiga, K., Rebollar, G., Avelar, M., Campos-Terán, J., Torres, E., 2022. Nanomaterial-Based Sensors for the Detection of Glyphosate. Water (Switzerland) 14. https://doi.org/10.3390/w14152436

Declaration of interests

☒ The authors declare that they have no known competing financial interests or personal relationships that could have appeared to influence the work reported in this paper.

☐ The authors declare the following financial interests/personal relationships which may be considered as potential competing interests: